27
12-12-79
2 to NTIS

SAND79-7030
Unlimited Release

UC-70

Creep Behavior of Bedded Salt From Southeastern New Mexico at Elevated Temperature

Francis D. Hansen, Kirby D. Mellegard

Sandia Laboratories

SF-2900 Q(7-73)

SAND79-7030
Unlimited Release
Printed November 1979

Distribution
Category UC-70

TECHNICAL MEMORANDUM REPORT RSI-0062

CREEP BEHAVIOR OF BEDDED SALT FROM SOUTHEASTERN NEW MEXICO AT ELEVATED TEMPERATURE

Submitted To

Sandia Laboratories
Albuquerque, New Mexico

Operated By

Sandia Corporation

for the

Energy Research and Development Administration

By

Francis D. Hansen
and
Kirby D. Mellegard

MASTER

of

RE/SPEC Inc.
P. O. Box 725
Rapid City, South Dakota

November 9, 1977

FOREWORD

This report summarizes the results obtained from a series of triaxial creep experiments on specimens of bedded salt recovered from a depth interval of 2605 to 2679 feet in ERDA Hole No. 9 located in southeastern New Mexico. The objective of this experimental effort was to determine the time-dependent deformational characteristics of the salt under differential stress and elevated temperature. The tests encompassed differential axial stress levels ranging from 1500 to 6000 psi, confining stress levels from zero to 3000 psi, and temperatures of 24, 70 and 100°C. Time durations were variable and ranged from 15 minutes to 20 days. Data analysis consisted of thorough documentation and presentation of experimental results and power law fits to the creep strain-time measurements.

This report was prepared by RE/SPEC Inc. for Sandia Laboratories under Sandia Corporation Contract Document Nos. 02-8858 and 05-7466 under Contract AT (29-1)-789 with the United States Energy Research and Development Administration. The authors are indebted to staff members of RE/SPEC Inc. for contributions and support during the course of testing, data analysis and report preparation. Mr. Leslie A. Wagner and Mr. Daniel M. Schiermeister were instrumental to the entire testing effort including sample preparation, continual maintenance and initial data acquisition. Dr. Paul F. Gnirk reviewed the technical contents of this report and lent constructive criticism. A special acknowledgement is in order for Ms. Julie S. Annicchiarico and Ms. Elizabeth A. Speer for their extra efforts in preparation of this report. The authors also would like to thank Dr. Wolfgang R. Wawersik for his support in this effort throughout the year.

TABLE OF CONTENTS

LIST OF FIGURES

LIST OF TABLES

R S RE/SPEC INC.

P. O. Box 725 • Rapid City, S.D. 57709 • 605/343-7868

November 9, 1977

TECHNICAL MEMORANDUM REPORT RSI-0062

TO: Sandia Laboratories
Albuquerque, NM 87115

Attn.: Dr. Les R. Hill
Dr. Darrell E. Munson
Dr. Wolfgang R. Wawersik

FROM: Mr. Francis D. Hansen
and
Mr. Kirby D. Meliegard
RE/SPEC Inc.
P. O. Box 725
Rapid City, SD 57701

SUBJECT: Triaxial Creep Behavior of Bedded Salt from Southeastern New Mexico at Elevated Temperature (Sandia Corporation, Contract Nos. 02-8858 and 05-7466).

1. INTRODUCTION

This report presents the results of a series of triaxial creep experiments conducted on bedded salt specimens from ERDA Hole 9 in southeastern New Mexico. The salt core and matrix of test conditions were provided by Dr. Wolfgang R. Wawersik, Sandia Laboratories. The purpose of the experiments was to measure creep response of salt at temperatures of 24, 70 and 100°C under confinement pressures of 0, 1500, 2000, 2500 and 3000 psi and differential axial stress levels of 1500, 3000, 4500 and 6000 psi. Test durations ranged from 15 minutes to over 500 hours.

The specimens, obtained by recoring four-inch diameter cores in the axial direction, were nominally two inches in diameter and four inches in length. The crystal size ranged from very small to one-half inch diameter; the specimens contained various amounts of clay impurities. A total of 19 specimens were prepared of which 14 were tested.

The collected data included axial and lateral strain, axial and confinement stresses, time and temperature. Periodically, axial stress was adjusted to account for specimen strain in order to maintain a constant differential stress. Frequency of the stress correction was dependent on the rate of deformation; two or more corrections in a 24 hour period were typical. Data were automatically recorded with a printer, manually recoded from the print-out to punched cards and reduced by means of a computer. A preponderance of the data (see Section 4.1) was collected in the transient creep regime. In some tests specimen rupture occurred, while in others an accelerating creep rate brought the specimen in contact with the pressure vessel wall. Also, a considerable amount of data was collected during stress application to creep stress level.

It is the purpose of this report to present all of the data obtained in a concise manner such that use can be made of these results by Dr. Wawersik in his more comprehensive experimental program. For that matter, the contents have been divided into sections which present summaries of the collective results. The experimental data have been fit with equations which describe transient creep. All of the data is presented in plots in the Appendices. Considerable attention was also given to specimen characterization and measurements after deformation.

3. BACKGROUND AND PROCEDURES

2.1. Test Matrix

The Statement of Work Section of Contract 05-7466 specified eighteen creep (constant stress) tests be conducted on fourteen salt specimens. Specifics of principal stress difference, confining pressure, temperature, and duration for the tests were transmitted in a letter from Wolfgang R. Wawersik to Paul F. Gnirk on October 22, 1976. Table 1 lists the parameters as projected at that time.

2.2. Specimen Preparation

Several four-inch diameter cores of various lengths from the ERDA 9 drillhole located in southeastern New Mexico were received by RE/SPEC on April 8, 1977. The four-inch cores were sawed using a bandsaw into five-inch lengths and subsequently recored to two-inch diameter specimens on a vertical milling machine. A thin-walled diamond bit and recirculating saturated brine were used for coring. Table 2 contains a summary of the cores received and the resultant testable specimens prepared from each piece. Lapping of the specimen ends was accomplished on the vertical milling machine using a diamond wheel. Specimen preparation was extremely precise; ends were parallel $\pm$ 0.001 inches and diameters were 1.997 $\pm$ 0.002 inches.

2.3. Apparatus and Procedure

All of the tests with the exception of those conducted at room temperature and atmospheric (zero psi) confining pressures (Tests 1, 4, and 9) were conducted on two machines designed by Dr. Wawersik and shown in Figure 1. Procedural detail and data acquisition involved with the operation of these machines has been presented previously (1). Tests 1, 4 and 9 were conducted on a triaxial machine equipped with precharged accumulators for maintaining constant axial stress, as shown in Figure 2.

Each specimen was first subjected to a hydrostatic stress state and allowed to achieve equilibrium; tests were normally allowed to stabilize overnight. After equilibration under hydrostatic conditions, differential axial stress was applied at a rate of 100 psi/min. for a majority of the tests. Variances in the rate on five tests ranged from 75 to 275 psi/min. (Table 3). During differential stress application, axial

displacement data were collected at one minute intervals on all of the tests; lateral strain data were collected on only those specimens subjected to confinement pressures.

TABLE 1

STRAWMAN OF PROJECTED RE/SPEC CREEP TESTS FY77

TEST SPECIMENS	TEMPERATURE (^{o}C)	PRINCIPAL STRESS DIFFERENCE (PSI)	CONFINING PRESSURE (PSI)	TEST DURATION (DAYS)
1	24	1500	0	15
2	70	1500	0	15
3	100	1500	0	10
4	24	3000	0	≤ 10
5	24	3000	2500	15
6	70	3000	2500	10
7	100	3000	2500	10
8	100	1500	3000	15
9	24	1500/3000	0	7/5=12
10	24	1500/3000	2500	7/7=14
11	100	1500/3000	0	5/5=10
12	100	1500/3000	2500	5/5=10
13	24	4500	2000	10
14	24	6000	1500	10

NOTE: Tests 9, 10, 11, 12 are two stage tests; differenital axial stresses and durations are separated by a slash (/).

TABLE 2

FOUR-INCH CORES FROM ERDA 9 AND FINISHED TWO-INCH SPECIMENS

ERDA CORE	*DEPTH INTERVAL (FT.)*	*APPROX. LENGTH (IN.)*	*TWO-INCH SPECIMENS RECORED AND FINISHED (TEST - DEPTH (FT.))**
1	*2605.0 to 2606.5*	*18*	*8-2605.0(B), 10-2606.0(B), 13-2605.5(B), UT-2605.0(A), UT-2606.0(A), UT-2605.5(A)*
2	*2678.0 to 2679.0*	*15*	*12-2678.3(B), 14-2678.7(B), 7-2679.0(B), UT-2678.3(A), UT-2678.7(A), 11-2679.0(A)*
3	*2678.0*	*5*	*4-2678.0(A), 9-2678.0(B)*
4	*2674.5*	*5*	*6-2674.5(B), 5-2674.5(A)*
5	*2622.0*	*5*	*3-2622.0*
6	*2668.5*	*5*	*1-2668.5(A), 2-2668.5(B)*

** The prefix UT denotes untested specimen. The suffix (A) or (B) differentiates between specimens recored from the same depth.*

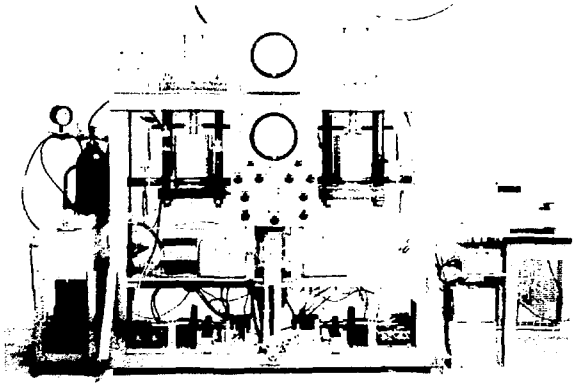

Figure 1. Photograph of Testing Apparatus Housing Machine 1 on Right, Machine 2 on Left.

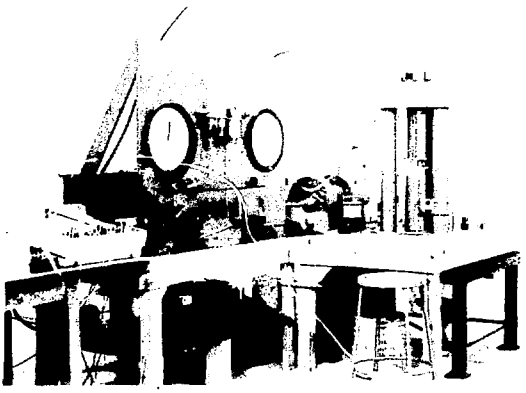

Figure 2. Photograph of Tesing Machine 3.

Subsequent to achieving the differential axial stress level desired for creep, the axial system was closed. A constant axial stress was held on the specimen by means of a one gallon capacity nitrogen charged bladder accumulator. A correction of the differential axial stress to account for specimen distortion was periodically applied. The necessity and frequency of correctional measures were dependent upon the rate of deformation of the specimen. The correction for cross-sectional area change was taken as:

$$A_R \cong A_o (1 + \epsilon_2)^2 \qquad (1)$$

where:

A_R = Corrected area of the specimen (sq. in.)
A_o = Original area of the specimen (sq. in.)
ϵ_2 = Lateral strain.

Where lateral strain measurements were not available, the correction was taken as:

$$A_R \cong A_o (1 + \epsilon_1) \qquad (2)$$

where:

$\epsilon_1 = 2\epsilon_2$ (assuming $-\epsilon_2/\epsilon_1 \equiv 0.5$)

It is recognized that Equation 1 and Equation 2 are not entirely consistent; Equation 2 neglects higher order terms.

2.4. Calibration of Testing Apparatus

Calibration of the testing apparatus involved two considerations; i.e., axial and lateral displacements and temperature of the test specimen versus oil temperature. Uniaxial and triaxial compression tests were performed on metal specimens of brass, aluminum and steel. Calibrations were performed at 24 and 100°C temperatures and under confinement pressures of 0, 500, 1500 and 3000 psi. A total of 81 separate quasi-static calibration tests were completed among the three machines. In addition, thermal calibration tests involved assembly of a triaxial experiment with thermocouples placed within a specimen of salt.

2.4.1. Calibration of Axial and Lateral Systems

Unconfined compression calibrations of metal specimens resulted in initially nonlinear displacement (DCDT) as a function of stress; direct strain gauge data, however, were linear and consistent. Triaxial compression calibrations resulted in linear stress-strain responses with the contribution of the assembly pistons consistent between metal types. Axial calibration consisted of a simple comparison of indirect displacement measurements with strain gauge results. The "machine softness" calculations resulted in axial displacement calibrations essentially identical as obtained and reported previously (1).

Calibration of the lateral displacement system was directed toward determining an effective length of the test column inside the pressure vessels, L_p. Lateral strain measurements obtained from volumetric displacements were used to calculate L_p. Despite the relatively large number of calibration tests, refinement of a value for L_p was extremely difficult due to scatter in the data. As an illustration, the values for L_p ranged from 7.0 to 9.0 inches and were consistently of the order of the values reported previously (1). Influences of L_p values on determination of lateral strain are basically a function of the magnitude of strain. That is, for small strains, such as obtained from calibration tests on metals, the value of L_p is more significant than it is for larger strains, such as obtained during triaxial creep experiments on rock salt. This partially accounts for the scatter encountered during calibrations. It was determined that errors in lateral strain calculations due to L_p for reduction of actual creep data were minimal (< 1.0%). For reduction of experimental data in this report, L_p values as reported previously (1) were used.

2.4.2. Calibration of Temperatures

Temperature of the tests was measured by means of a thermocouple probe inserted in the pressure vessel wall to point flush with the inside diameter (Figure 3). This thermocouple also served as a feedback for temperature control. Calibrations were performed to evaluate the difference between the temperature at the pressure vessel wall and the temperature within the salt specimen at the top, middle and bottom. To accomplish the calibration, three thin(0.020 in. diameter) flexible thermocouples were inserted into a 1/16" diameter hole drilled in a specimen of Jefferson Island domal salt and arranged as illustrated in Figure 3. The vessel oil was heated from

room temperature to 70°C and later to 100°C while measurements of temperature were taken from the four thermocouples. Tests were conducted with no confinement pressure and with 500 psi confinement pressure.

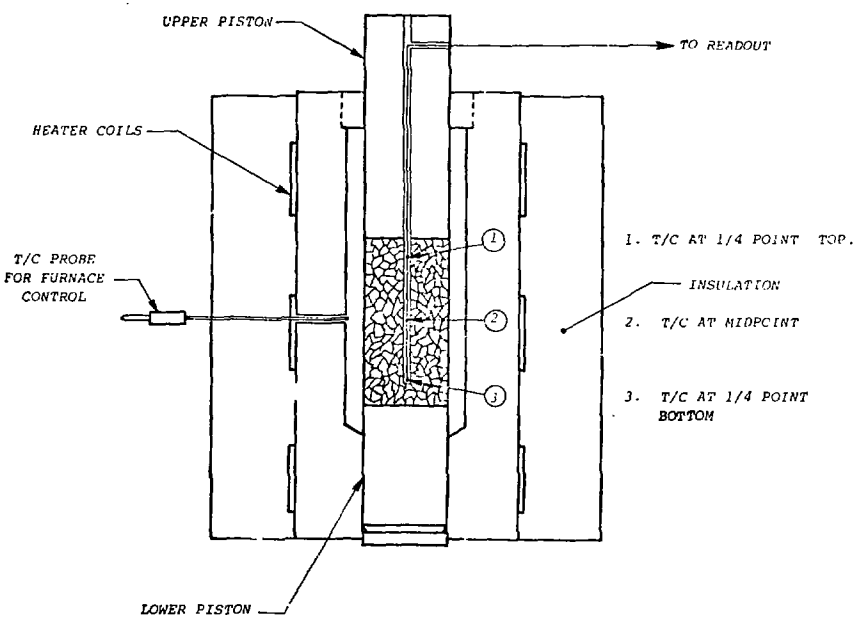

Figure 3. *Temperature Calibration Assembly.*

As a result of these calibration tests, the internal specimen temperature was found to be less than the vessel oil temperature by 6 to 8°C at 100°C and 3 to 5°C at 70°C. As a consequence of this determination, tests specified 100°C were conducted at 106°C and tests specified 70°C were conducted at 74°C. Calibration also showed an axial thermal gradient of about 2°C to exist in specimens subjected to elevated temperatures.

3. DIFFERENTIAL STRESS APPLICATION TO CREEP INITIATION

After the test assembly had achieved equilibrium under hydrostatic stress conditions, initiation of creep tests involved application of differential stress to the desired level for creep, whereupon the differential stress was held constant. During differential stress application, measurements of axial and, when possible, lateral displacements were made. As these data are representative of limited quasi-static compression tests, the resulting mechanical properties and behavior of the material are of interest. For that matter, Figure 4 illustrates the stress-strain response of all of the tests and Figure 5 illustrates the variation of principal strain ratio of the tests when lateral strains were measured. Table 3 is a summary of the axial and lateral pressures, temperatures, and load rates, as well as magnitudes of axial and lateral strain. Table 3 also includes an approximation of a modulus of deformation which was calculated by numerical integration of the stress-strain curve over a differential stress range of 0 to 1500 psi. Calculation of the modulus by integration resulted in slightly lower values than secant calculations.

Plots of the individual stress-strain curves for stress application are presented in Appendix A.

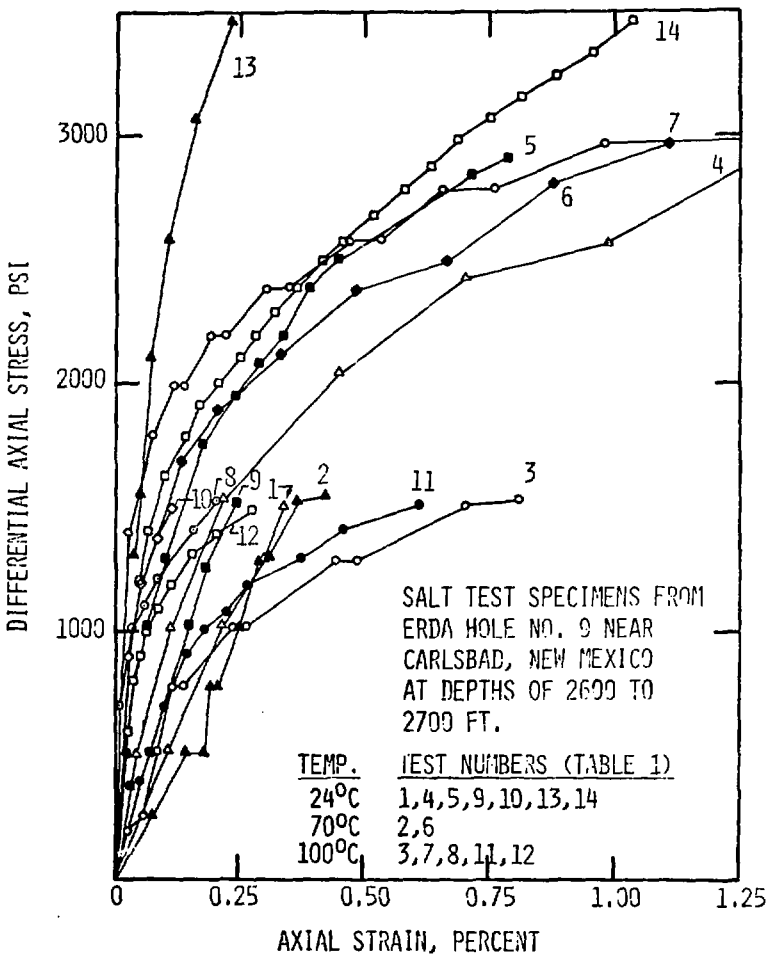

FIGURE 4. DIFFERENTIAL AXIAL STRESS AS A FUNCTION OF AXIAL STRAIN FOR STRESS APPLICATION TO INITIATE CREEP TESTS AT VARIOUS TEMPERATURES.

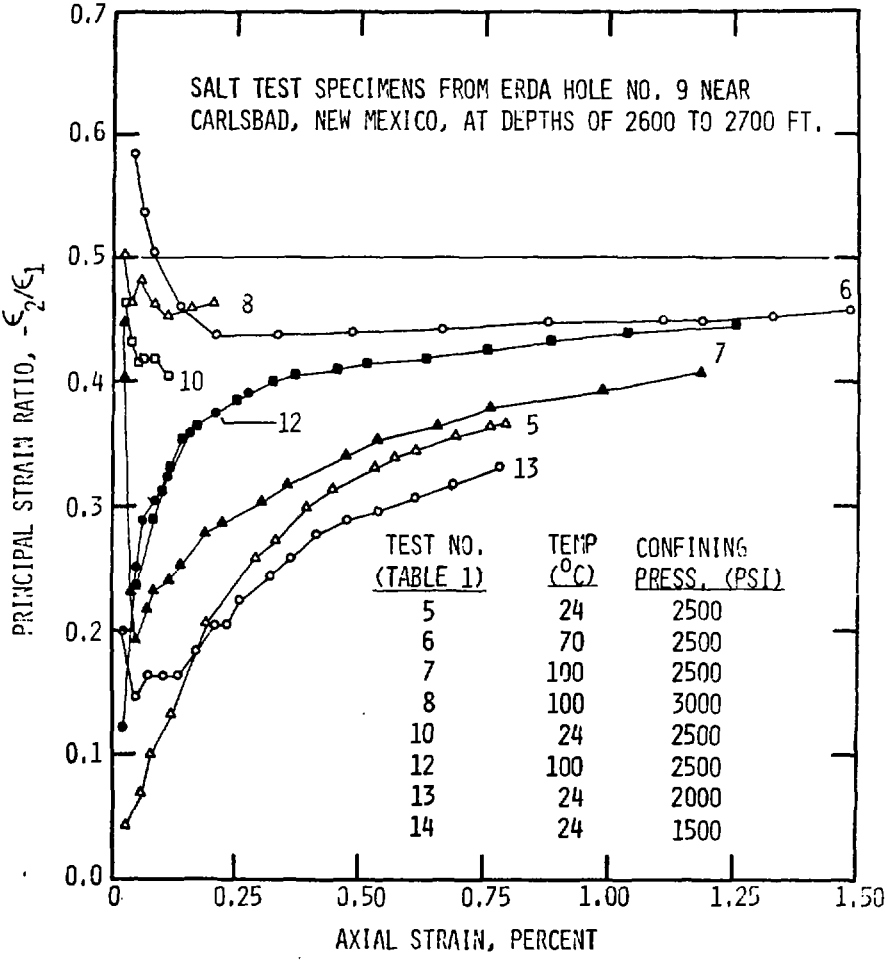

FIGURE 5. PRINCIPAL STRAIN RATIO VARIATIONS DURING DIFFERENTIAL STRESS APPLICATION TO INITIATE CREEP TESTS AT VARIOUS TEMPERATURES AND CONFINING PRESSURES.

TABLE 3

SUMMARY OF TEST DATA FOR TRIAXIAL COMPRESSION
TO INITIATE CREEP TESTS ON ERDA 9 SALT

TEST* NO.	SAMPLE ORIGIN (HOLE-DEPTH, FT.)	CONF. PRESS. (PSI)	TEST TEMP. (°C)	LOAD RATE (PSI/MIN)	DIFF. AXIAL STRESS (PSI)	TOTAL AXIAL STRAIN (%)	TOTAL LATERAL STRAIN (%)	INTEGRATED MODULUS FROM 0 to 1500 PSI (10^3 PSI)
1	9-2668.5(A)	0	24	125	1500	0.34	--	460
2	9-2668.5(B)	0	70	100	1500	0.42	--	396
3	9-2622.0	0	100	100	1500	0.81	--	275
4	9-2678.0(A)	0	24	275	3000	1.45	--	303
5	9-2674.5(A)	2500	24	75	3000	79	0.29	1,431
6	9-2674.5(B)	2500	70	160	3000	1.54	0.70	1,698
7	9-2679.0(B)	2500	100	100	3000	1.18	0.48	2,000**
8	9-2605.0(B)	3000	100	100	1500	0.20	0.09	1,204
9(1)	9-2678.0(B)	0	24	200	1500	0.25	--	692
10(1)	9-2606.0(B)	2500	24	100	1500	0.12	0.04	2,003
11(1)	9-2679.0(A)	0	100	100	1500	0.61	--	361
12(1)	9-2678.3(B)	2500	100	100	1500	0.28	--	833
13	9-2605.5(B)	2000	24	100	4500	0.78	0.26	3,928
14	9-2678.7(B)	1500	24	100	6000	4.37	2.11	2,418

* Numbers in parentheses indicate stress-strain data if from the initial stage of a multistage test. Secondary applications are given in Appendix A.

** Approximated, DCDT temporary malfunction.

4. RESULTS OF TRIAXIAL CREEP EXPERIMENTS

4.1. Introductory Remarks

This testing effort encompassed 17 creep tests conducted at an ambient temperature of 24°C and at elevated temperatures of 70°C and 100°C. Discussion in Section 3 covered the behavioral properties of the salt specimens during stress application to the desired stress level for creep. This section will discuss both axial and lateral deformation as a function of time under constant stress conditions. First, the transient creep behavior which comprises the bulk of experimental data will be presented and discussed. Axial and lateral strains have been plotted and fit to power law equations. A section is also devoted to discussion of the specimens at post-failure and photographs of the specimens are presented. Then, brief analyses concerning activation energy and observed steady state creep are presented. Finally, some comparisons of this set of data to previous data will conclude this section.

Data were collected by means of printed output in engineering units. The mV signals from transducers were amplified, conditioned and calibrated to engineering units. During initial portions of a test, data were collected at a rate of one set of readings per minute. Dependent on the rate of deformation, the time increments between scans were gradually increased. Assembly of data into punched cards was accomplished by hand coding. The card decks were processed on a CDC 3400 computer, which reduced displacement measurements to strains, plotted raw data and numerically fit the experimental data with power law functions.

4.2. Axial Strain as a Function of Time

Initially, data were plotted in terms of strains as a function of time and given a cursory evaluation. Predominantly, the results displayed transient creep behavior; most strain rates continually decreased. This led to a decision to describe the data in terms of $\log_{10}$ strain versus $\log_{10}$ time, which for a majority of the tests resulted in a nearly straight line and can be fit by an equation of the form:

$$\varepsilon_1 = kt^n \qquad (3)$$

where:

ε_1 = axial strain

t = time (sec.) ($t > 1$ hour)

k = experimental constant

Evaluation of Equation 3 was by the method of least squares for t > 1 hour. This procedure is described in more detail in Reference 1. Selection of time greater than one hour for evaluation was arbitrary, but appeared to be a reasonable time for which experimental data showed consistent and linear log-log plots. Equation 3 was then used to describe the complete transient creep response (from t = 0) and for subsequent calculations of strain magnitude and rates. Again, this is a reasonable simplification substantiated by "spot" checking experimental data versus calculated data. For example, actual individual strains were compared to calculated strain magnitudes at a time of one hour and found to be essentially identical; similarly experimental strain rate data were compared to calculated strain rates and found to be consistently of the same order of magnitude. An illustrative example of a typical result is shown in Figure 6-A and 6-B. Figure 6-A illustrates $\log_{10}$ strain as a function of $\log_{10}$ time, including the fit of a least squares line. Figure 6-B is a comparison of the axial strain as a function of time calculated from the resultant equation and the raw experimental data. Experiments which exhibited faster strain rates and greater magnitudes of strain were fit extremely well. Experiments which exhibited slower rates and less strain contained thermal variations and comparison was good but scattered.

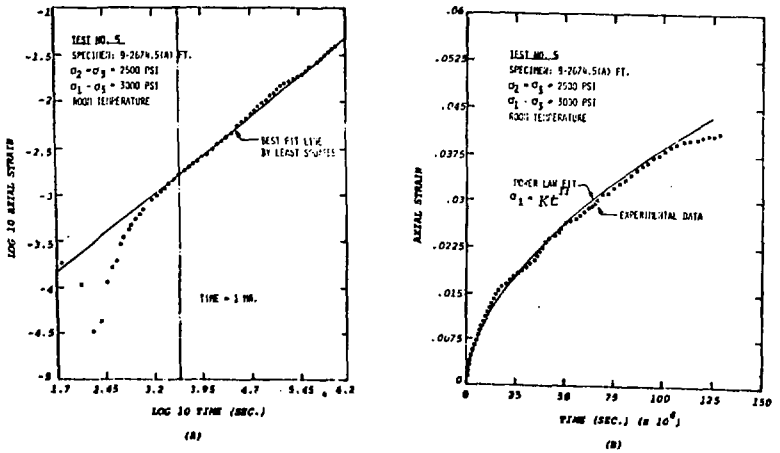

Figure 6. Typical Results of Curve Fitting to Experimental Data.

All of the experiments resulted in at least an initial portion of creep which was definitely transient; most of the tests conducted at elevated temperature ($70^{o}C$ and $100^{o}C$) appeared to exhibit some steady-state creep, though interpretation is somewhat arbitrary. Also, some of the experiments resulted in accelerating creep rate prior to contacting the vessel wall, terminating the test. Tertiary creep data was omitted for purposes of fitting curves to transient creep. Most of the data appearing steady-state on the time-strain curves also appeared rather linear on $\log_{10}$ time versus $\log_{10}$ strain curves and was included in these calculations. Appendix B contains plots of axial strain as a function of time as well as $\log_{10}$ axial strain as a function of $\log_{10}$ time for each of the experiments.

Table 4 contains a summary of the creep data including test conditions, duration and resultant magnitudes of strain. A power law of the form of Equation 3 is listed for the transient portion of each test. Experimental variations, such as cyclic response to ambient temperature variations, make handling of raw experimental data cumbersome. A power law fit facilitates calculation of creep rates and strain magnitudes without the experimental scatter. It should be noted that the powers on time and the constant coefficients are given with more significant digits than justifiable. The idea is to allow subsequent rounding of the numbers a discretion of the reader.

By use of a computerized multiple regression analysis utilizing raw experimental data, a power law was evaluated which incorporates the influence of temperature and stress as well as time. Such a power law may be written:

$$\varepsilon_1 = -Kt^n\sigma^m T^p \qquad (4)$$

where:

σ = differential axial stress (psi)

T = absolute temperature (^{o}K)

The other parameters have been previously defined.

As a result of the fourth order multiple regression on experimental data, a power law of the form of Equation 4 is:

TABLE 4

SUMMARY OF EXPERIMENTAL AXIAL STRAIN DATA

TEST NO.	SPECIMEN ORIGIN	TEST MACH. NO.	TEST TEMP. (^{o}C)	σ_2 (PSI)	$\Delta\sigma$ (PSI)	STAGE OF TEST	DURATION	ε_1^* %	ε_2 %	LEAST SQUARES FIT TO EXPERIMENTAL DATA IN TRANSIENT REGIME	COMMENTS
1 1A	9-2668.5(A)	3	24	0	1,500	App. Creep App. Creep	12 MIN. 123 HRS. 13 MIN. 361 HRS.	0.34 0.47 0.17 0.07	- - - -	$\varepsilon_1 = 3.622(10^{-5})t^{0.3631}$	Leak Necessitated, Unloading at 123 Hrs., Test was Restarted, Data was Added.
2	9-2668.5(B)	2	70	0	1,500	App. Creep	15 MIN. 503 HRS.	0.42 3.27	- -	$\varepsilon_1 = 2.190(10^{-5})t^{0.4991}$	Good Test.
3	9-2622.0	1	100	0	1,500	App. Creep	15 MIN. 503 HRS.	0.81 10.87	- -	$\varepsilon_1 = 1.800(10^{-4})t^{0.4400}$	Good Test.
4	9-2678.0(A)	3	24	0	3,000	App. Creep	11 MIN. 5 HRS.	1.45 2.75	- -	$\varepsilon_1 = 5.475(10^{-5})t^{0.6151}$	Specimen Ruptured.
5	9-2674.5(A)	2	24	2,500	3,000	App. Creep	40 MIN. 360 HRS.	0.79 4.11	0.29 1.80	$\varepsilon_1 = 1.756(10^{-5})t^{0.5572}$	Good Test.
6	9-2674.5(B)	1	70	2,500	3,000	App. Creep	19 MIN. 160 HRS.	1.54 43.00	0.70 20.50	$\varepsilon_1 = 6.151(10^{-5})t^{0.6138}$	Accelerated @ 80 to 100 Hrs., Contacted Vessel Walls @ About 150 Hrs.
7	9-2679.0(B)	1	100	2,500	3,000	App. Creep	31 MIN. 43 HRS.	1.18 39.81	0.48 28.36	$\varepsilon_1 = 1.391(10^{-4})t^{0.6230}$	Accelerated @ 20 Hrs., Contacted Vessel Wall @ End of Test.

* Strain indicated in this column is total strain at test termination. The least squares equation fits only the transient data.

TABLE 4 (CONT'D)

SUMMARY OF EXPERIMENTAL STRAIN DATA

TEST NO.	SPECIMEN ORIGIN	TEST MACH. NO.	TEST TEMP. (^{o}C)	σ_2 (PSI)	$\Delta\sigma$ (PSI)	STAGE OF TEST	DURATION	ε_1 (%)	ε_2 (%)	LEAST SQUARES FIT TO EXPERIMENTAL DATA IN TRANSIENT REGIME	COMMENTS
8	9-2605.0(B)	1	100	3,000	1,500	App. Creep	15 Min. 362 Hrs.	0.20 6.55	0.09 3.14	$\varepsilon_1 = 1.255(10^{-5})t^{0.6022}$	Good Test
9-STG1	9-2678.0(B)	3	24	0	1,500	App. Creep	7 Min. 162 Hrs.	0.24 0.36	- -	$\varepsilon_1 = 3.886(10^{-5})t^{0.3368}$	Good Test
9-STG2	9-2678.0(B)	3	24	0	3,000	App. Creep	15 Min. 15 Min.	0.87 0.89	- -	--	Specimen Ruptured
10-STG1	9-2606.0(B)	1	24	2,500	1,500	App. Creep	15 Min. 170 Hrs.	0.12 0.35	0.05 0.22	$\varepsilon_1 = 2.805(10^{-5})t^{0.3579}$	Good Test
10-STG2	9-2606.0(B)	1	24	2,500	3,000	App. Creep	15 Min. 189 Hrs.	0.51 2.91	0.22 1.43	$\varepsilon_1 = 3.467(10^{-5})t^{0.5024}$	Good Test
11-STG1	9-2679.0(A)	2	100	0	1,500	App. Creep	15 Min. 124 Hrs.	0.61 7.82	- -	$\varepsilon_1 = 3.978(10^{-5})t^{0.5804}$	Stage 1, Good Test, Contacted Vessel Wall
11-STG2	9-2679.0(A)	2	100	0	3,000	App.	21 Min.	6.97	-		Second Stress Application
12-STG1	9-2678.3(B)	1	100	2,500	1,500	App. Creep	15 Min. 137 Hrs.	0.28 5.27	0.11 2.67	$\varepsilon_1 = 1.980(10^{-5})t^{0.6000}$	Good Test
12-STG2	9-2678.3(B)	1	100	2,500	3,000	App. Creep	15 Min. 13 Hrs.	1.66 20.53	0.82 11.18	$\varepsilon_1 = 2.883(10^{-4})t^{0.6060}$	Steady State for Last 6 Hrs.
13	9-2605.5(B)	1	24	2,000	4,500	App. Creep	45 Min. 262 Hrs.	0.78 12.18	0.26 6.55	$\varepsilon_1 = 1.136(10^{-4})t^{0.5090}$	Good Test
14	9-2678.7(B)	1	24	1,500	6,000	App. Creep	60 Min. 89 Hrs.	4.37 23.77	2.11 13.51	$\varepsilon_1 = 7.538(10^{-4})t^{0.4457}$	Terminated Just Prior to Contacting Vessel Wall

$$\varepsilon_1 = 1.1(10^{-35})\ t^{0.4656}\ \sigma^{2.475}\ T^{8.969} \qquad (4\text{-a})$$

Table 5 is a tabulation of the various axial creep strains for 16 experiments to which the data were fit with power law of the form of Equation 3. Near the bottom of Table 5 are several comparative values of axial strains as calculated using the power law given above. Subsequent Figures 7 and 8 are plots of experimental data at differential stress levels of 1500, 3000 and 4500 psi at room temperature and at differential stress levels of 1500 and 3000 psi at 100°C, respectively. Superimposed on actual data plots are the curves calculated on the basis of the best fit power law, Equation 4-a. Notably, the power law fits a majority of the experimental data quite well with the exception of tests at a differential stress level of 3000 psi at 100°C, Tests 7 and 12 - Stage 2. Both of these experiments exhibited large strain and relatively rapid (10^{-6}/sec.) strain rates. For the most part, those experiments exhibiting predominently transient creep are modeled well with the power law equation.

4.3. Lateral Strain as a Function of Time

Lateral strain response was measured during ten of the creep experiments. Lateral strain was measured volumetrically by means of a servo-control system which controls lateral pressure. As a consequence, the volumetric changes of experiments with confinement pressures of zero psi (atmospheric) could not be measured. Lateral strain data was acquired by measuring the turns of a potentiometer in intimate contact with the cylinder of the servometer. Lateral data acquired was handled in the same manner as axial strain, first documented, plotted and then fitted to equations by least squares.

Appendix C contains the individual plots of lateral strain as a function of time and $\log_{10}$ lateral strain as a function of $\log_{10}$ time. Collectively, the qualitative shape of the lateral strain curves are the same as the corresponding axial strain curves. Similarly, the experimental curves lent themselves well to a power law curve fit of lateral strain as a function of time of the form of Equation 3. To summarize the results, Table 6 was prepared which lists test information, a power law equation which fits the transient experimental data, and calculations of principal strain ratios. Overall, the amount of data generated in these tests is too small to arrive at definitive conclusions. The majority of the results appears to indicate constant volume deformation. Response of lateral strain as a function of

TABLE 5

AXIAL CREEP STRAIN AT VARIOUS TIMES

TEST NO.	$\Delta\sigma$ (PSI)	TEMP. ($^{\circ}C$)	LEAST SQUARES EQUATION	AXIAL STRAIN AT VARIOUS TIMES*					
				4 HRS.	12 HRS.	1 DAY	2 DAYS	5 DAYS	10 DAYS
1	1,500	24	$\varepsilon_1 = 3.622(10^{-5})t^{0.3631}$	$1.17(10^{-3})$	$1.75(10^{-3})$	$2.25(10^{-3})$	$2.89(10^{-3})$	$4.04(10^{-3})$	$5.18(10^{-3})$
2	1,500	70	$\varepsilon_1 = 2.190(10^{-5})t^{0.4991}$	$2.61(10^{-3})$	$4.51(10^{-3})$	$6.37(10^{-3})$	$9.01(10^{-3})$	0.0142	0.0201
3	1,500	100	$\varepsilon_1 = 1.800(10^{-5})t^{0.4400}$	0.0122	0.0197	0.0268	0.0363	0.0543	0.0737
4	3,000	24	$\varepsilon_1 = 5.475(10^{-5})t^{0.6151}$	0.0198	(0.0390)	--	--	--	--
5	3,000	24	$\varepsilon_1 = 1.756(10^{-5})t^{0.5572}$	$3.64(10^{-3})$	$6.72(10^{-3})$	$9.89(10^{-3})$	0.0146	0.0242	0.0357
6	3,000	70	$\varepsilon_1 = 6.151(10^{-5})t^{0.6138}$	0.0219	0.0429	0.0659	0.1009	0.1770	(0.2693)
7	3,000	100	$\varepsilon_1 = 1.391(10^{-4})t^{0.6230}$	0.0542	0.1075	0.1655	(0.2549)	--	--
8	1,500	100	$\varepsilon_1 = 1.255(10^{-5})t^{0.6022}$	$4.01(10^{-3})$	$7.76(10^{-3})$	0.0118	0.0179	0.0311	0.0472
9	1,500	24	$\varepsilon_1 = 3.886(10^{-5})t^{0.3368}$	$9.72(10^{-4})$	$1.42(10^{-3})$	$1.79(10^{-3})$	$2.26(10^{-3})$	$3.07(10^{-3})$	$(3.88(10^{-3}))$
10(1)	1,500	24	$\varepsilon_1 = 2.805(10^{-5})t^{0.3579}$	$8.63(10^{-4})$	$1.28(10^{-3})$	$1.64(10^{-3})$	$2.10(10^{-3})$	$2.92(10^{-3})$	$(3.74(10^{-3}))$
10(2)	3,000	24	$\varepsilon_1 = 3.467(10^{-5})t^{0.5024}$	$4.26(10^{-3})$	$7.39(10^{-3})$	0.0105	0.0148	0.0235	(0.0333)
11	1,500	100	$\varepsilon_1 = 3.978(10^{-5})t^{0.5804}$	0.0103	0.0195	0.02916	0.0436	0.0742	(0.1110)
12(1)	1,500	100	$\varepsilon_1 = 1.980(10^{-5})t^{0.6000}$	$6.19(10^{-3})$	0.0120	0.0181	0.0275	0.0476	(0.0722)
12(2)	3,000	100	$\varepsilon_1 = 2.883(10^{-4})t^{0.6060}$	0.0955	0.1858	(0.2827)	--	--	--
13	4,500	24	$\varepsilon_1 = 1.136(10^{-4})t^{0.5090}$	0.0149	0.0260	0.0370	0.0526	0.0839	0.1193
14	6,000	24	$\varepsilon_1 = 7.538(10^{-4})t^{0.4457}$	0.0538	0.0878	0.1195	0.1630	(0.2449)	--
MULTIPLE REGRESSION POWER LAW EQUATIONS	1,500	24	$\varepsilon_1 = 1.203(10^{-5})t^{0.4656}$	$1.04(10^{-3})$	$1.73(10^{-3})$	$2.39(10^{-3})$	$3.30(10^{-3})$	$5.06(10^{-3})$	$6.99(10^{-3})$
	3,000	24	$\varepsilon_1 = 6.690(10^{-5})t^{0.4656}$	$5.78(10^{-3})$	$9.63(10^{-3})$	0.0133	0.0184	0.0281	0.0389
	4,500	24	$\varepsilon_1 = 1.820(10^{-4})t^{0.4656}$	0.0158	0.0263	0.0363	0.0501	0.0768	0.1060
	1,500	100	$\varepsilon_1 = 9.290(10^{-5})t^{0.4656}$	$8.02(10^{-3})$	0.0134	0.0185	0.0255	0.0391	0.0539
	3,000	100	$\varepsilon_1 = 5.160(10^{-4})t^{0.4656}$	0.0446	0.0743	0.1027	0.1418	0.2172	0.2999

* Numbers appearing in parentheses are extrapolated beyond experiment duration.

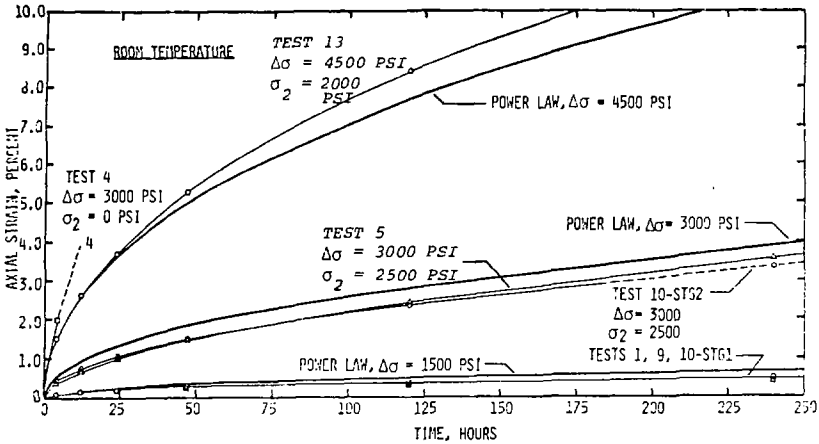

FIGURE 7. CREEP TEST RESULTS; SALT FROM ERDA 9 AT 2700 FOOT DEPTH TESTED AT ROOM TEMPERATURE.

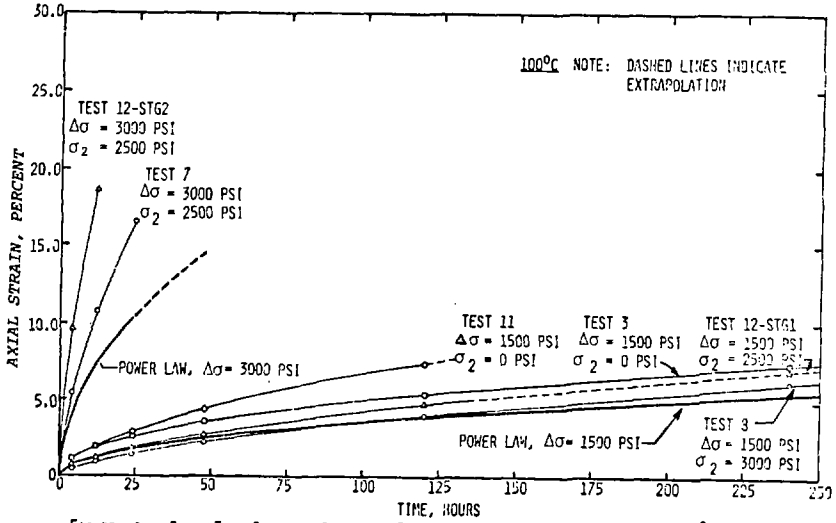

FIGURE 8. CREEP TEST RESULTS; SALT FROM ERDA 9 AT 2700 FOOT DEPTH TESTED AT 100°C.

TABLE 6

LATERAL CREEP STRAIN AT VARIOUS TIMES

TEST NO.	Δσ (PSI)	TEMP. (°C)	LEAST SQUARES EQUATION	LATERAL STRAIN AT VARIOUS TIMES*					
				4 HRS.	12 HRS.	1 DAY	2 DAYS	5 DAYS	10 DAYS
5	3,000	24	$\epsilon_2=9.569(10^{-6})t^{0.5386}$	$1.66(10^{-3})$	$3.00(10^{-3})$	$4.36(10^{-3})$	$6.34(10^{-3})$	0.0104	0.0151
		PRINCIPAL STRAIN RATIOS		0.46	0.45	0.44	0.43	0.43	0.43
6**	3,000	70	$\epsilon_2=2.710(10^{-5})t^{0.6196}$	0.0102	(0.0202)	---	---	---	--
		PRINCIPAL STRAIN RATIOS		0.47	0.47				
7	3,000	100	$\epsilon_2=4.751(10^{-5})t^{0.6640}$	0.0274	0.0569	0.0901	(0.1427)	---	---
		PRINCIPAL STRAIN RATIOS		0.51	0.53	0.54	0.56		
8	1,500	100	$\epsilon_2=8.532(10^{-6})t^{0.5721}$	$2.04(10^{-3})$	$3.83(10^{-3})$	$5.69(10^{-3})$	$8.46(10^{-3})$	0.0143	0.0212
		PRINCIPAL STRAIN RATIOS		0.51	0.49	0.48	0.47	0.46	0.45
10-1	3,000	24	$\epsilon_2=8.312(10^{-6})t^{0.4215}$	$4.70(10^{-4})$	$7.47(10^{-4})$	$1.00(10^{-3})$	$1.34(10^{-3})$	$1.97(10^{-3})$	$(2.64(10^{-3}))$
		PRINCIPAL STRAIN RATIOS		0.54	0.58	0.61	0.64	0.67	0.71
10-2	3,000	24	$\epsilon_2=1.246(10^{-5})t^{0.5157}$	$1.91(10^{-3})$	$3.41(10^{-3})$	$4.91(10^{-3})$	$7.06(10^{-3})$	0.0114	(0.0165)
		PRINCIPAL STRAIN RATIOS		0.45	0.45	0.47	0.48	0.49	0.50
12-1	1,500	100	$\epsilon_2=9.892(10^{-6})t^{0.6006}$	$3.11(10^{-3})$	$6.02(10^{-3})$	$9.12(10^{-3})$	0.0138	0.0240	(0.0364)
		PRINCIPAL STRAIN RATIOS		0.50	0.46	0.50	0.50	0.50	0.50
12-2	3,000	100	$\epsilon_2=1.005(10^{-4})t^{0.6437}$	0.0477	0.0965	(0.1513)	---	---	---
		PRINCIPAL STRAIN RATIOS		0.50	0.52	0.54			
13	4,500	24	$\epsilon_2=3.780(10^{-5})t^{0.5427}$	$6.83(10^{-3})$	0.0124	0.0181	0.0263	0.0432	0.0630
		PRINCIPAL STRAIN RATIOS		0.46	0.48	0.49	0.50	0.51	0.53
14	6,000	24	$\epsilon_2=2.690(10^{-4})t^{0.4832}$	0.0275	0.0467	0.0653	0.0913	(0.1422)	---
		PRINCIPAL STRAIN RATIOS		0.51	0.53	0.55	0.56	0.58	

* Numbers appearing in parentheses are extrapolated beyond actual experimental duration.

**Lateral measurements were lost after eight hours due to broken limit switch.

time was near one-half the magnitude of the axial strain, and the powers on time, t, in the least squares equations are nearly identical between equations for axial and lateral strain.

As noted in Section 3 (Figure 5), the principal strain ratio for the various tests was generally trending toward 0.5. During the creep tests, the principal strain ratio slowly increased with time to values greater than 0.5. A notable exception was Test 5, which was contained in Vessel 2. Vessel 2 is prone to very small leaks, which probably negated the increase in principal strain ratio. Another notable exception is Test 10-Stage 1. This variation, and consequential high values for principal strain ratio, can probably be attributed to the very small magnitudes measured. Some cyclic thermal drift is inherent to all tests; when very small strains are involved, the drift causes a relatively greater percent error.

4.4. Deformed Specimens

The purpose of this section is to present photographs of the specimen along with general description of the specimens after testing. Though these specimens were obtained from the same general location, ERDA 9 @ 2600 to 2700 foot depth, considerable variance between specimens exists. Figures 9 through 12 are photographs of the tested as well as untested specimens concerned in this experimental program. A general knowledge of the specimen characterization may assist in qualitative interpretation of data. For that matter, Appendix D contains general descriptions of the test specimen as it was set up for testing, as well as geometry of the specimen before and after testing.

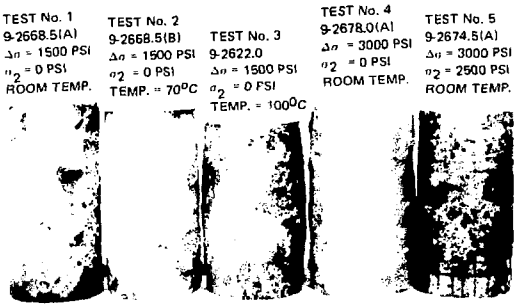

Figure 9. Photographs of Test Specimens 1 through 5.

(a) Test 1: no visible cracks; (b) Test 2: few medium cracks between large crystals, minor cracking in large crystals; (c) Test 3: few major cracks, many hairline cracks; (d) Test 4: failed; (e) Test 5: no visible cracks.

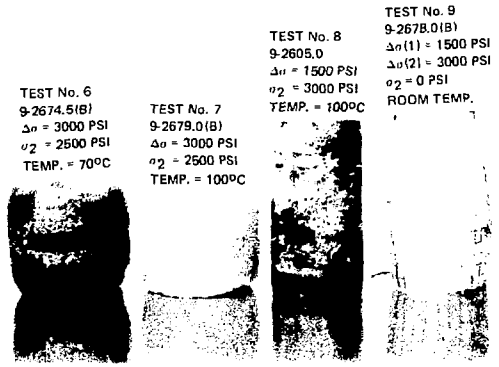

Figure 10. Photograph of Test Specimens 6 through 9.

(a) Test 6: major cracking on ridges, specimen well-deformed with no visible cracks; (b) Test 7: same; (c) Test 8: minor hairline cracks; (d) Test 9: failed.

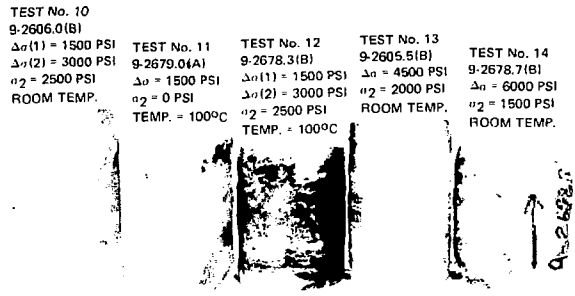

Figure 11. Photograph of Test Specimens 10 through 14.

(a) Test 10: large crystals show cracking, few hairline cracks throughout; (b) Test 11: major cracks, many medium and small cracks; (c) Test 12: some major cracks on ends, hairline cracks throughout; (d) Test 13: large crystals are cracked, no other visible cracks; (e) Test 14: major cracking on ends, large crystals cracked, many hairline cracks throughout.

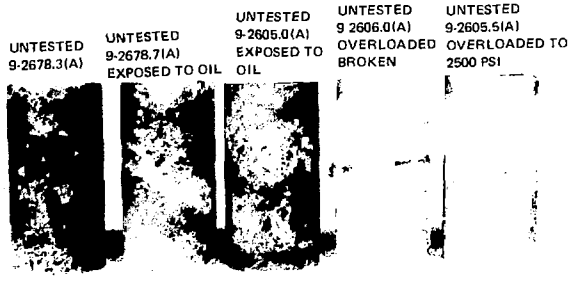

Figure 12. Photograph of Untested Specimens.

4.5. Activation Energy

The purpose of this section is to present the results of activation energy calculations. Several experiments in this test matrix exhibited a constant, or nearly so, creep rate. The activation energy, Q_c, for rock salt can be calculated if the creep rate is known at two temperatures, T_1 and T_2. From Sherby and Burke (2), the equation is:

$$Q_c\Big|_{\sigma,\varepsilon} = R \ln (\dot{\varepsilon}_1/\dot{\varepsilon}_2)/(1/T_2 - 1/T_1) \qquad (5)$$

where:

$\dot{\varepsilon}_1$ and $\dot{\varepsilon}_2$ = axial strain rates at T_1 and T_2, respectively.

R = gas constant

In application of this equation to the experimental results, the strain-time plots were visually examined and steady state was assumed over portions of the plots which were linear. Table 7 summarizes the results obtained in this manner.

From the data contained in Table 7, four calculations of activation energy have been made:

$$Q_{2,3} = 8{,}460 \text{ cal/mole}$$

$$Q_{2,8} = 9{,}100 \text{ cal/mole}$$

$$Q_{6,7} = 10{,}990 \text{ cal/mole}$$

$$Q_{6,12} = 19{,}715 \text{ cal/mole}$$

Certainly this amount of data cannot be construed as conclusive, however, it is comforting to note that these activation energies are in the range of values published by Le Compte (3).

Though it is not practical to over-analyze minimal data, it is interesting to note correlation of these data to an equation from Heard (4):

$$\dot{\varepsilon} = A\exp^{(-Q_c/RT)}\sigma^N \qquad (5)$$

where:

$\dot{\varepsilon}$ = steady state strain rate

A = experimental constant

σ = differential axial stress

Evaluation of the power on stress, N, for steady state creep is illustrated in Figure 13.

As a result, N is shown to be of the order of 6. From Heard (4), the value of N = 3, 4.5 and 6, depending on the specific dislocation mechanism assumed to prevail. Aside from illustrating an apparent close fit to Equation 5 , no further analyses of these data are justified.

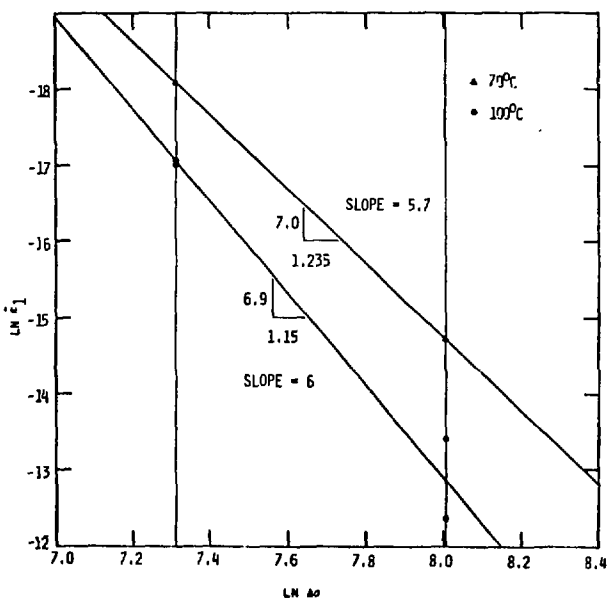

FIGURE 13. PLOT OF LN $\dot{\epsilon}_1$ AS A FUNCTION OF LN $\Delta\sigma$

TABLE 7

STEADY STATE AXIAL CREEP

TEST NO.	TEMP. (^{o}C)	DIFFERENTIAL AXIAL STRESS/ CONFINING PRESSURE (PSI/PSI)	TIME OVER WHICH STEADY CREEP OCCURRED	APPROXIMATE STEADY STATE CREEP RATE (ϵ_1 sec.$^{-1}$)
2	70	1500/0	140 to 500 HRS.	$1.4(10^{-8})$
3	100	1500/0	110 to 360 HRS.	$3.8(10^{-8})$
4	24	3000/0	1.4 to 5.0 HRS.	$1.0(10^{-6})$
6	70	3000/2500	16 to 83 HRS.	$4.1(10^{-7})$
7	100	3000/2500	8 to 20 HRS.	$1.5(10^{-6})$
8	100	1500/3000	140 to 360 HRS.	$4.1(10^{-8})$
9	24	3000/0	3 to 12 MIN.	$7.4(10^{-6})$
12	100	3000/2500	6 to 12.5 HRS.	$4.2(10^{-6})$
14	24	6000/1500	42 to 88 HRS.	$4.8(10^{-7})$

4.6. Comparison with Previous Results

Many of the experiments in this investigation were conducted under similar stresses and temperatures to tests reported in Reference 1. Principal differences between these two test efforts are: (1) Specimens tested in this investigation were obtained from ERDA Hole No. 9 at 2605 to 2679 foot depth while those tested previously were from AEC Hole No. 8 at 2711 to 2722 foot depth; (2) Less time elapsed between field drilling and laboratory testing than previously and core from ERDA #9 was carefully protected from environmental effects; (3) Differential stress was corrected to account for specimen deformation in this work, whereas, previously the stress was not corrected; and (4) Temperature of the tests in this study were actual specimen temperatures rather than oil temperature. General characterization of the salt was similar; each group was relatively clean though ERDA #9 salt contained minor amounts of clay impurities.

Finally, it is interesting to compare results. For that purpose, Table 8 has been compiled which lists strain rates obtained this year and rates of similar tests reported previously. The experiments conducted at room temperature, 24°C, compare very favorably. The experiments conducted at 100°C illustrate the different rates attained by correcting differential stress opposed to not correcting. Also included in this difference is the effect of temperature differences, though thought to be much less significant.

Another way of presenting the difference between results of this experimental program and the previous program is by comparison of power laws which include differential stress and temperature dependence:

$$\varepsilon_1 = 1.693(10^{-39})\, t^{0.4808}\, \sigma^{2.676}\, T^{10.17} \qquad \text{(Reference 1)}$$

$$\varepsilon_1 = 1.1(10^{-35})\, t^{0.4656}\, \sigma^{2.475}\, T^{8.969} \qquad \text{(Equation 4-a)}$$

Generally, the strain dependence on time, differential stress and temperature are very comparable. However, the experimental coefficient differs by four orders of magnitude. As far as application of these two equations to calculate strain magnitudes at a given time ($t \leq 10$ days), the results are surprisingly comparable.

TABLE 8

COMPARISON OF EXPERIMENTAL DATA FOR TESTS INCLUDED IN THIS REPORT AND FOR TESTS AS REPORTED IN REFERENCE 1

TEST*	DATE (YR)	CONFINING PRESSURE (PSI)	AXIAL STRAIN RATES (SEC^{-1}) AT VARIOUS TIMES**			
			2 HR	10 HR	100 HR	200 HR
CONDUCTED AT 24°C AND Δσ = 1500 PSI						
RC-1(STG 1)	76	500	$5.62(10^{-8})$	$1.80(10^{-8})$	$3.53(10^{-9})$	$2.16(10^{-9})$
RC-3(STG 1)	76	2000	$4.58(10^{-8})$	$1.56(10^{-8})$	$3.34(10^{-9})$	$2.10(10^{-9})$
1	77	0	$4.50(10^{-8})$	$1.58(10^{-8})$	$3.53(10^{-9})$	$2.25(10^{-9})$
9(STG 1)	77	0	$3.69(10^{-8})$	$1.29(10^{-8})$	$2.89(10^{-9})$	$1.84(10^{-9})$
10(STG 1)	77	2500	$3.35(10^{-8})$	$1.19(10^{-8})$	$2.72(10^{-9})$	$1.74(10^{-9})$
CONDUCTED AT 100°C AND Δσ = 1500 PSI						
RC-2(STG 1)	76	500	$2.69(10^{-7})$	$1.22(10^{-7})$	$3.91(10^{-8})$	$2.78(10^{-8})$
RC-5(STG 1)	76	2000	$3.77(10^{-7})$	$1.54(10^{-7})$	$4.30(10^{-8})$	$2.93(10^{-8})$
3	77	0	$5.27(10^{-7})$	$2.12(10^{-7})$	$5.78(10^{-8})$	$3.91(10^{-8})$
11	77	0	$5.56(10^{-7})$	$2.83(10^{-7})$	$1.08(10^{-7})$	$8.05(10^{-8})$
12(STG 1)	77	2500	$3.40(10^{-7})$	$1.79(10^{-7})$	$7.12(10^{-8})$	$5.40(10^{-8})$
CONDUCTED AT 24°C AND Δσ = 3000 PSI						
RC-1(STG 2)	76	500	$2.64(10^{-7})$	$1.11(10^{-7})$	$3.24(10^{-8})$	$2.23(10^{-8})$
RC-3(STG 2)	76	2000	$2.39(10^{-7})$	$8.74(10^{-8})$	$2.07(10^{-8})$	$1.34(10^{-8})$
RC-4(STG 1)	76	2000	$2.20(10^{-7})$	$8.58(10^{-8})$	$2.21(10^{-8})$	$1.47(10^{-8})$
4	77	0	$1.10(10^{-6})$	RUPTURED	--	--
9(STG 2)	77	0	RUPTURED	--	--	--
5	77	2500	$1.92(10^{-7})$	$9.40(10^{-8})$	$3.39(10^{-8})$	$2.49(10^{-8})$
10(STG 2)	77	2500	$2.10(10^{-7})$	$9.42(10^{-8})$	$2.99(10^{-8})$	$2.12(10^{-8})$
CONDUCTED AT 100°C AND Δσ = 3000 PSI						
RC-2(STG 2)	76	500	$2.01(10^{-6})$	$9.00(10^{-7})$	$2.84(10^{-7})$	$2.01(10^{-7})$
RC-5(STG 2)	76	2000	$1.87(10^{-6})$	$8.39(10^{-7})$	$2.71(10^{-7})$	$1.93(10^{-7})$
RC-6(STG 1)	76	2000	$2.10(10^{-6})$	$8.44(10^{-7})$	$2.29(10^{-7})$	$1.55(10^{-7})$
7	77	2500	$3.20(10^{-6})$	$1.91(10^{-6})$	--	--
12(STG 2)	77	2500	$5.29(10^{-6})$	$2.86(10^{-6})$	--	--
CONDUCTED AT 24°C AND Δσ = 4500 PSI						
RC-1(STG 3)	76	500	$7.42(10^{-7})$	$3.03(10^{-7})$	$8.38(10^{-8})$	$5.70(10^{-8})$
RC-3(STG 3)	76	2000	$7.06(10^{-7})$	$2.67(10^{-7})$	$6.62(10^{-8})$	$4.36(10^{-8})$
RC-4(STG 2)	76	2000	$6.67(10^{-7})$	$2.65(10^{-7})$	$7.08(10^{-8})$	$4.76(10^{-8})$
13	77	2000	$7.38(10^{-7})$	$3.35(10^{-7})$	$1.08(10^{-7})$	$7.69(10^{-8})$

* Nomenclature RC-X refers to tests documented in Reference 1. Information in parentheses, eg: (STG-X), refers to stage of test where multiple stage creep tests were conducted on a single specimen.

** Calculated from individual best fit equation (Section 4.2)

5. CONCLUDING REMARKS

This report has presented the results of seventeen creep experiments completed on two-inch diameter rock salt specimens from ERDA Hole #9 in southeastern New Mexico. The results also include limited triaxial compression data as a result of stress application to creep levels. The vast majority of the report discusses and presents axial and lateral strain behavior as a result of creeping under conditions of differential axial stresses ranging from 1500 to 6000 psi, lateral stresses ranging from 0 to 3000 psi, and temperatures from ambient laboratory temperature to 100°C. Analyses of the test data are primarily in terms of curve fits to experimental data.

Quasi-static stress application to stress levels desired for creep experiments yielded relationships of differential axial stress as a function of strain. Axial strains were generally of the order of one percent and less. Moduli of deformation (determined by integration) ranged from 300,000 to 4,000,000 psi over the differential stress range of 0 to 1500 psi. In general, moduli decreased with increase in temperature. Principal strain ratio variation during quasi-static compression generally trended toward 0.5. At the end of quasi-static stress application, the principal strain ratio ranged between 0.33 to 0.48 and averaged 0.42.

All tests exhibited transient creep to various degrees; two experiments resulted in rupture; and some experiments exhibited apparent steady-state creep deformation which, in a few cases, accelerated prior to termination. The data are too limited to justify comprehensive analyses of primary, secondary and tertiary creep. The individual creep experiments were fit to power law forms of $\varepsilon_{1,2} = Kt^n$ over the transient portions. Subsequently, a regression analyses yielded an equation fitting axial creep data to a function of time, t, differential stress, σ, and temperature, T. The resultant equation is:

$$\varepsilon_1 = 1.1(10^{-35})\ t^{0.4656}\ \sigma^{2.475}\ T^{8.969}$$

Similar regression was not performed on the lateral strain data. However, on an individual basis, lateral strain was shown to track axial strain on a qualitatively identical curve. Actual principal strain ratios during creep tests ranged from 0.42 to 0.71, but for the most part, were nearly equal to 0.5. Principal strain ratios generally exhibited a gradual increase as the test progressed.

This testing program incorporated several refinements (improvements) as a result of last year's testing program. These improvements began with much improved sample preparation and continued through various changes in the experimental procedure. Broad comparisons of the previous results and these results have been incorporated in the text.

LIST OF REFERENCES

(1) Hansen, Francis D.: "Triaxial Quasi-Static Compression and Creep Behavior of Bedded Salt from Southeastern New Mexico", Technical Memorandum Report RSI-0055, Prepared for Sandia Laboratories operated by Sandia Corporation for the Energy Research and Development Administration, June 3, 1977.

(2) Sherby O. D. and Burke, P. M.: "Mechanical Behavior of Crystalline Solids at Elevated Temperature", Progr. Metal Sci., Vol. 13, pp. 325-390, 1968.

(3) Le Compte, P.: "Creep in Rock Salt", J. Geol., Vol. 73, pp. 469-484, 1965.

(4) Heard, H. C.: "Steady-State Flow in Polycrystalline Halite at Pressures of 2 Kilobars", Am. Geophys. Un. Mono., Vol. 16, 191-209, 1972.

APPENDIX A

PLOTS OF DIFFERENTIAL STRESS APPLICATION TO CREEP STAGE

APPENDIX A (CONT'D)

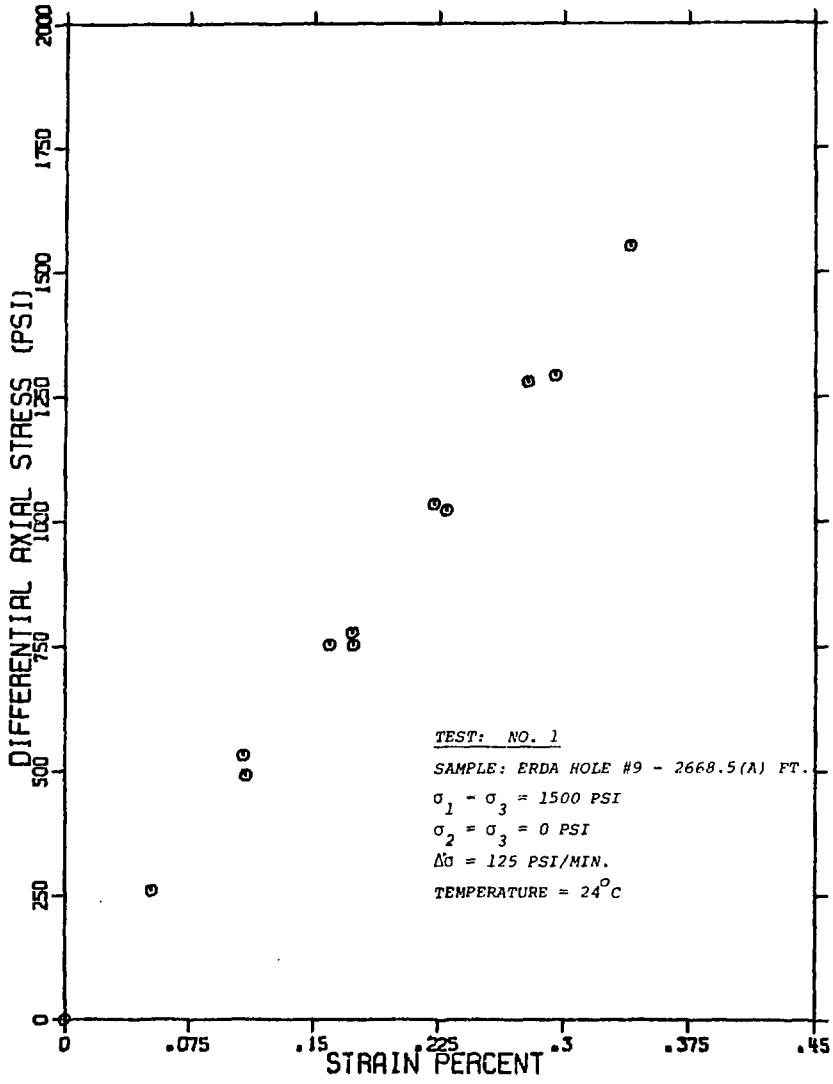

Figure A-1: Differential Axial Stress as a Function of Axial Strain, Test 1.

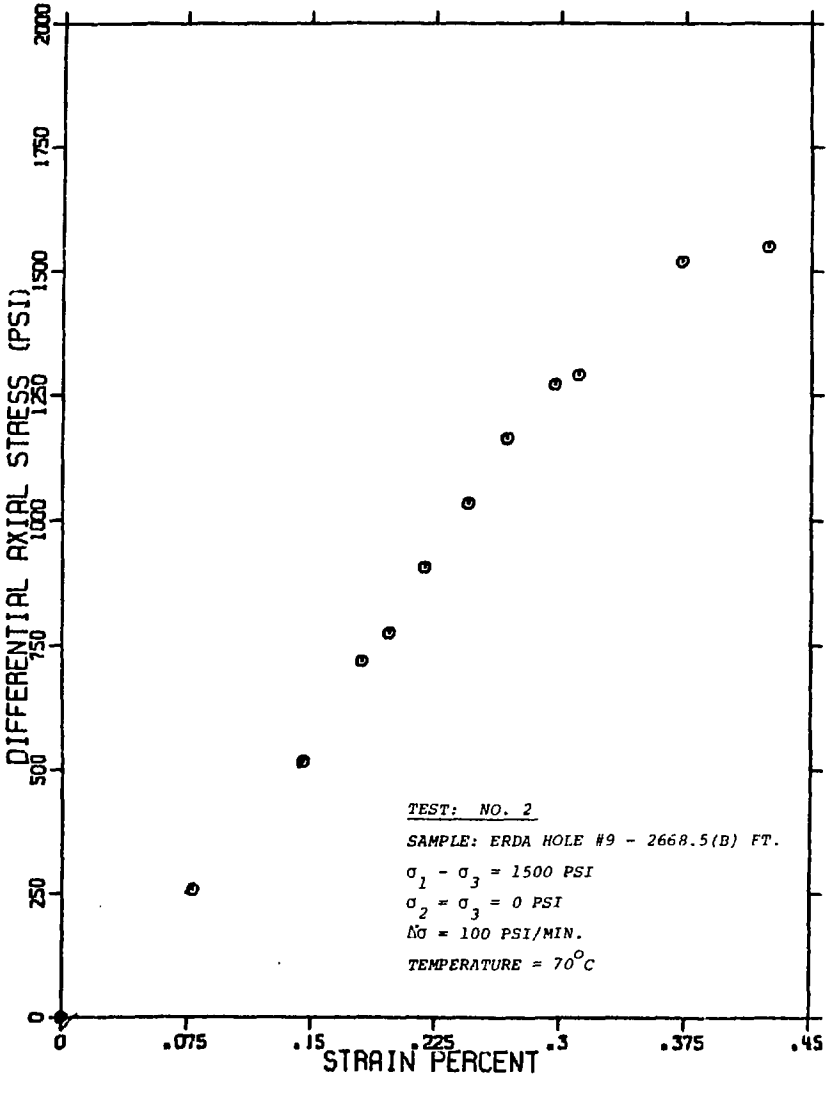

Figure A-2. Differential Axial Stress as a Function of Axial Strain, Test 2.

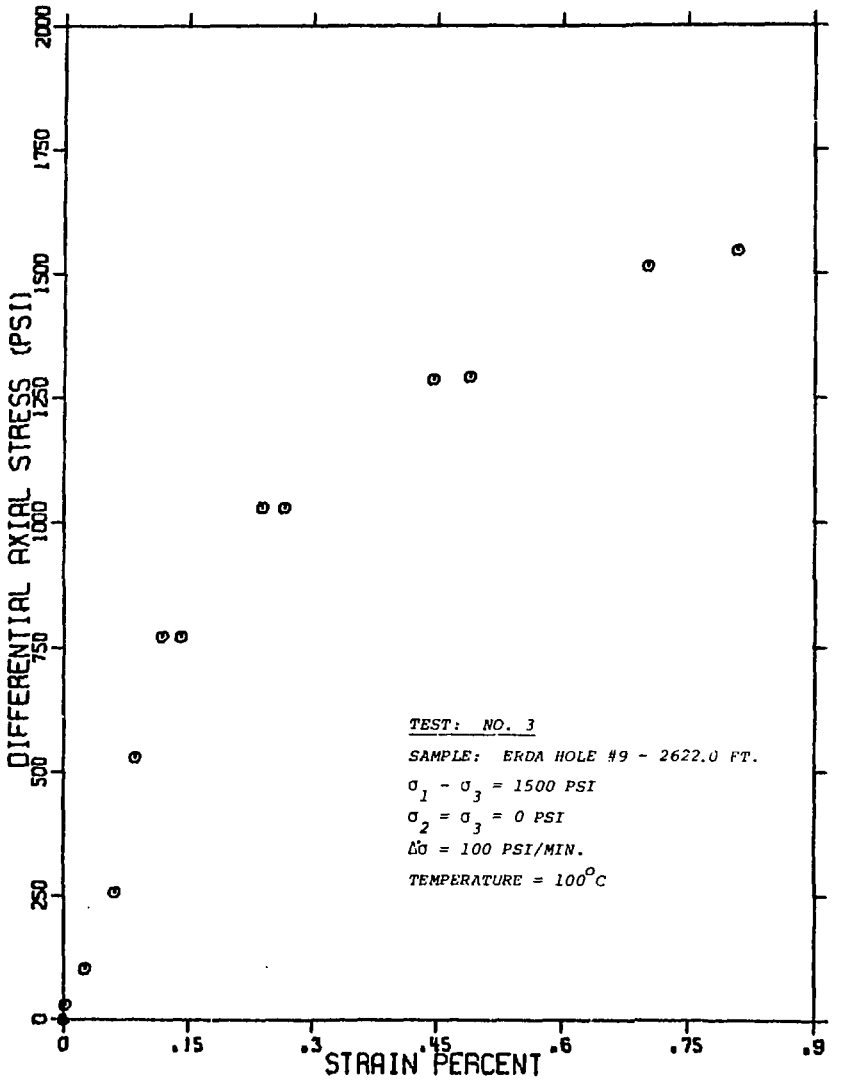

Figure A-3. Differential Axial Stress as a Function of Axial Strain, Test 3.

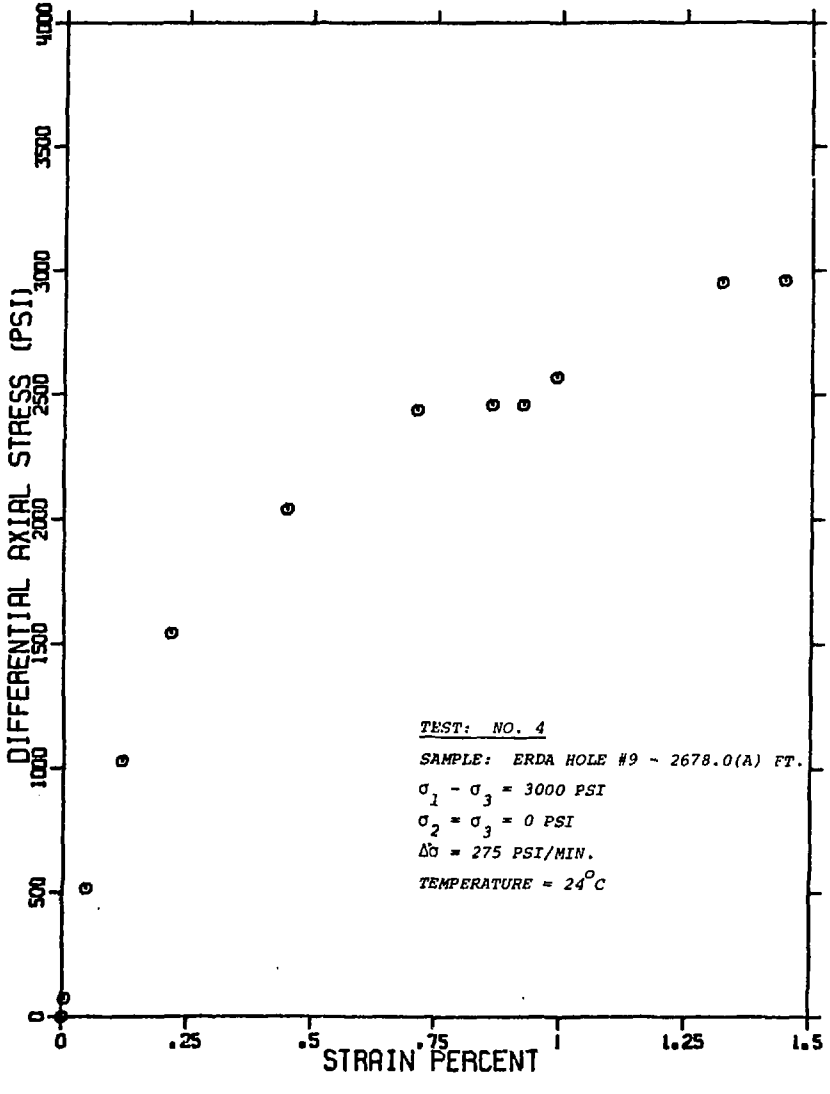

Figure A-4. Differential Axial Stress as a Function of Axial Strain, Test 4.

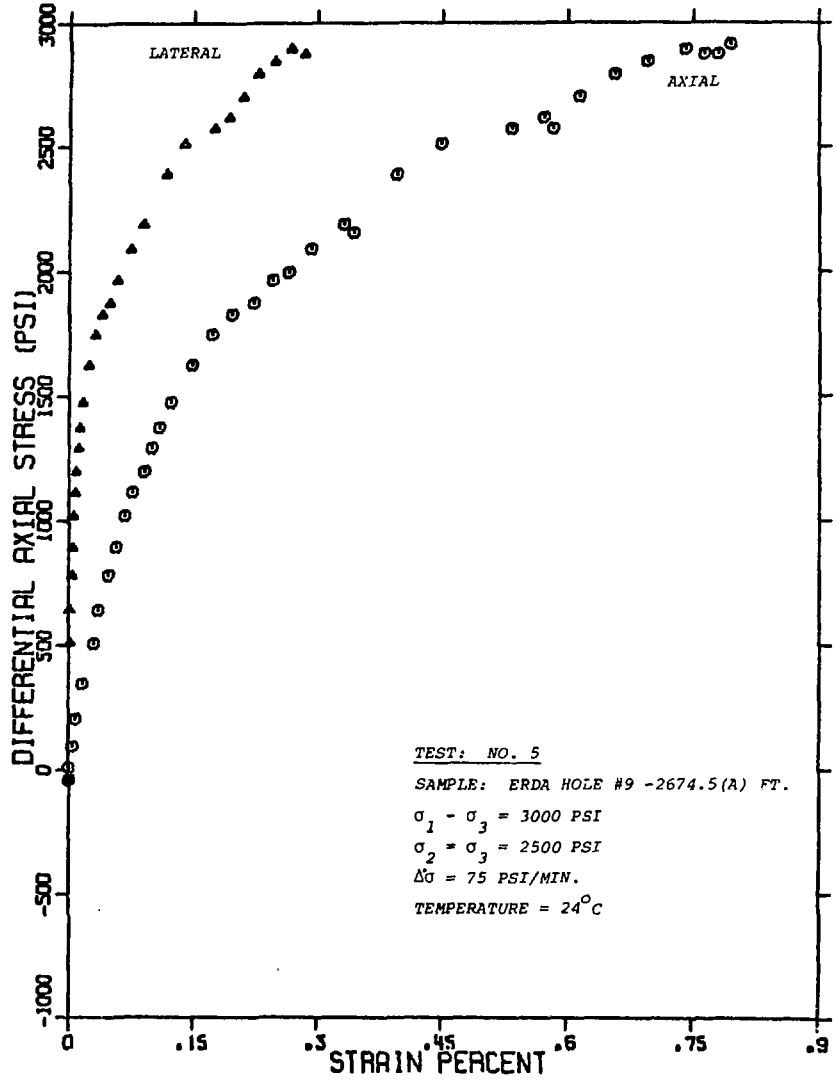

Figure A-5. Differential Axial Stress as a Function of Axial and Lateral Strain, Test 5.

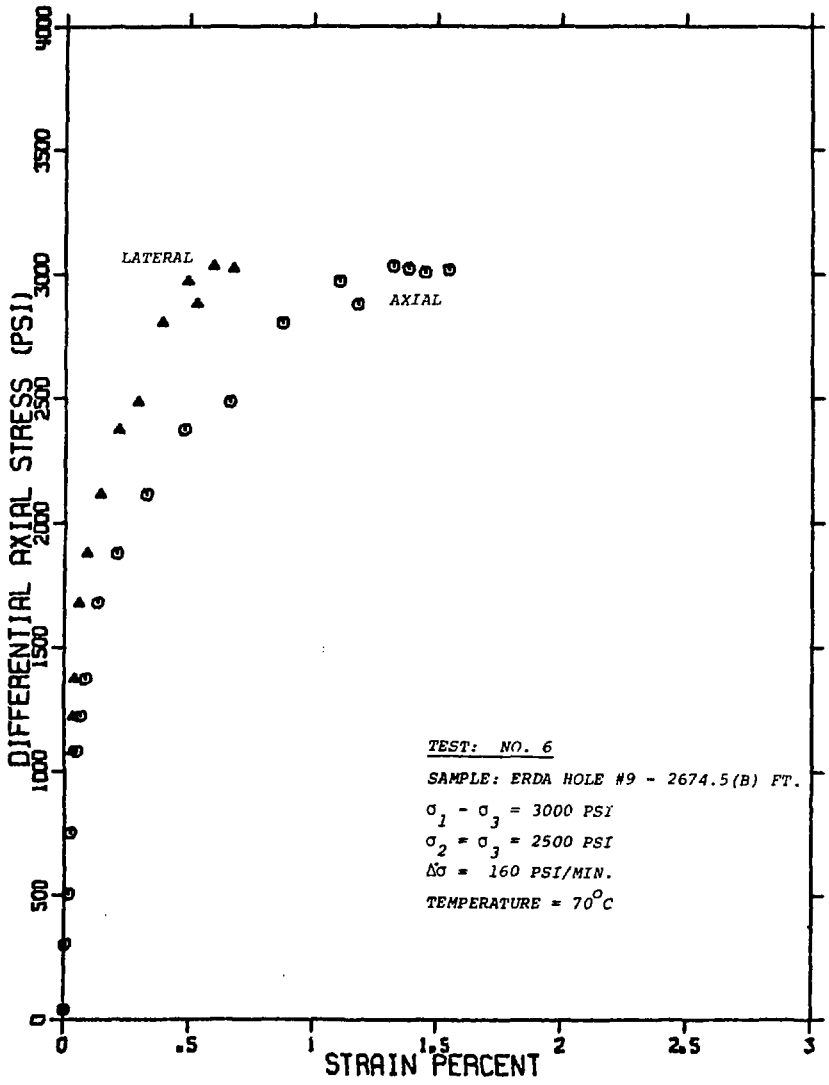

Figure A-6. Differential Axial Stress as a Function of Axial and Lateral Strain, Test 6.

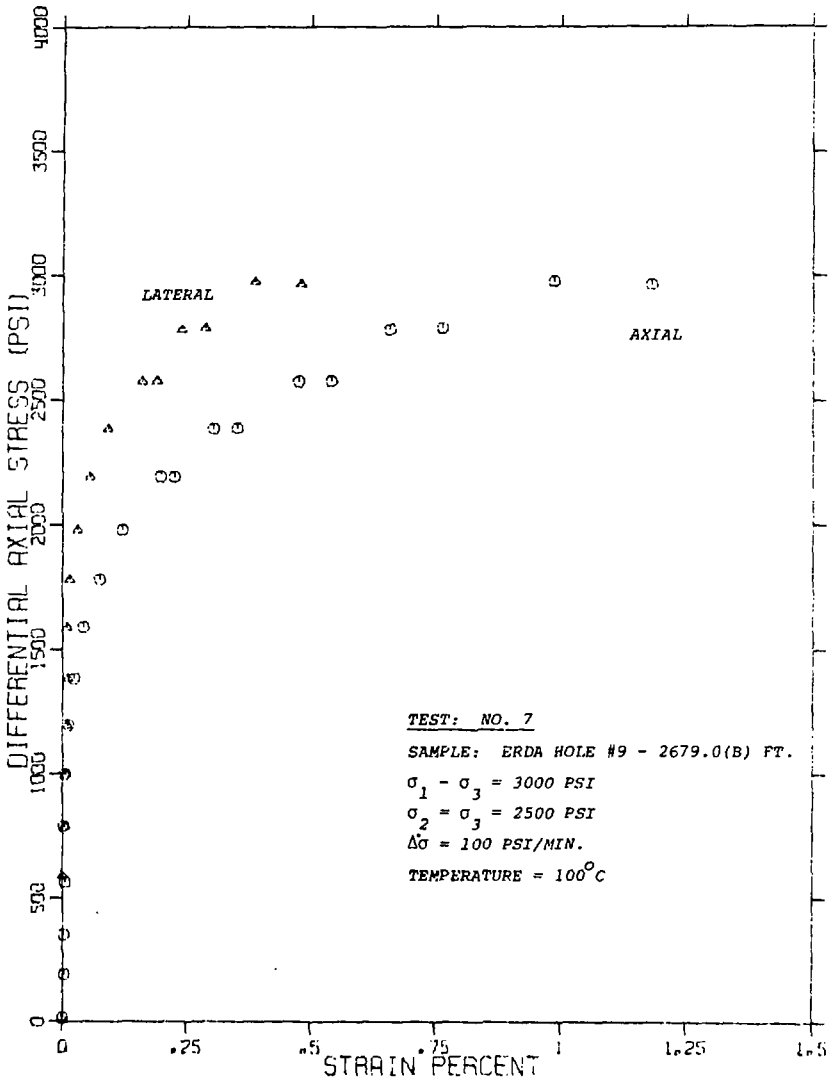

Figure A-7. Differential Axial Stress as a Function of Axial and Lateral Strain, Test 7.

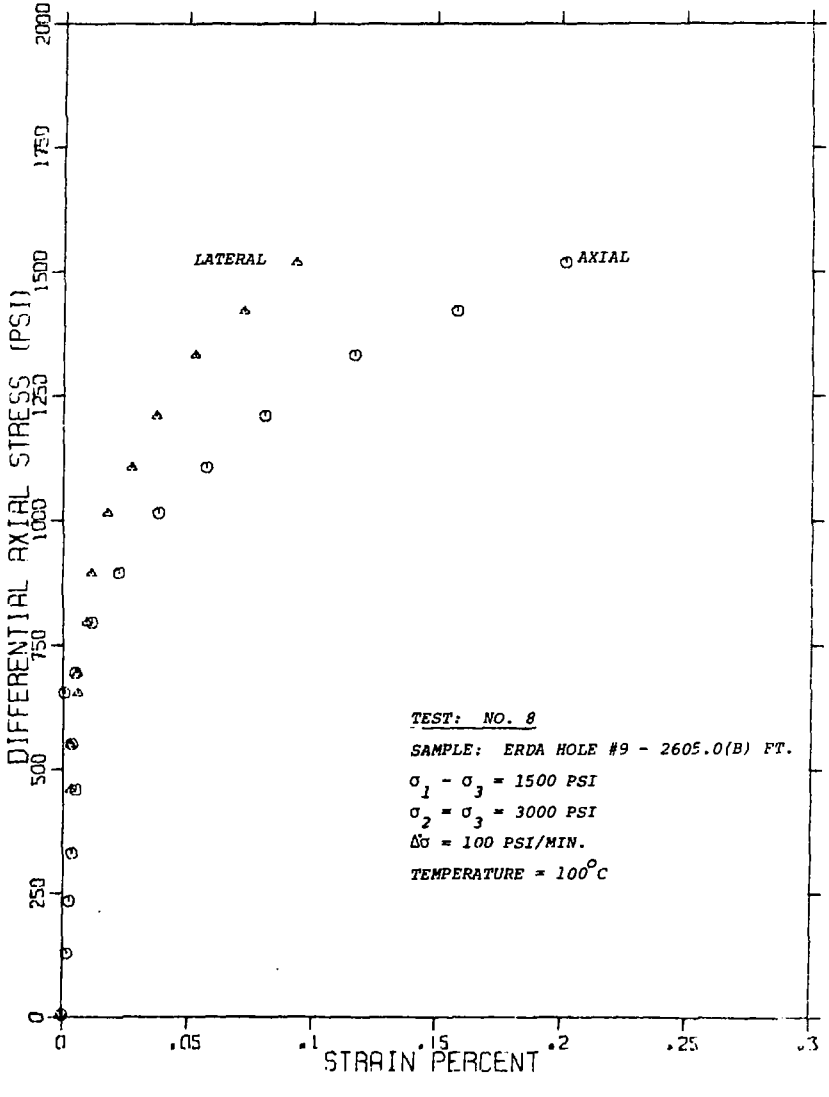

Figure A-8. Differential Axial Stress as a Function of Axial and Lateral Strain, Test 8.

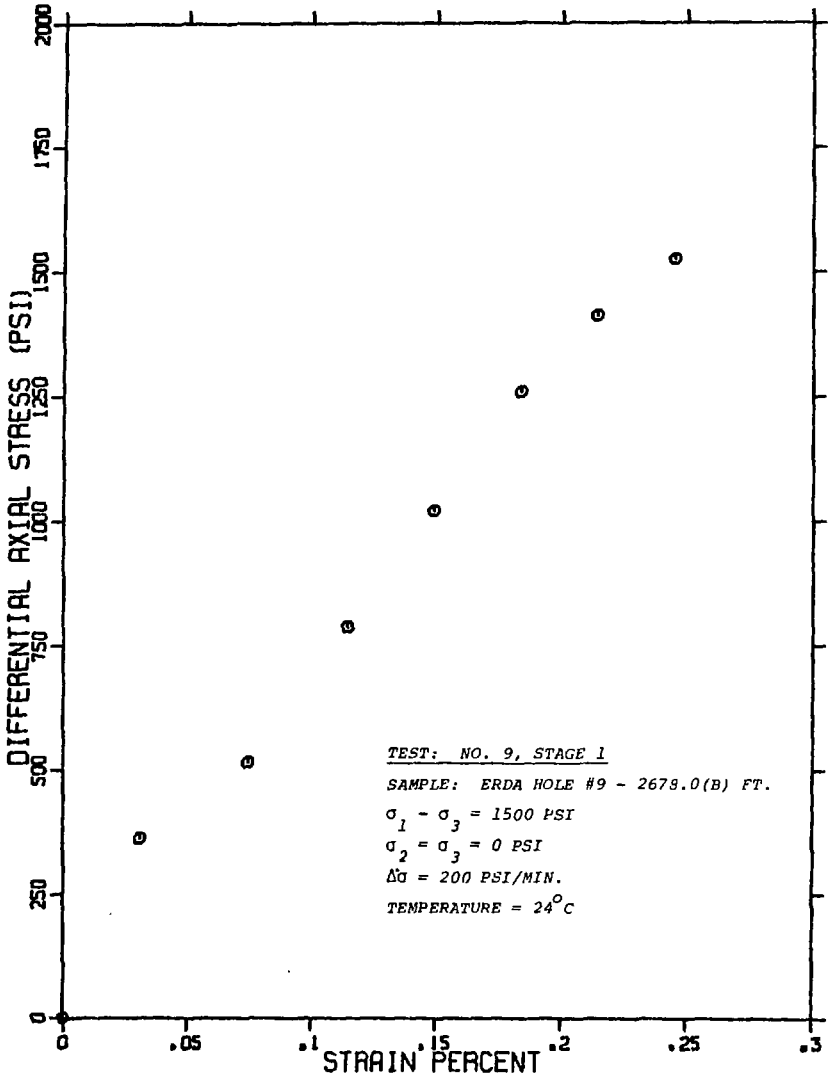

Figure A-9. Differential Axial Stress as a Function of Axial Strain, Test 9, Stage 1.

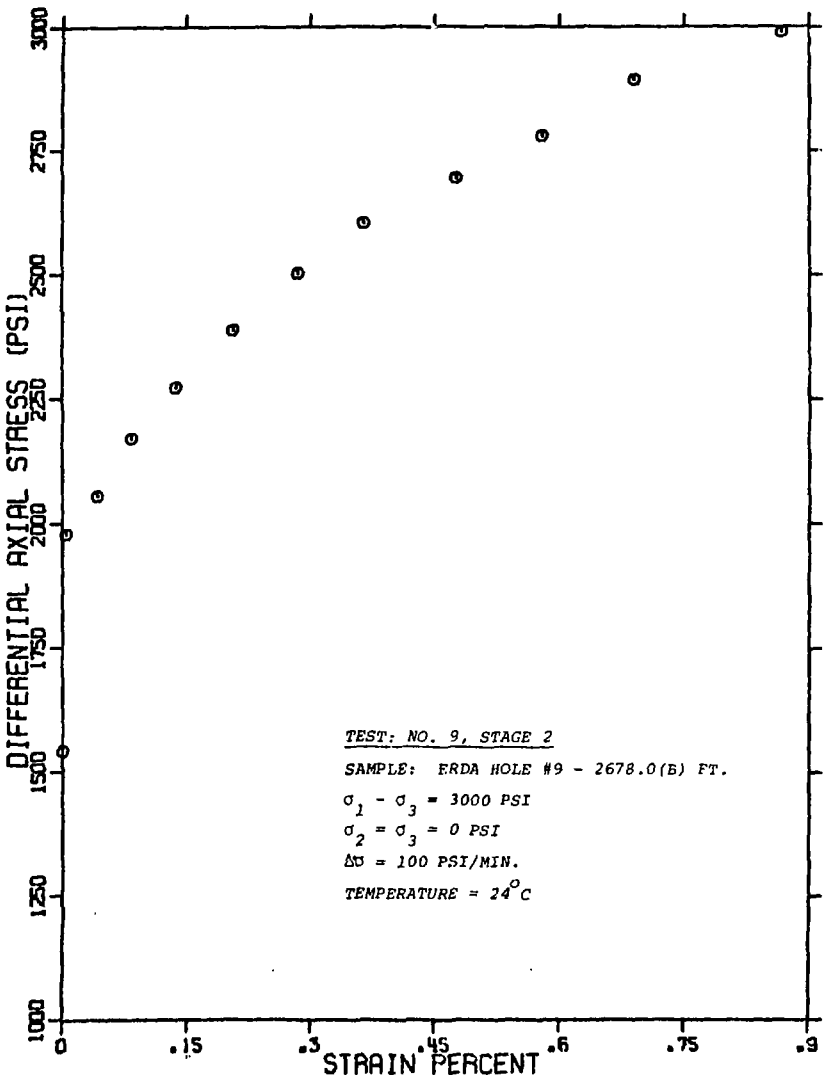

Figure A-10. Differential Axial Stress as a Function of Axial Strain, Test 9, Stage 2.

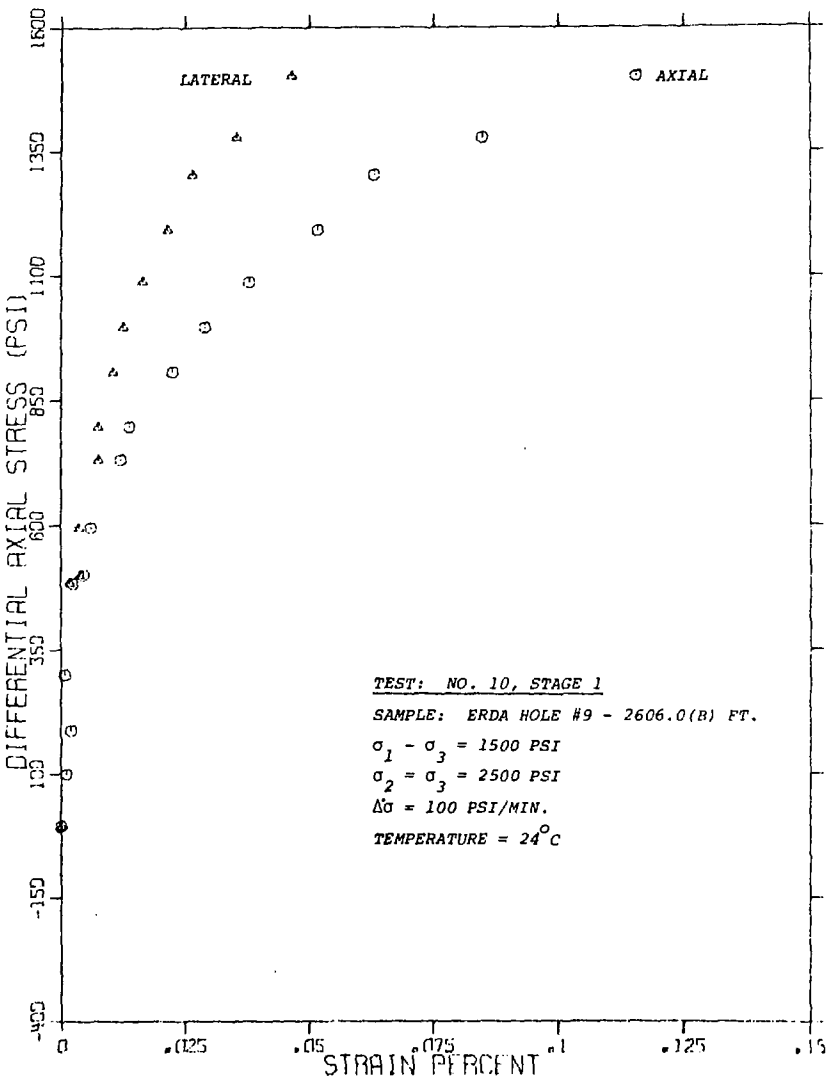

Figure A-11. Differential Axial Stress as a Function of Axial and Lateral Strain, Test 10, Stage 1.

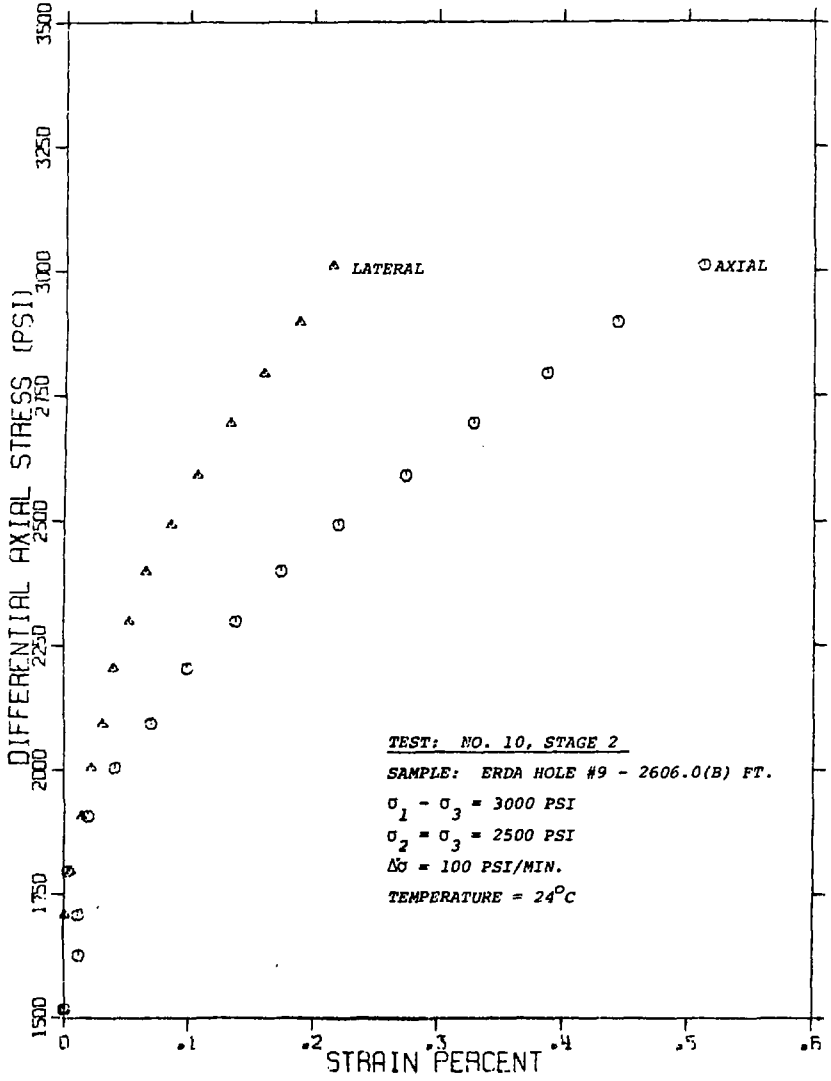

Figure A-12. Differential Axial Stress as a Function of Axial and Lateral Strain, Test 10, Stage 2.

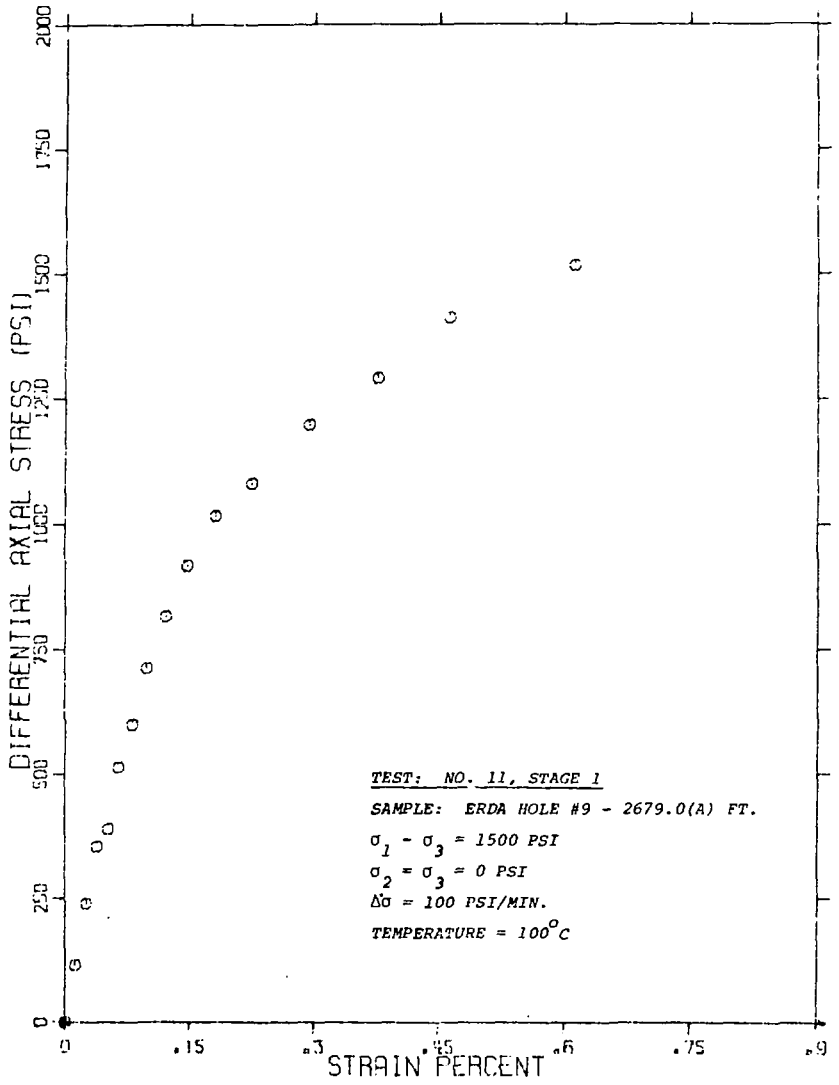

Figure A-13. Differential Axial Stress as a Function of Axial Strain, Test 11, Stage 1.

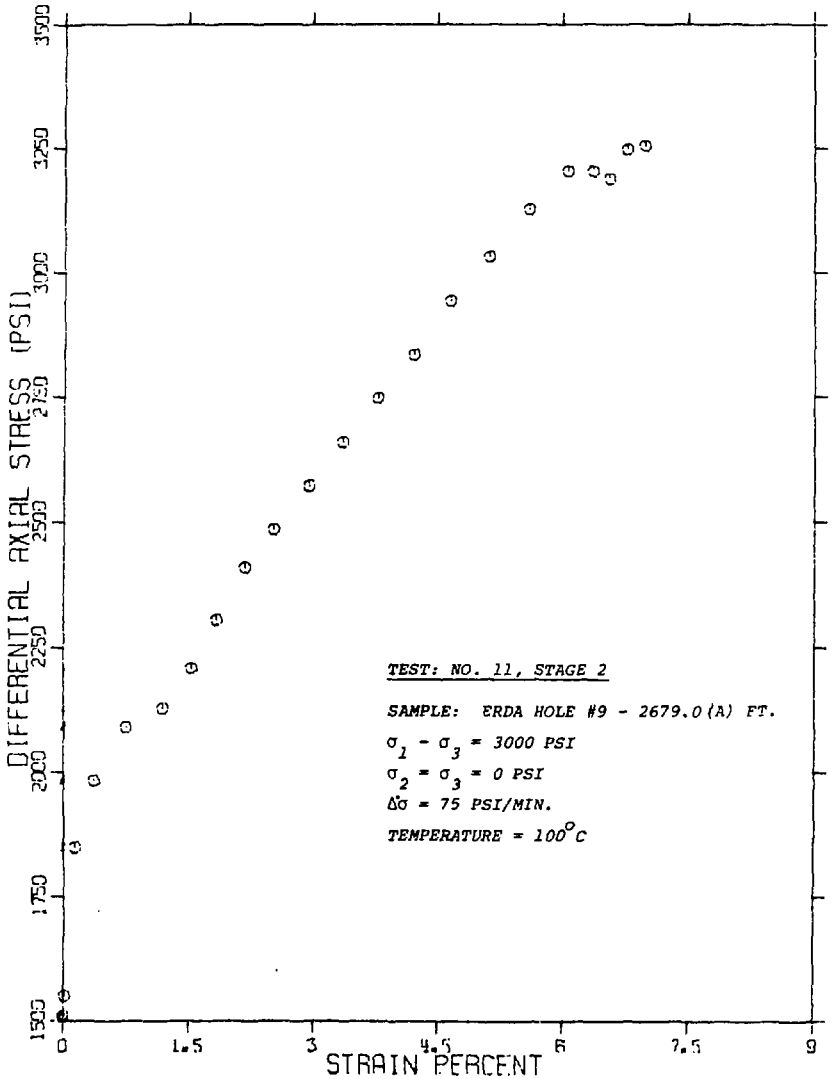

Figure A-14. Differential Axial Stress as a Function of Axial Strain, Test 11, Stage 2.

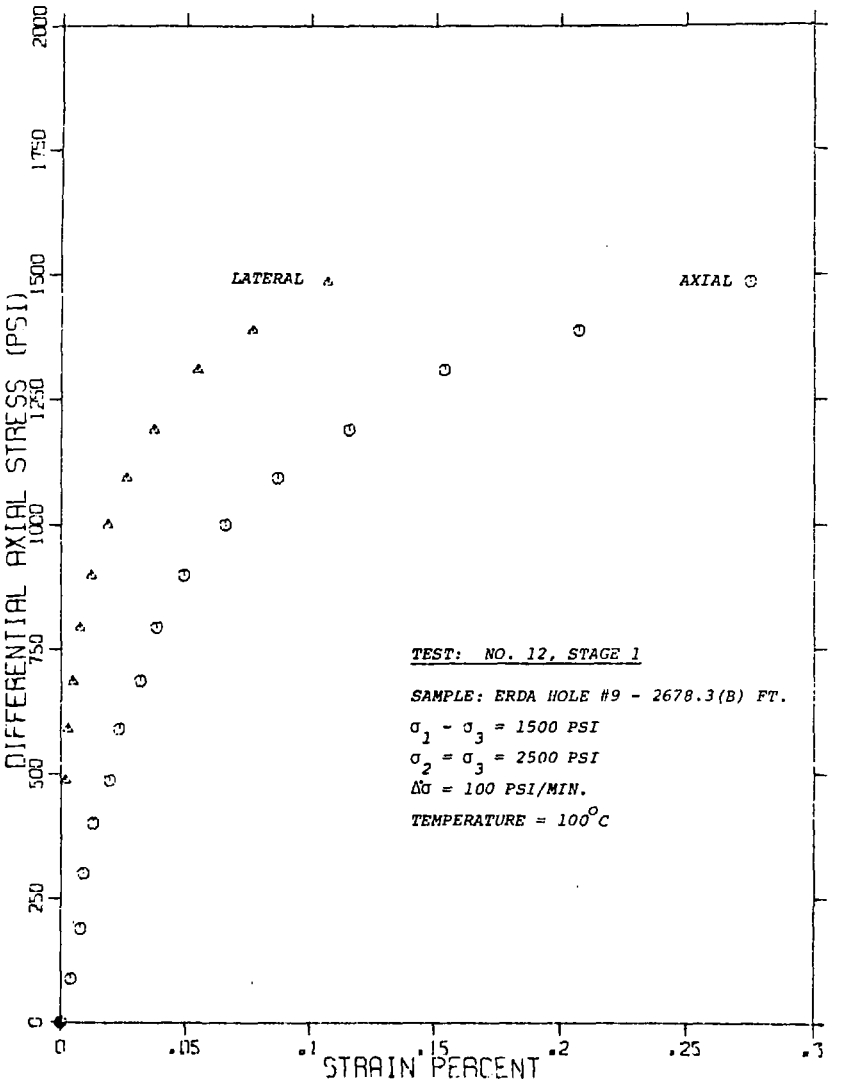

Figure A-15. Differential Axial Stress as a Function of Axial and Lateral Strain, Test 12, Stage 1.

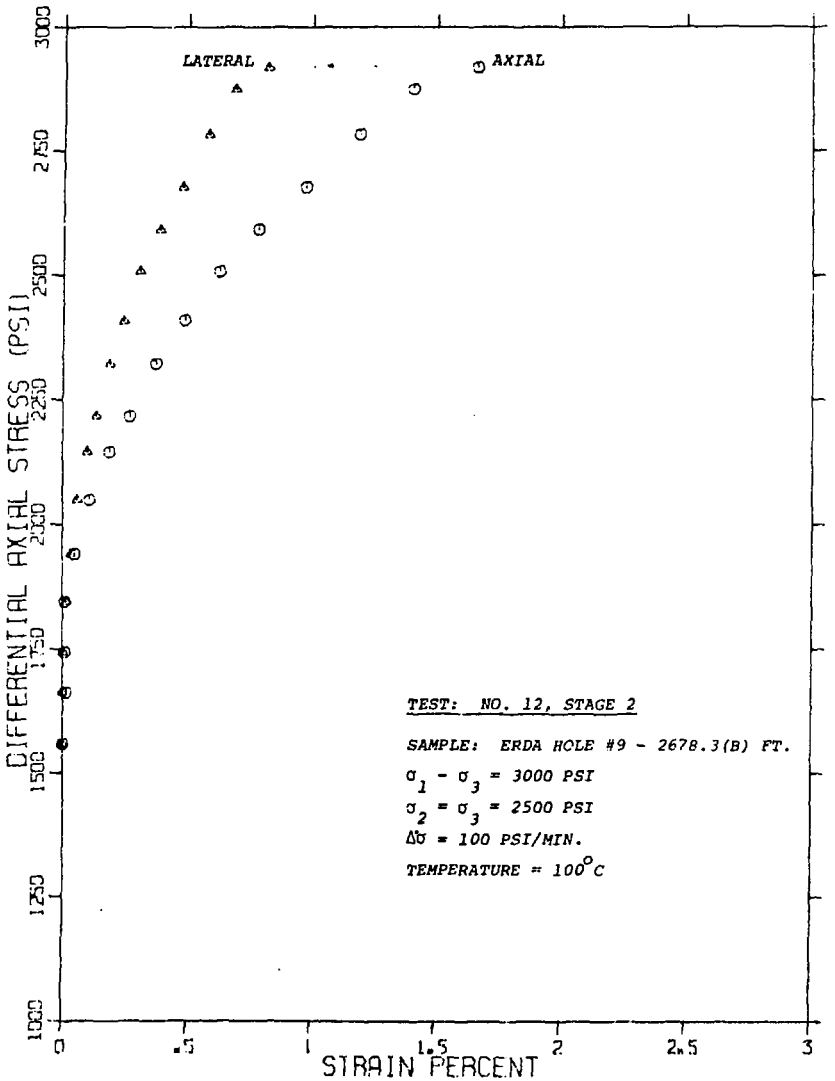

Figure A-16. Differential Axial Stress as a Function of Axial and Lateral Strain, Test 12, Stage 2.

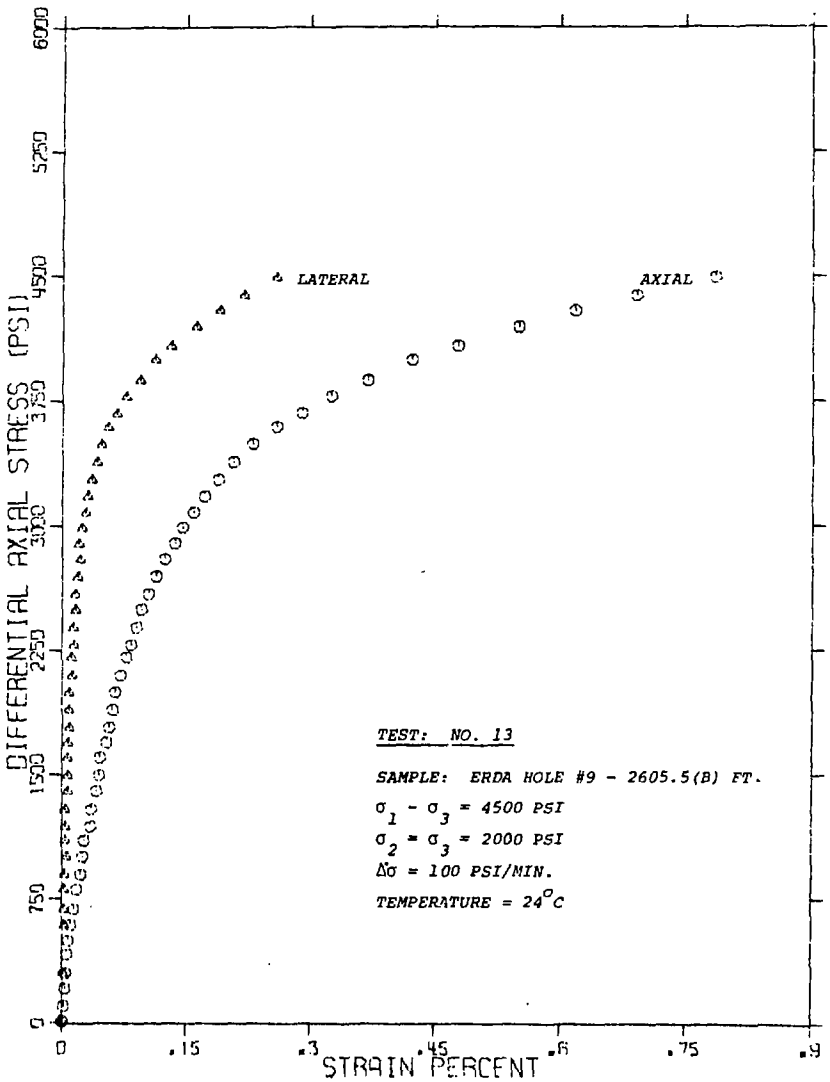

Figure A-17. Differential Axial Stress as a Function of Axial and Lateral Strain, Test 13.

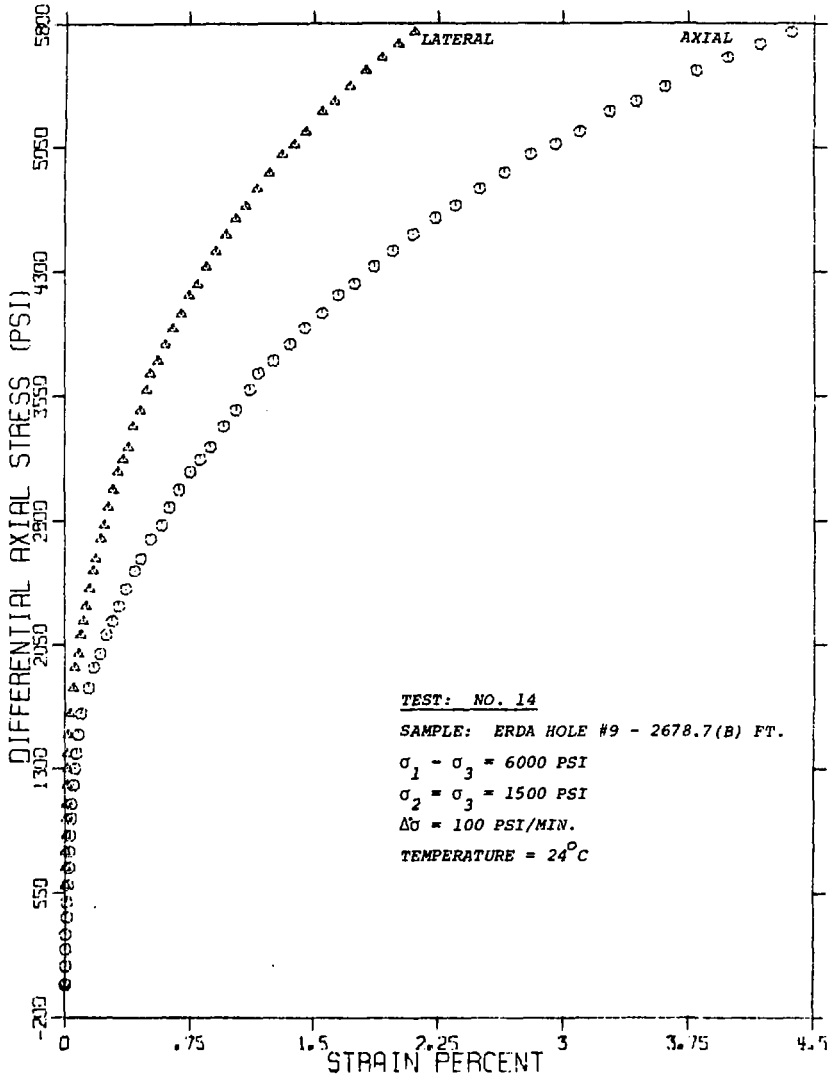

Figure A-18. Differential Axial Stress as a Function of Axial and Lateral Strain, Test 14.

APPENDIX B

PLOTS OF AXIAL STRAIN AS A FUNCTION OF TIME

APPENDIX B (CONT'D)

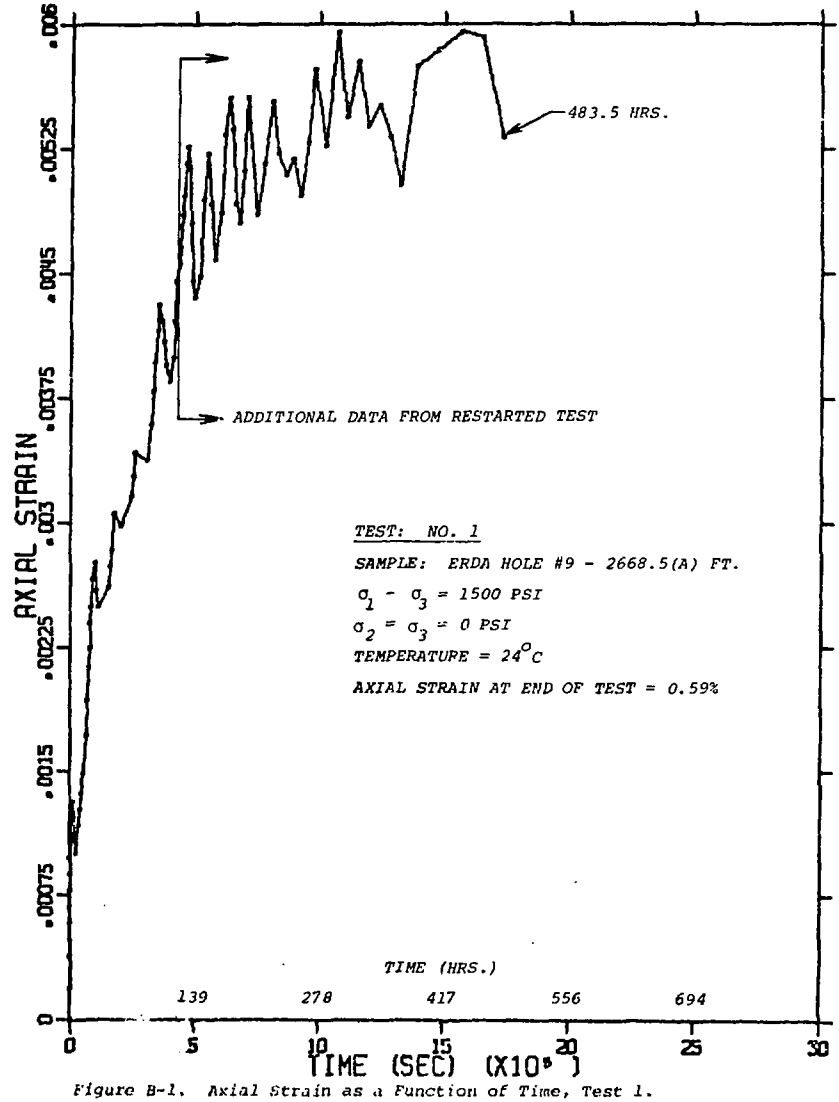

Figure B-1. Axial Strain as a Function of Time, Test 1.

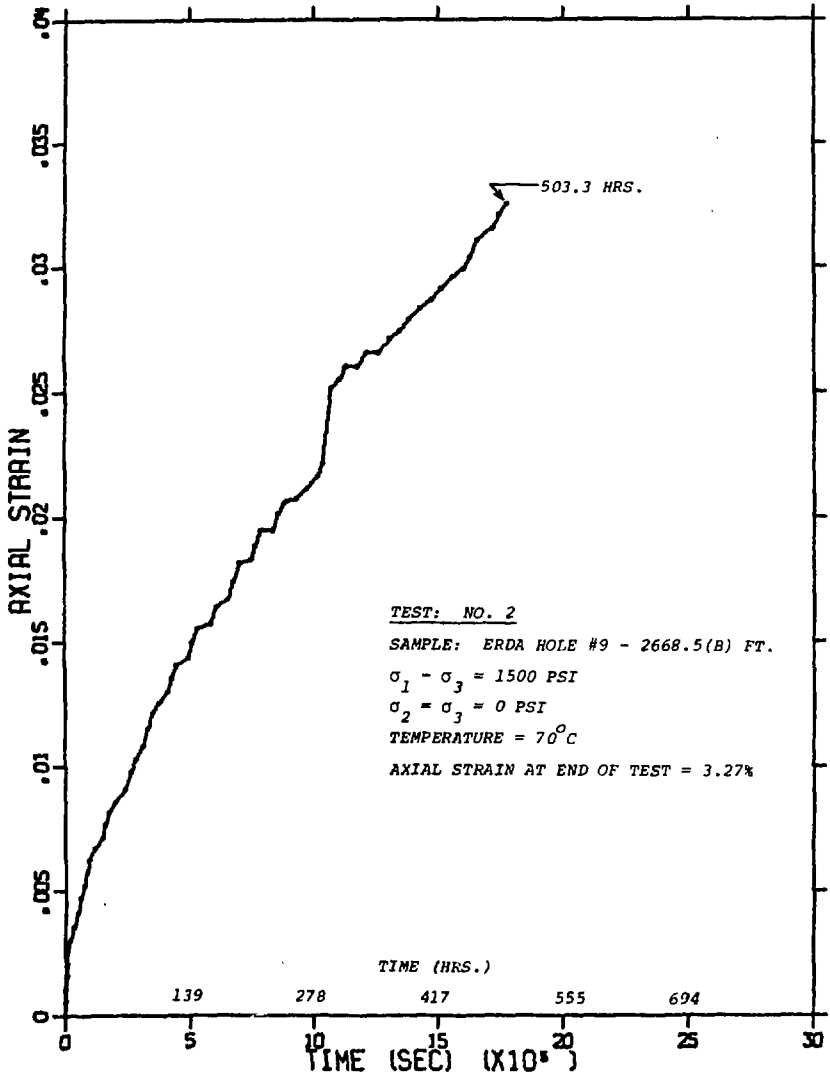

Figure B-2. Axial Strain as a Function of Time, Test 2.

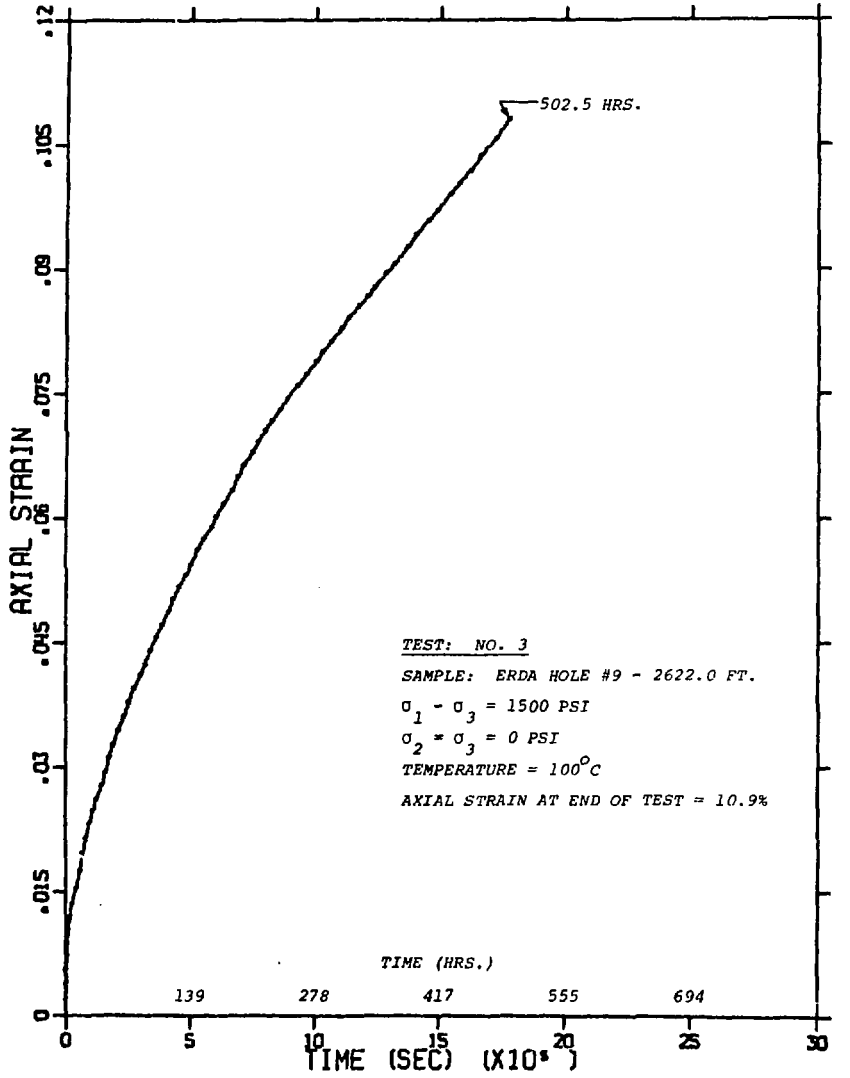

Figure B-3. Axial Strain as a Function of Time, Test 3.

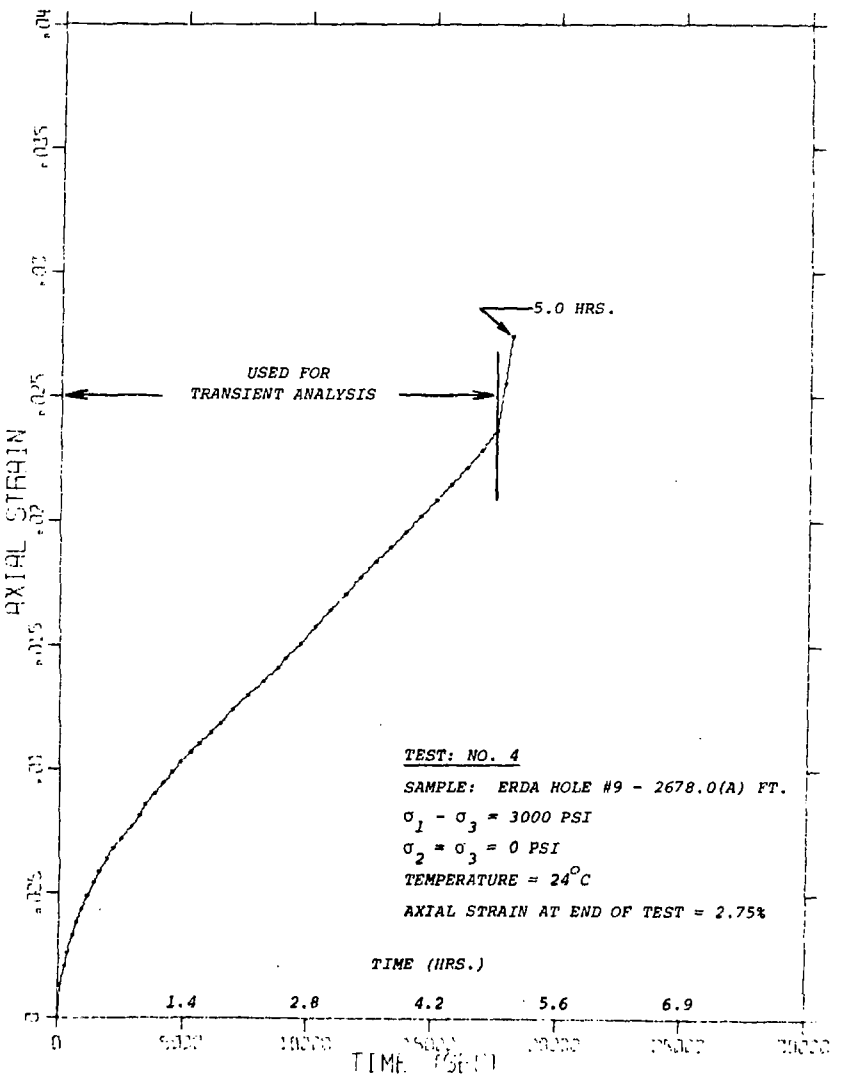

Figure B-4. Axial Strain as a Function of Time, Test 4.

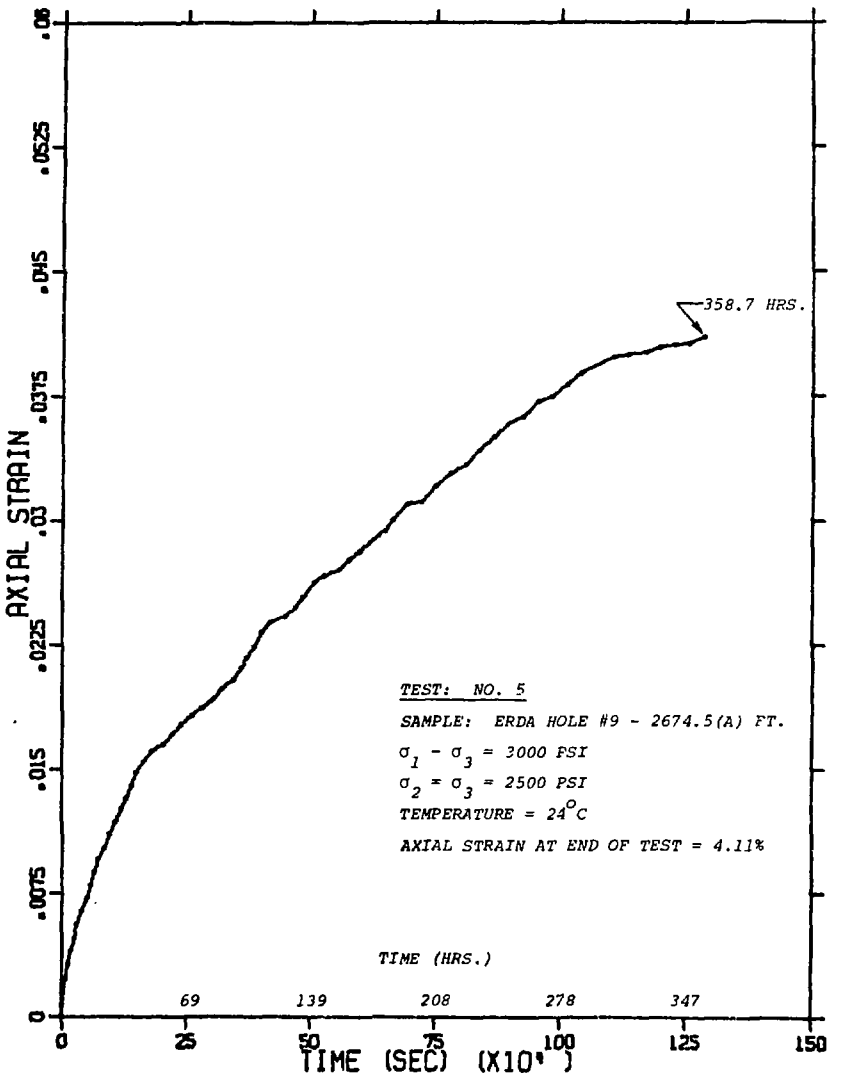

Figure B-5. Axial Strain as a Function of Time, Test 5.

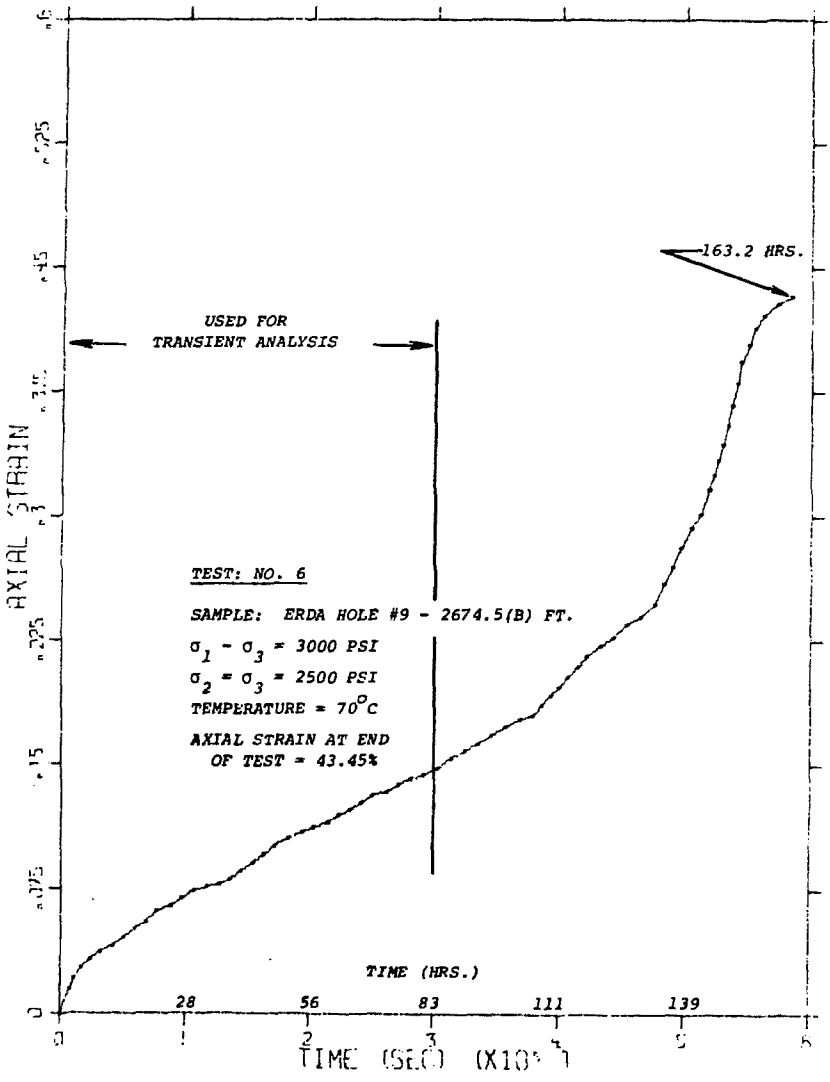

Figure B-6. Axial Strain as a Function of Time, Test 6.

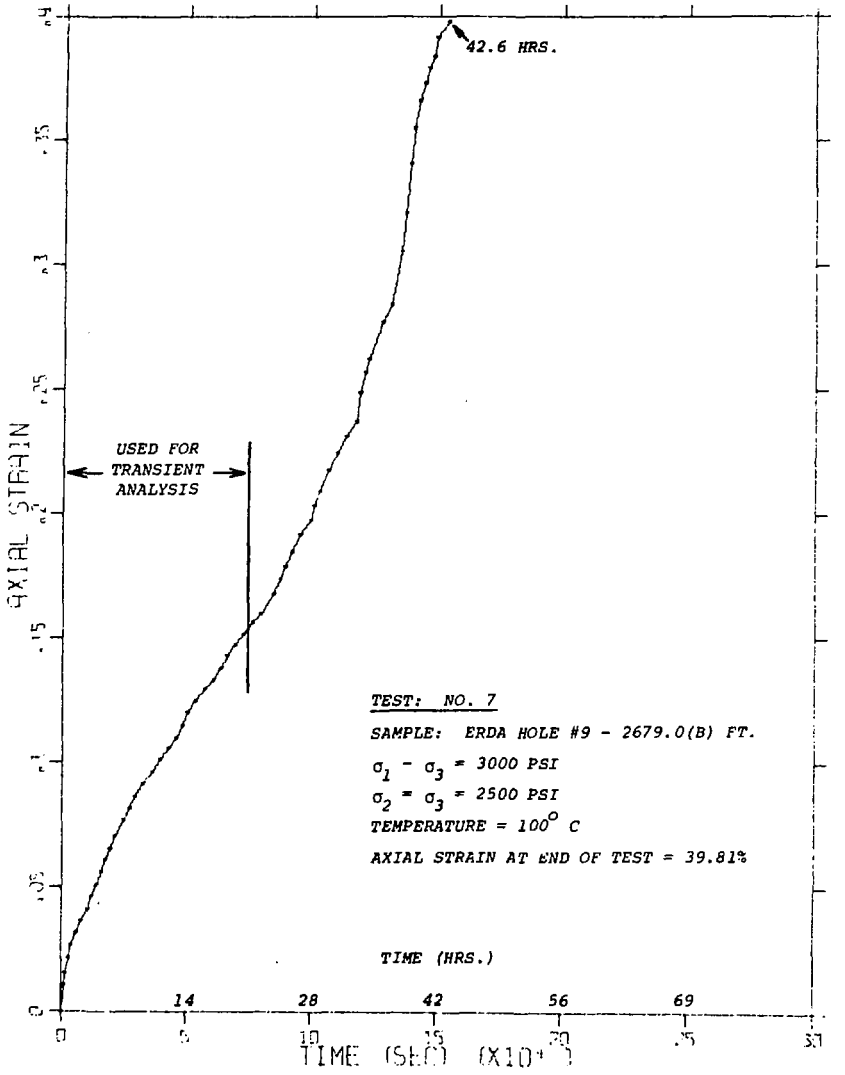

Figure B-7. Axial Strain as a Function of Time, Test 7.

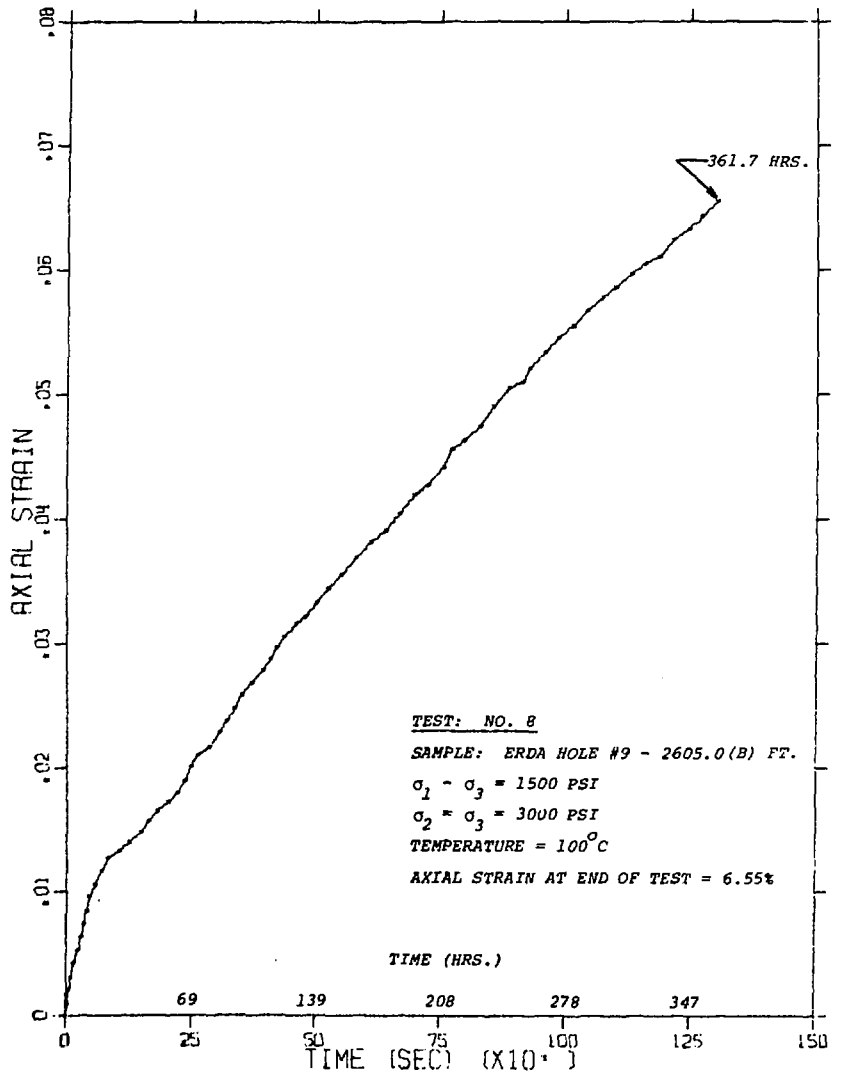

Figure B-8. Axial Strain as a Function of Time, Test 8.

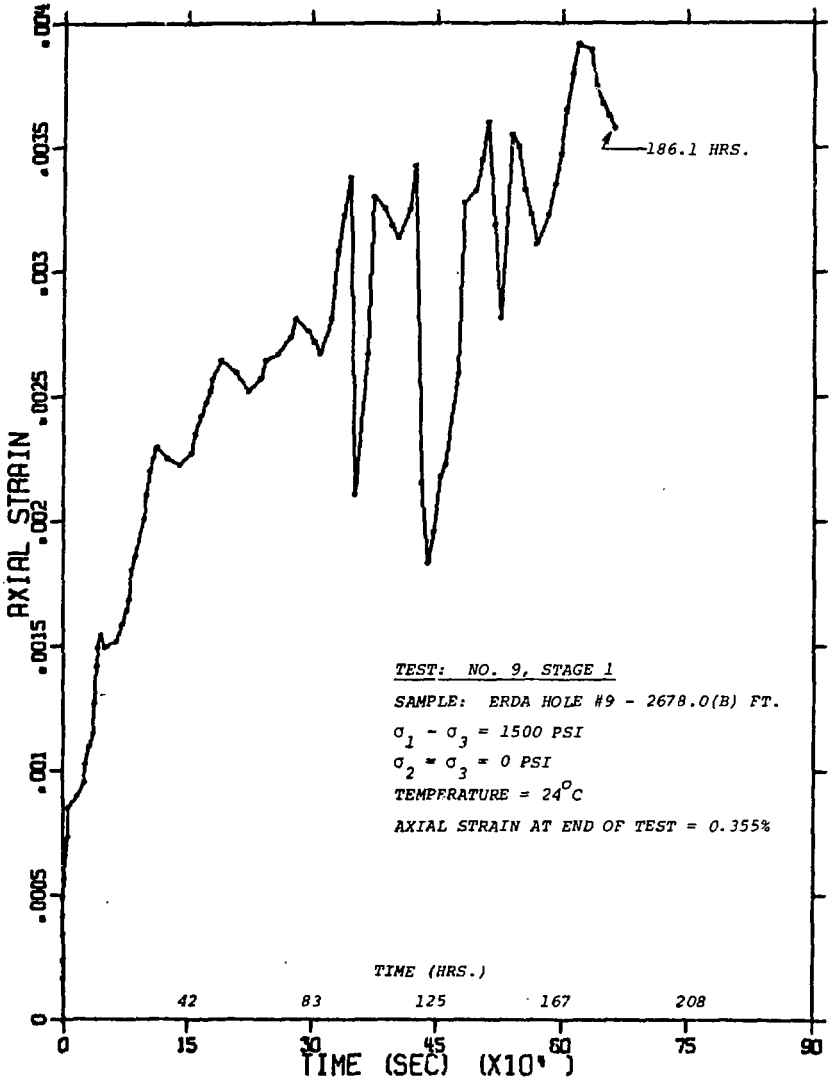

Figure B-9. Axial Strain as a Function of Time, Test 9, Stage 1.

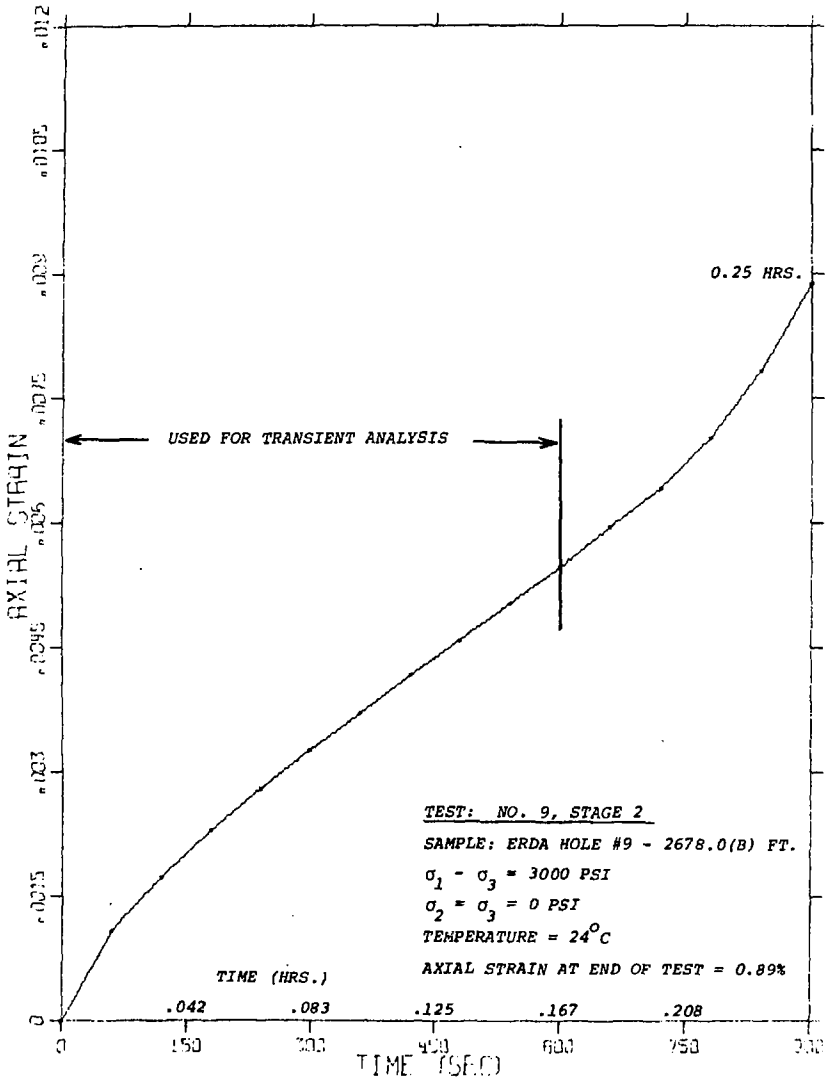

Figure B-10. Axial Strain as a Function of Time, Test 9, Stage 2.

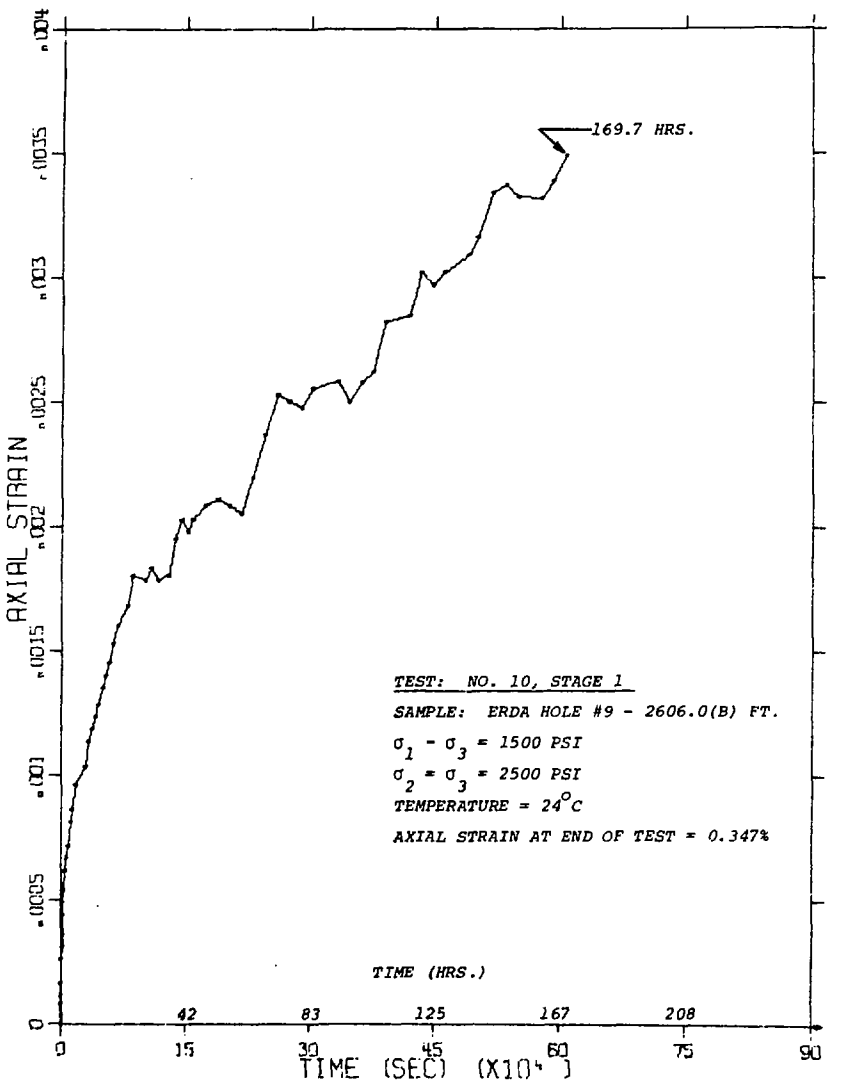

Figure B-11. Axial Strain as a Function of Time, Test 10, Stage 1.

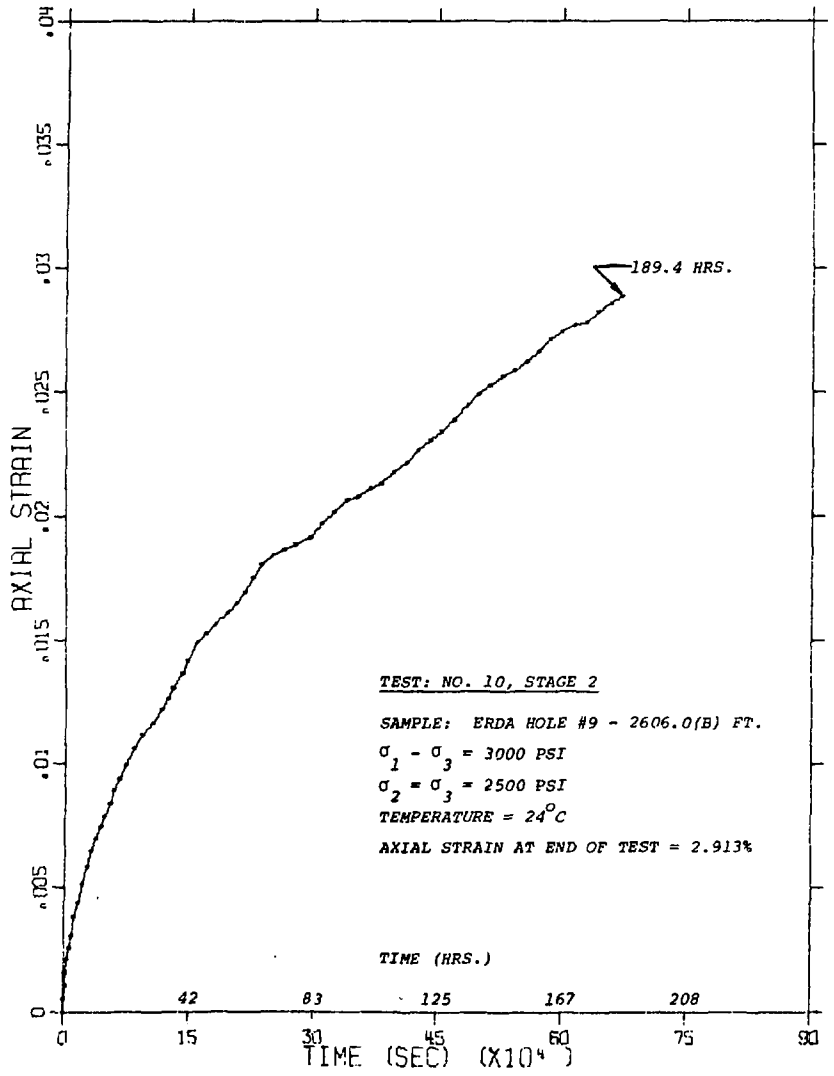

Figure B-12. Axial Strain as a Function of Time, Test 10, Stage 2.

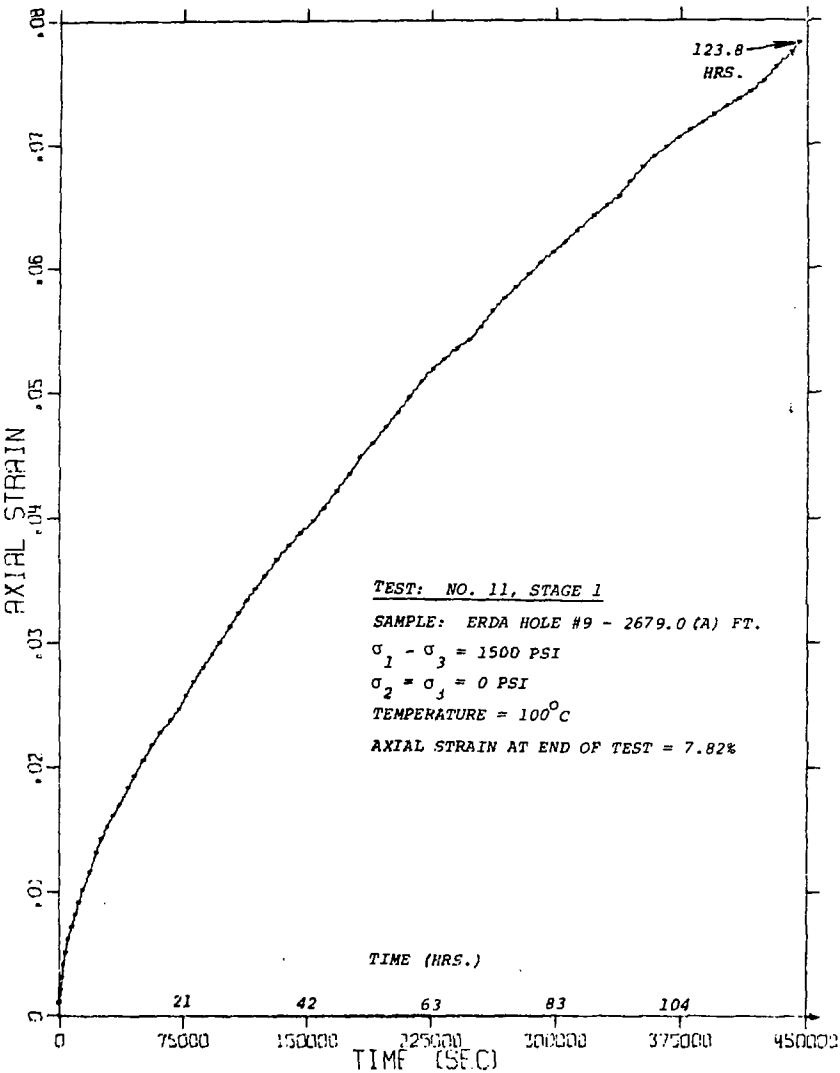

Figure B-13. Axial Strain as a Function of Time, Test 11, Stage 1.

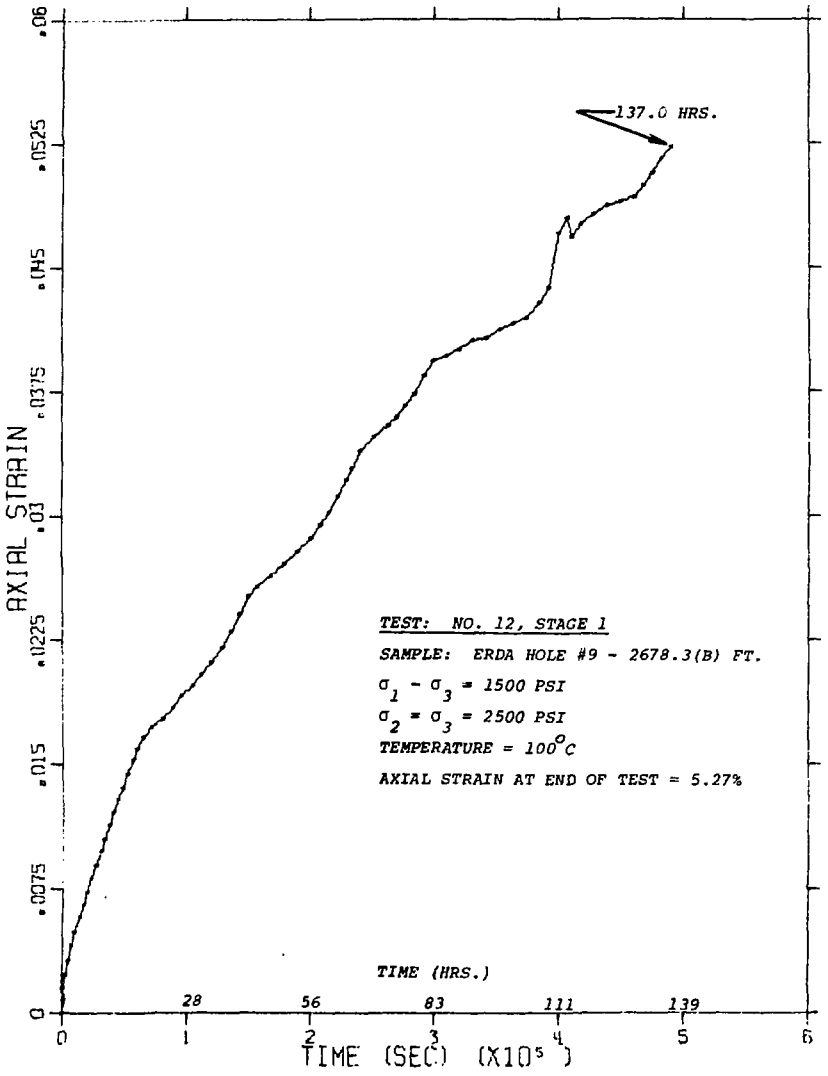

Figure B-14. Axial Strain as a Function of Time, Test 12, Stage 1.

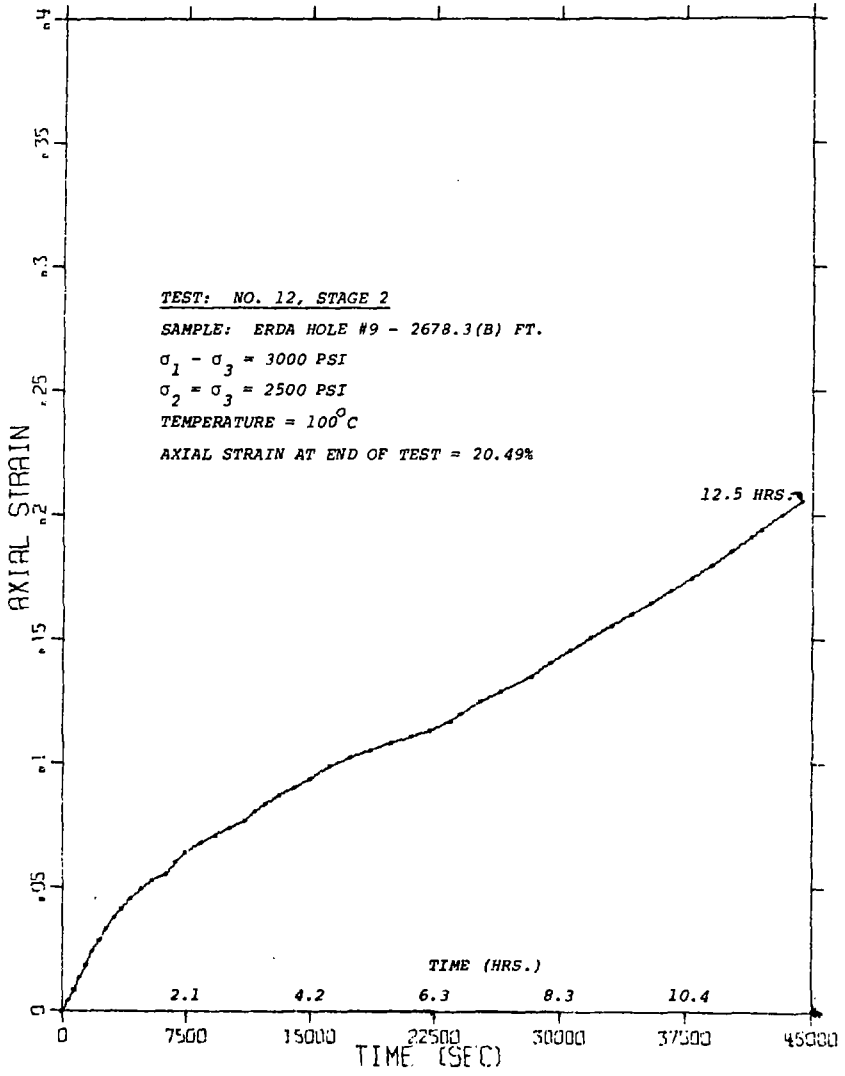

Figure B-15. Axial Strain as a Function of Time, Test 12, Stage 2.

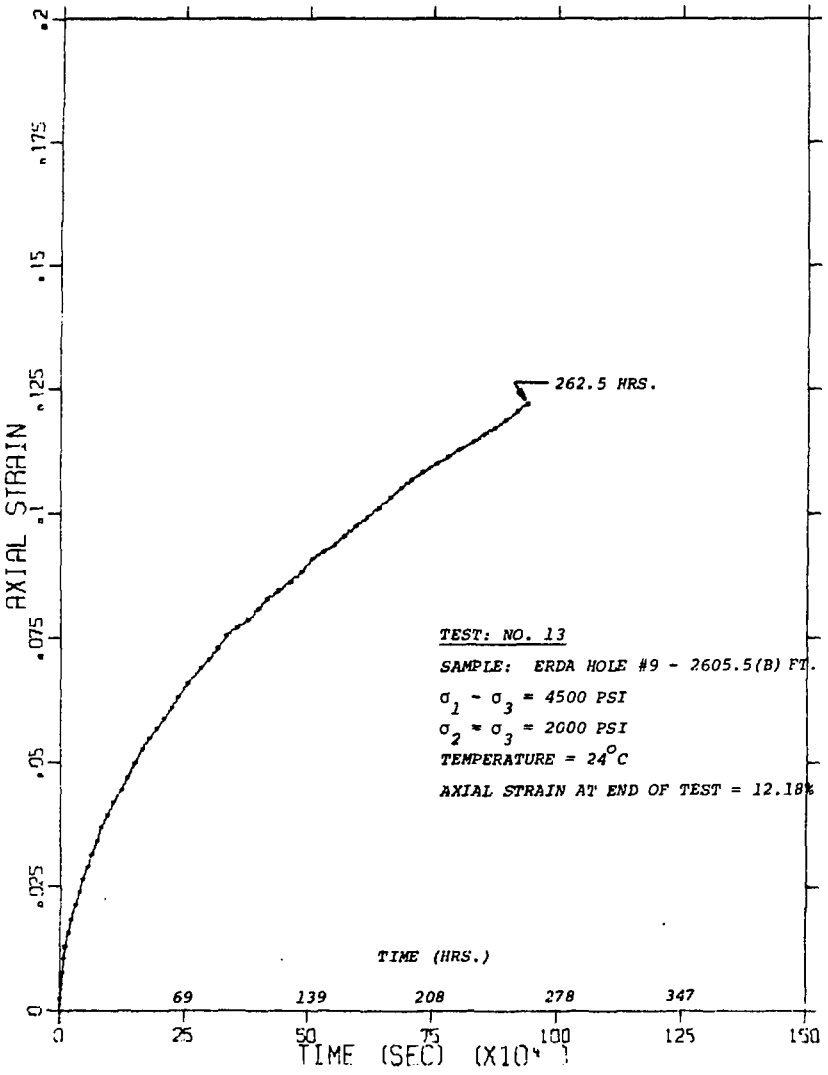

Figure B-16. Axial Strain as a Function of Time, Test 13.

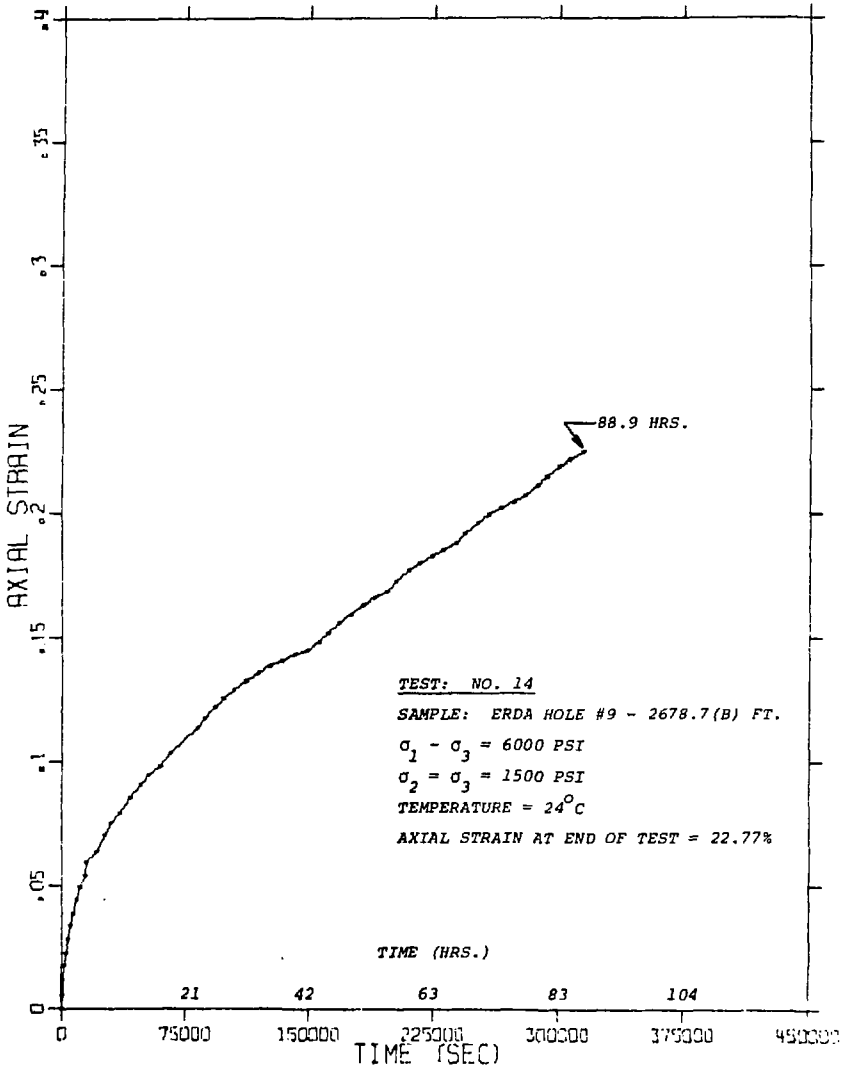

Figure B-17. Axial Strain as a Function of Time, Test 14.

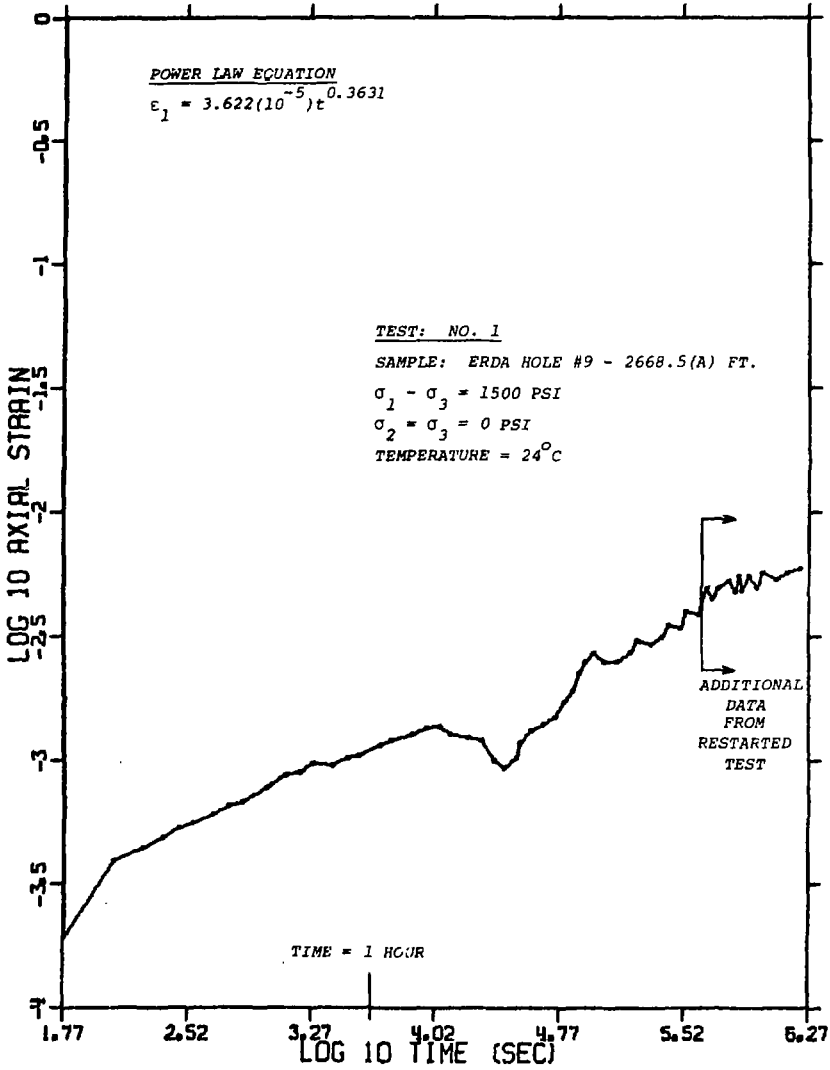

Figure B-18. Log_{10} Axial Strain as a Function of Log_{10} Time (Sec.), Test 1.

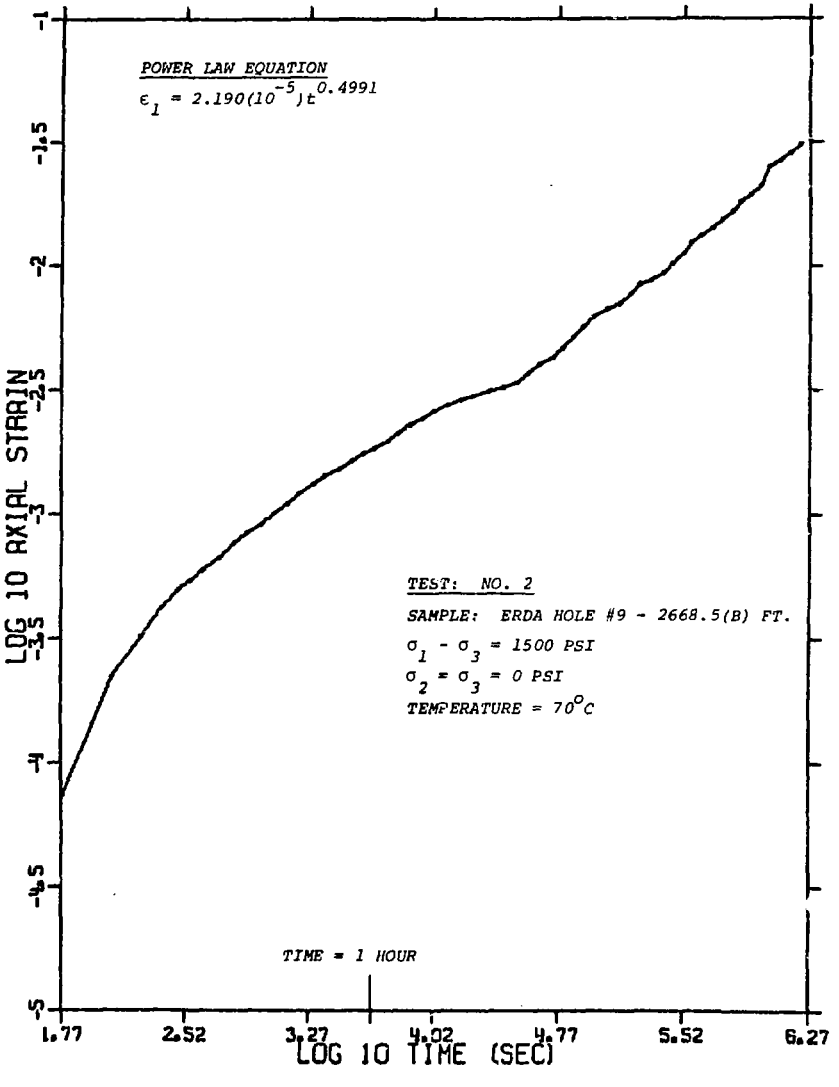

Figure B-19. Log_{10} Axial Strain as a Function of Log_{10} Time (Sec.), Test 2.

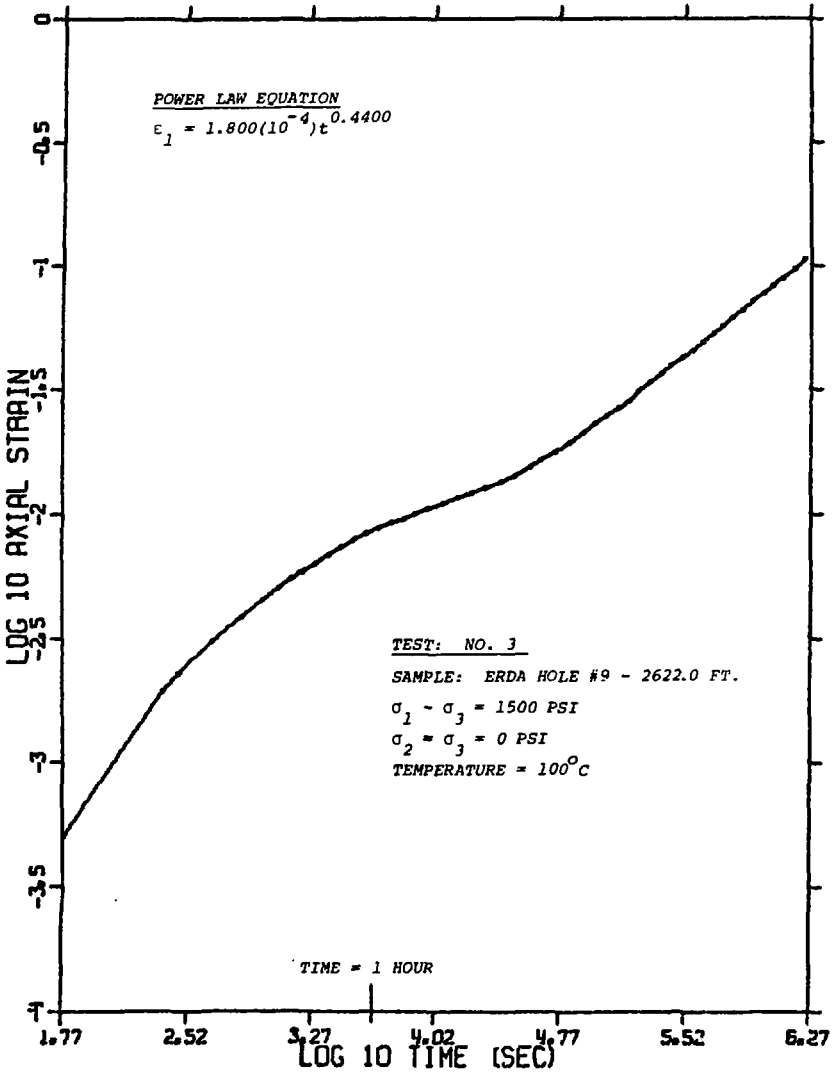

Figure B-20. Log_{10} Axial Strain as a Function of Log_{10} Time (Sec.), Test 3.

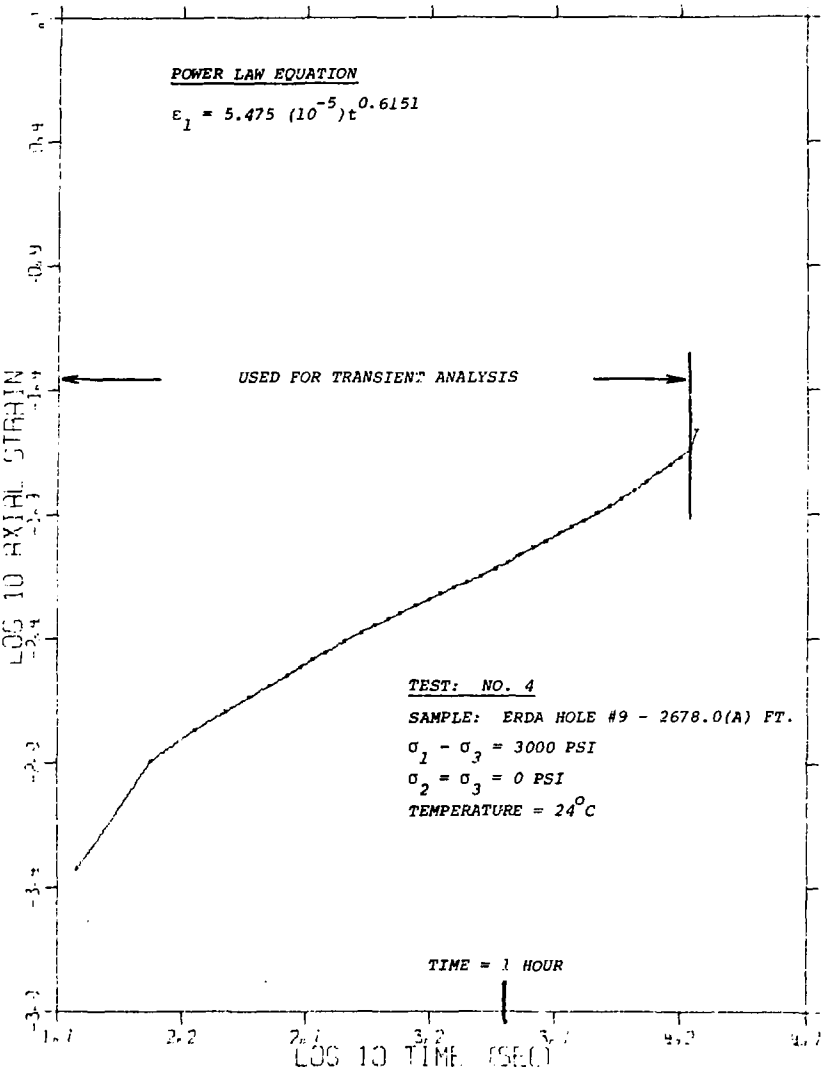

Figure B-21. Log_{10} Axial Strain as a Function of Log_{10} Time (Sec)., Test 4.

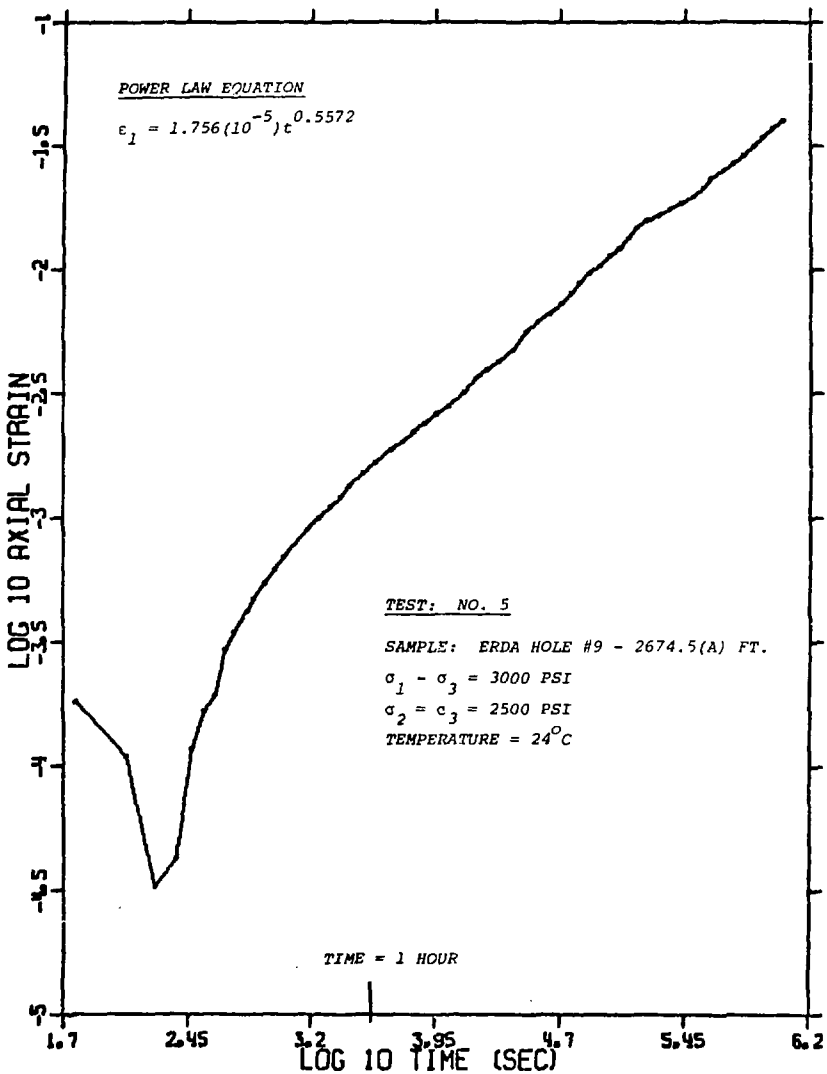

Figure B-22. Log_{10} Axial Strain as a Function of Log_{10} Time (Sec.), Test 5.

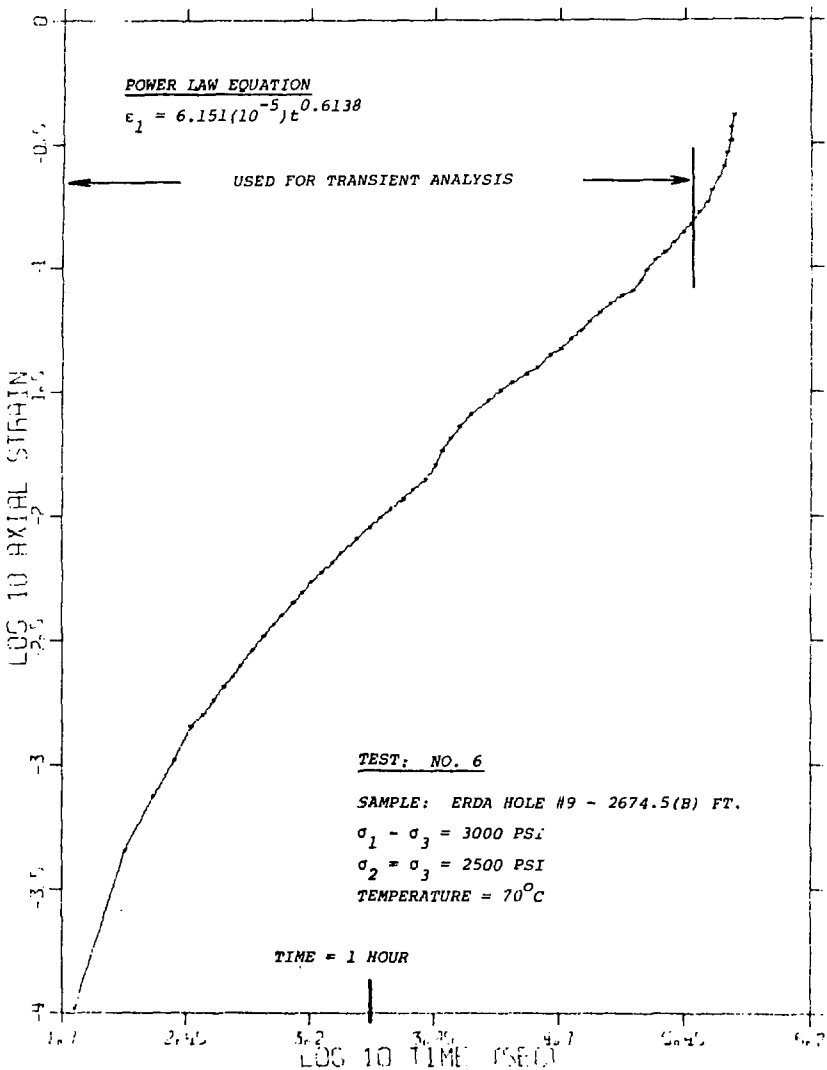

Figure B-23. Log_{10} Axial Strain as a Function of Log_{10} Time (Sec.), Test

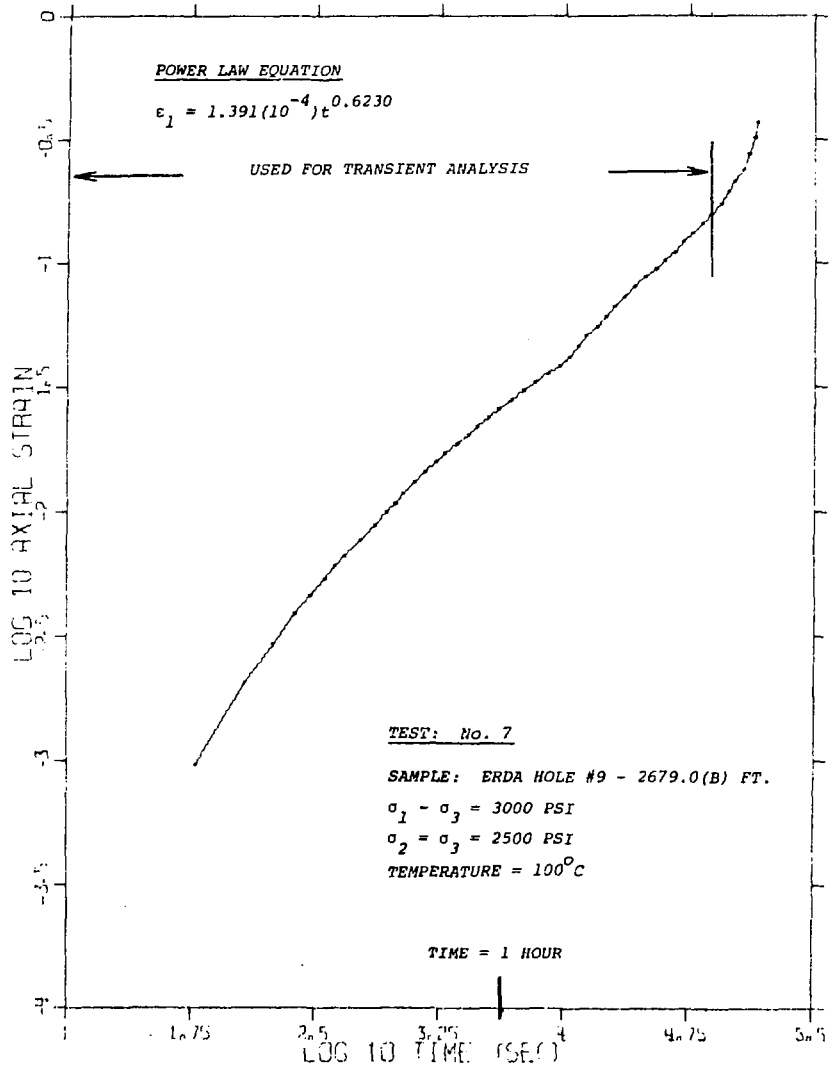

Figure B-24. Log_{10} Axial Strain as a Function of Log_{10} Time (Sec.), Test 7

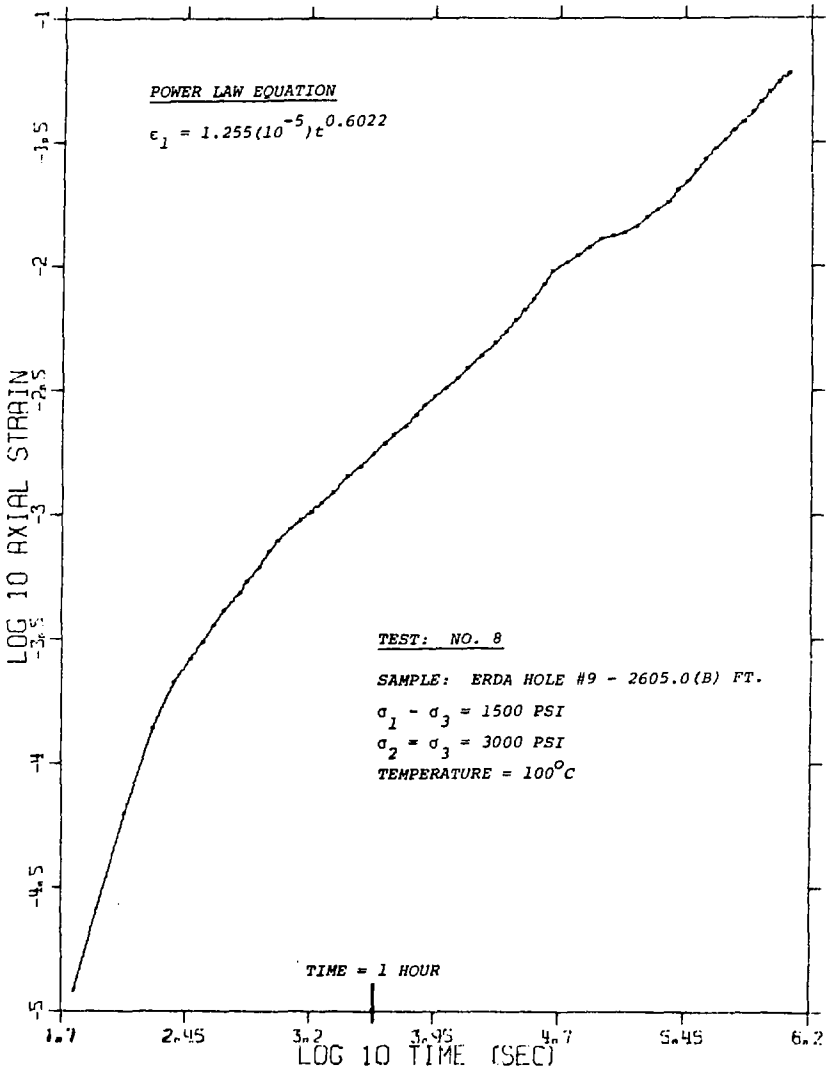

Figure B-25. Log_{10} Axial Strain as a Function of Log_{10} Time (Sec.), Test 8.

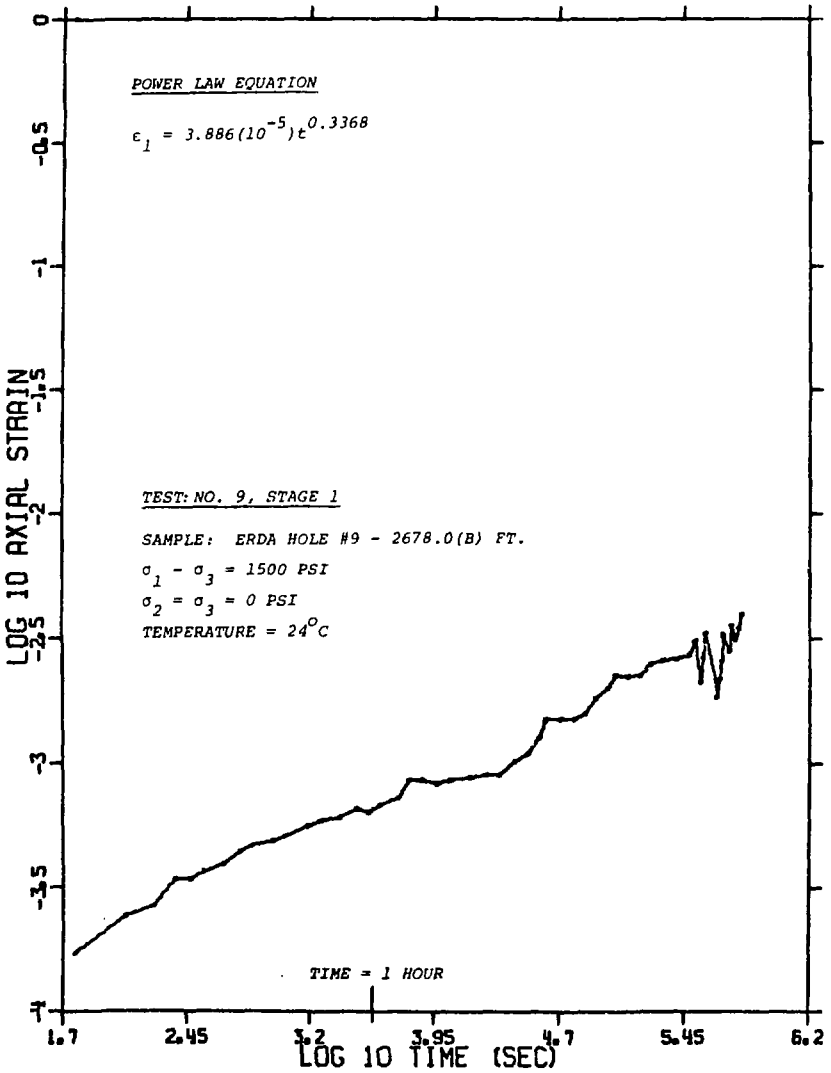

Figure B-26. Log_{10} Axial Strain as a Function of Log_{10} Time (Sec.), Test 9, Stage 1.

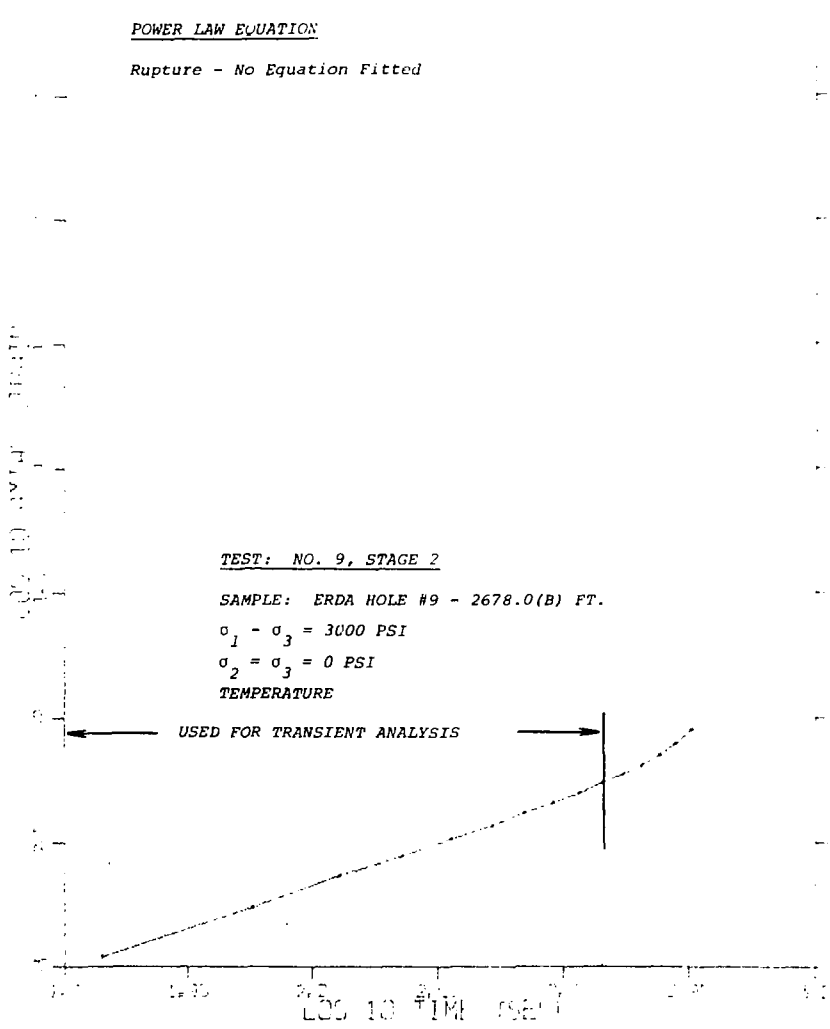

Figure B-27. Log_{10} Axial Strain as a Function of Log_{10} Time (Sec.), Test 9, Stage 2.

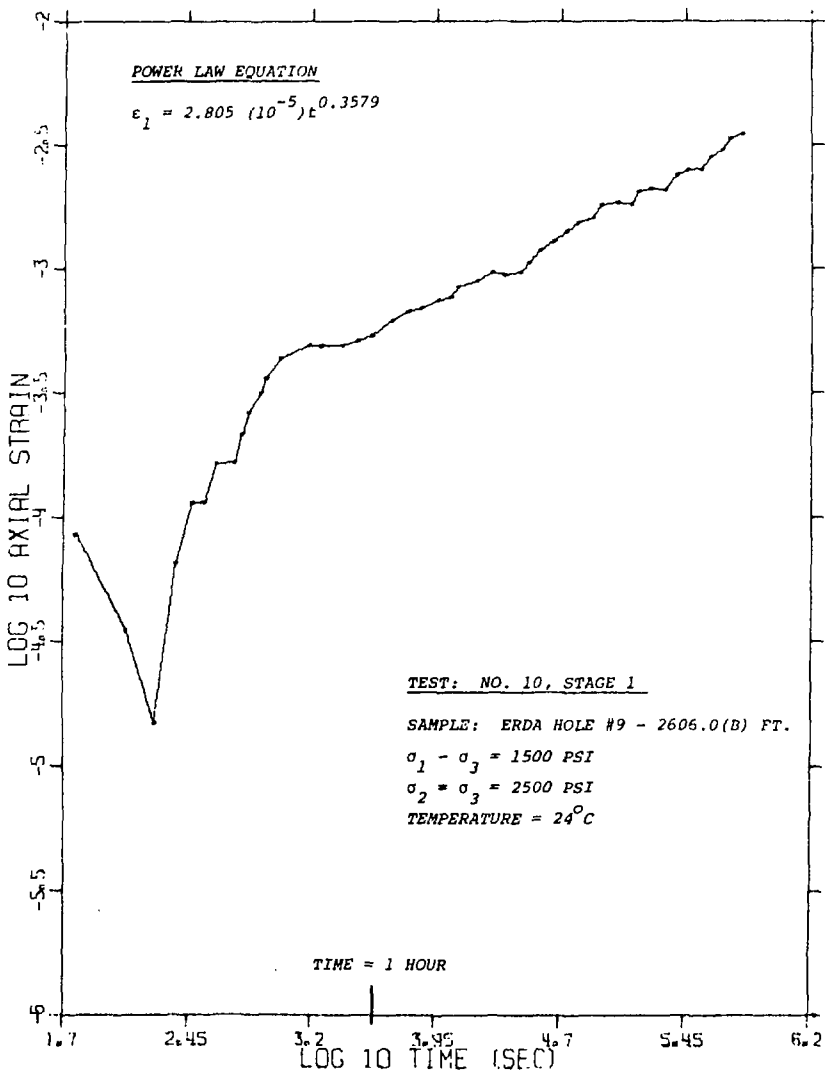

Figure B-28. Log_{10} Axial Strain as a Function of Log_{10} Time (Sec.), Test 10, Stage 1.

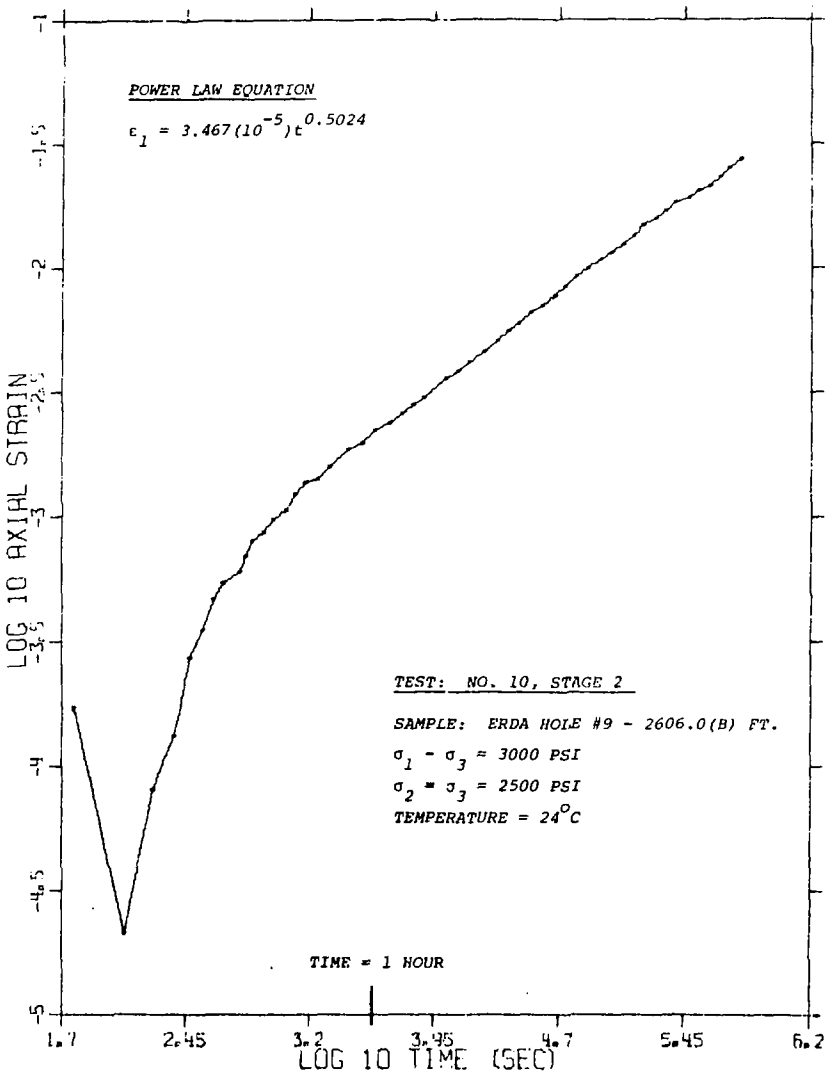

Figure B-29. Log_{10} Axial Strain as a Function of Log_{10} Time (Sec.), Test 10, Stage 2.

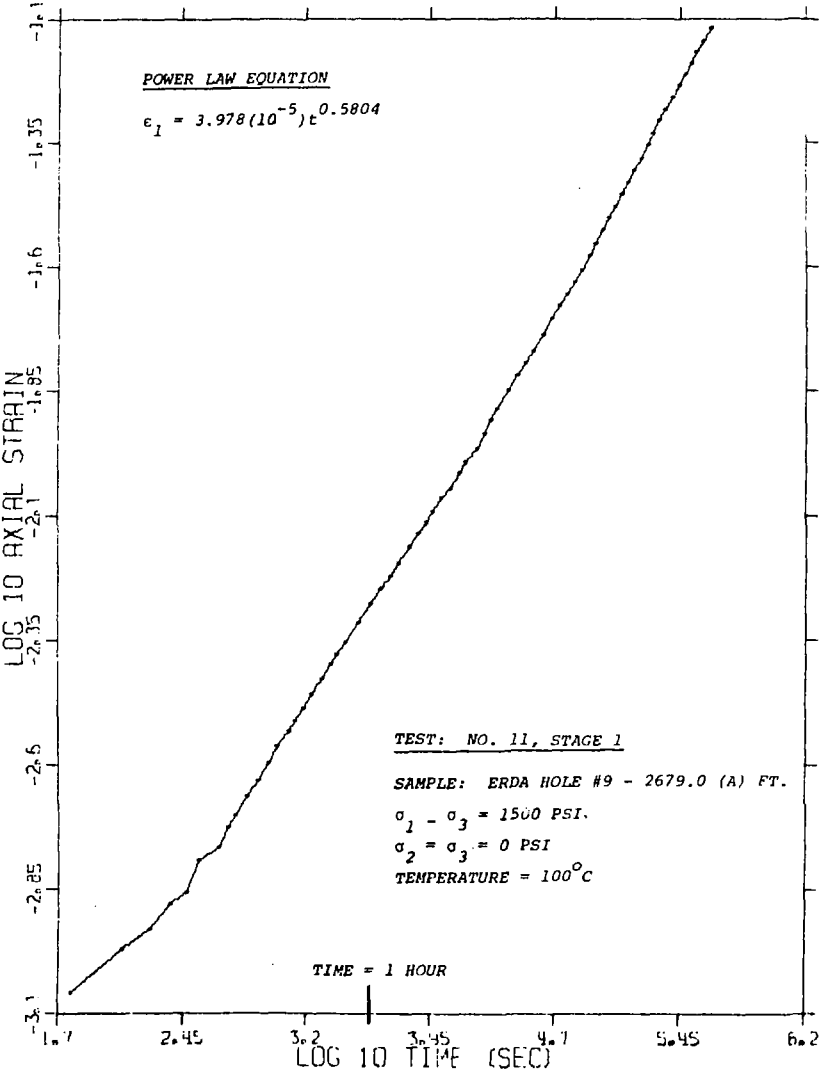

Figure B-30. Log_{10} Axial Strain as a Function of Log_{10} Time (Sec.), Test 11, Stage 1.

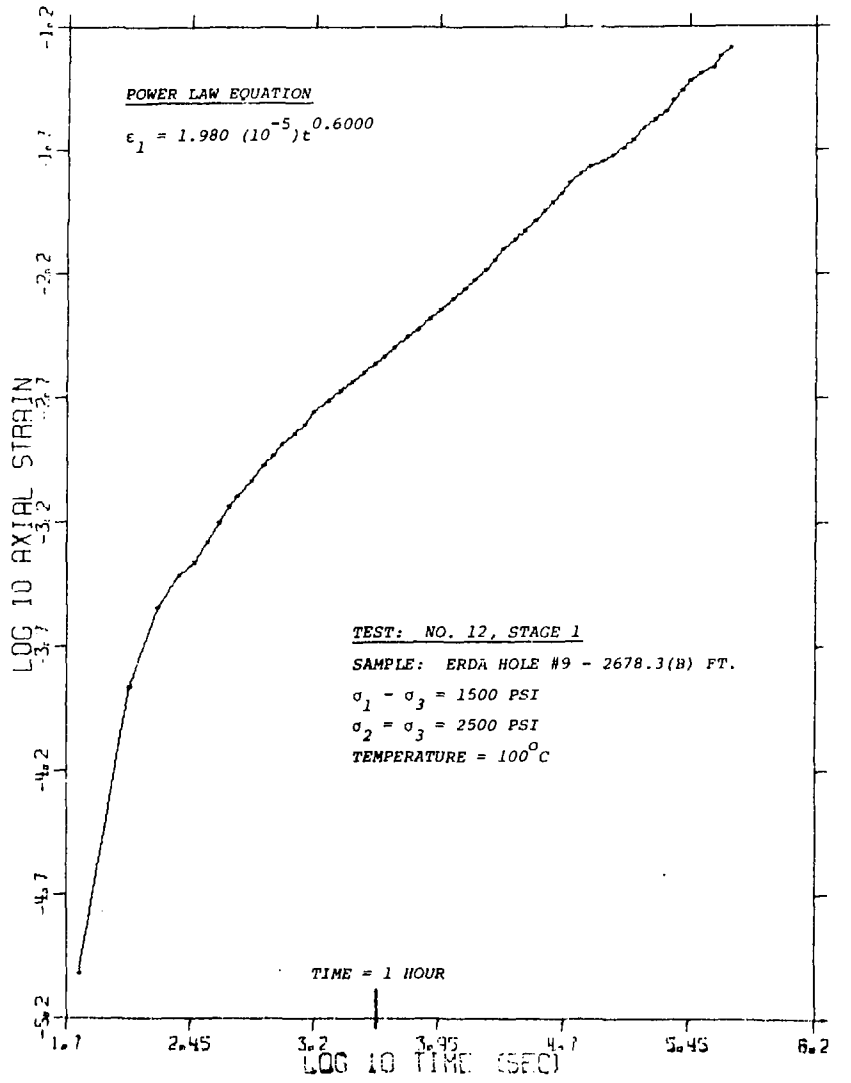

Figure B-31. Log_{10} Axial Strain as a Function of Log_{10} Time (sec), Test 12, Stage 1.

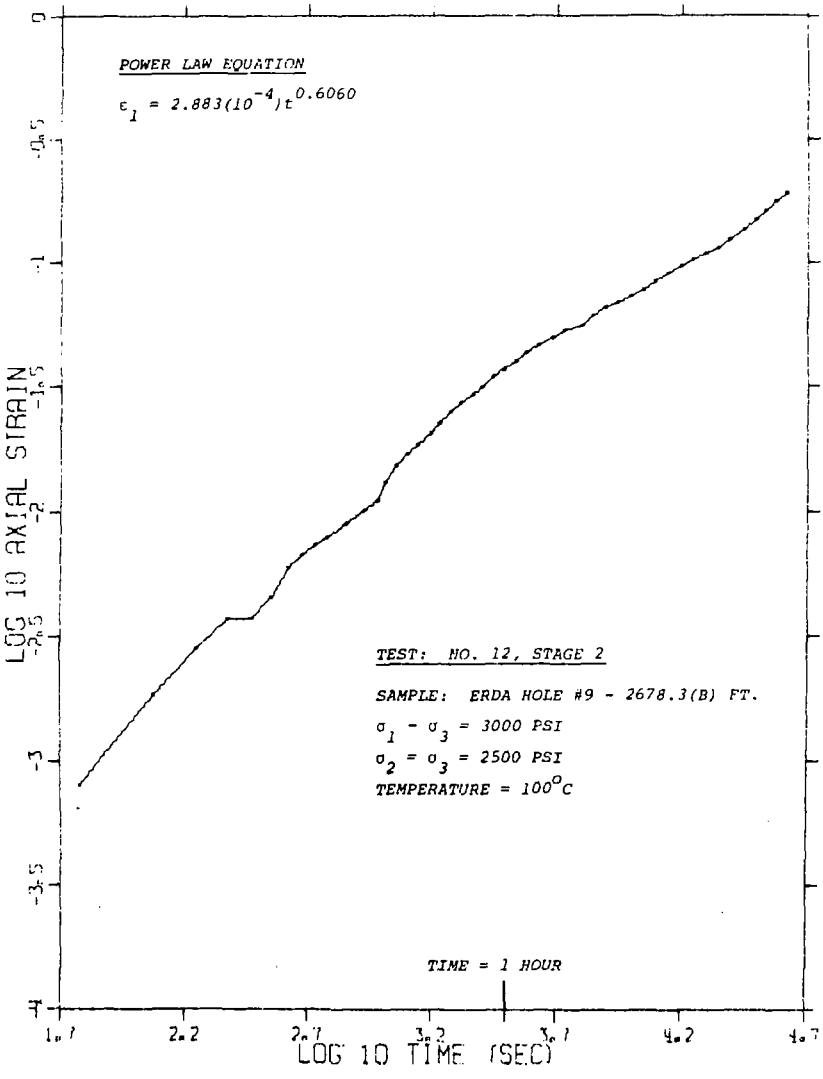

Figure B-32: Log_{10} Axial Strain as a Function of Log_{10} Time (Sec.), Test 12, Stage 2.

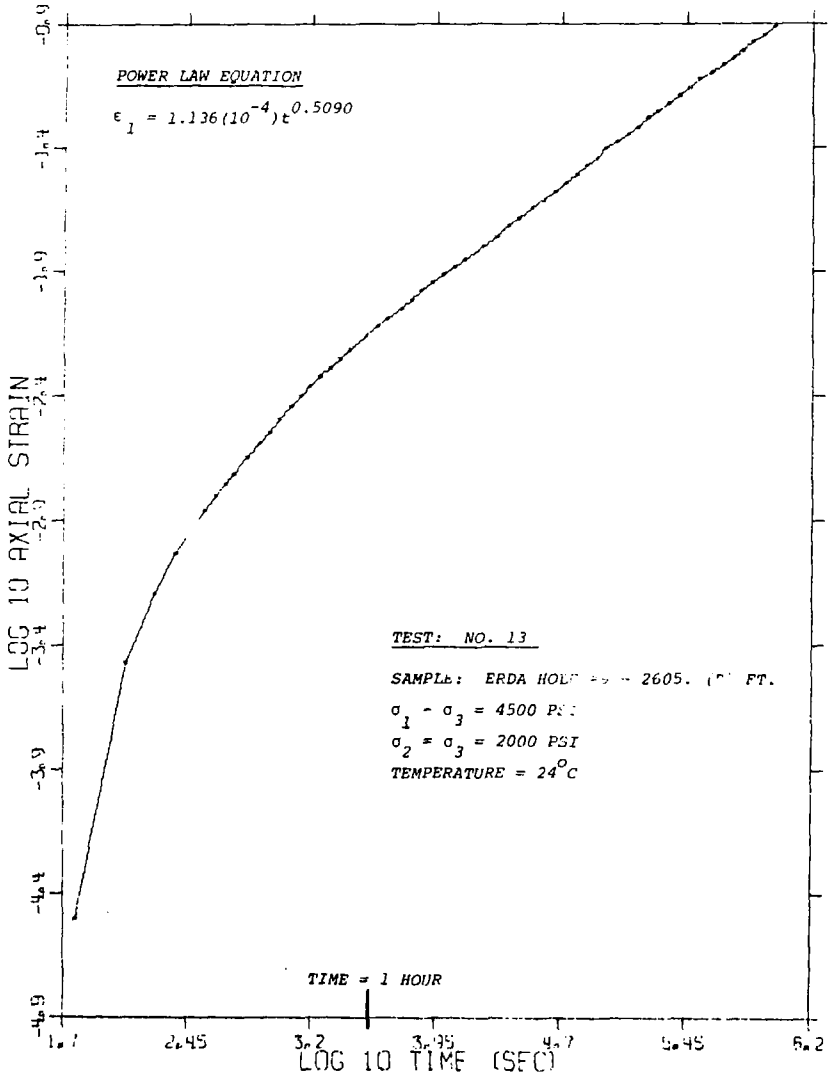

Figure B-33. Log_{10} Axial Strain as a Function of Log_{10} Time (Sec.), Test 13.

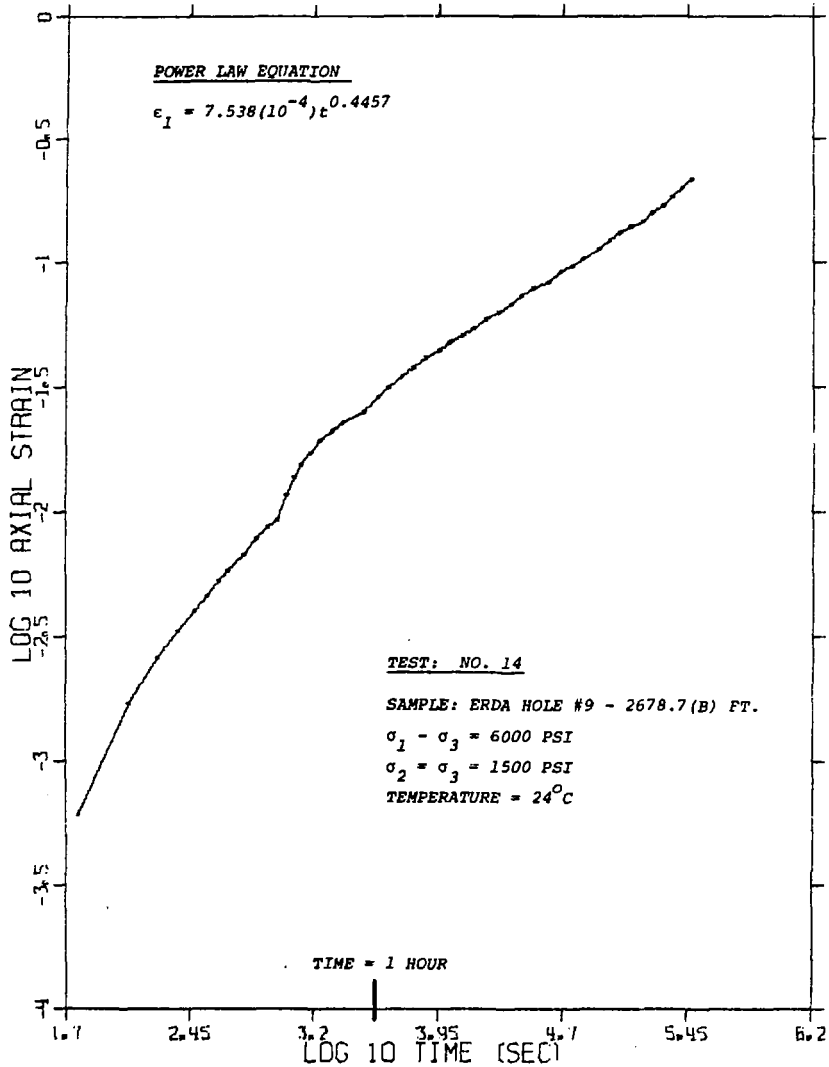

Figure B-34. Log_{10} Axial Strain as a Function of Log_{10} Time (Sec.), Test 14.

APPENDIX C

PLOTS OF LATERAL STRAIN

AS A FUNCTION OF TIME

APPENDIX C (CONT'D)

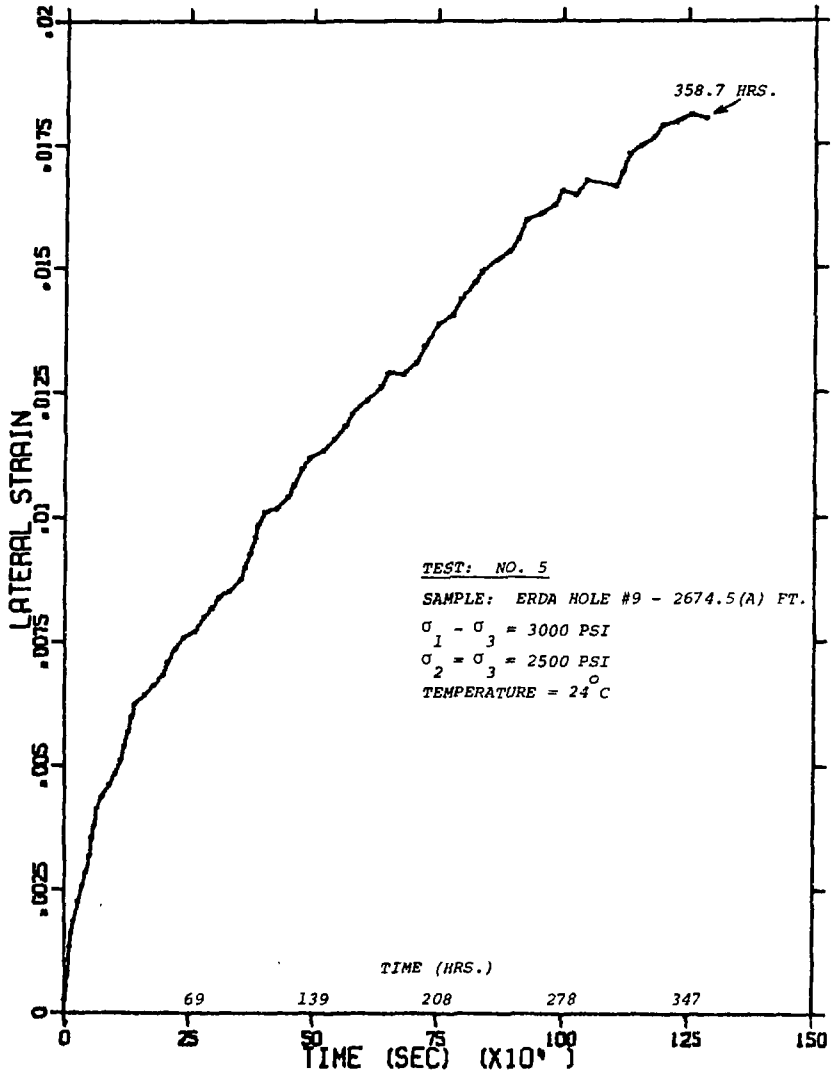

Figure C-1. Lateral Strain as a Function of Time, Test 5.

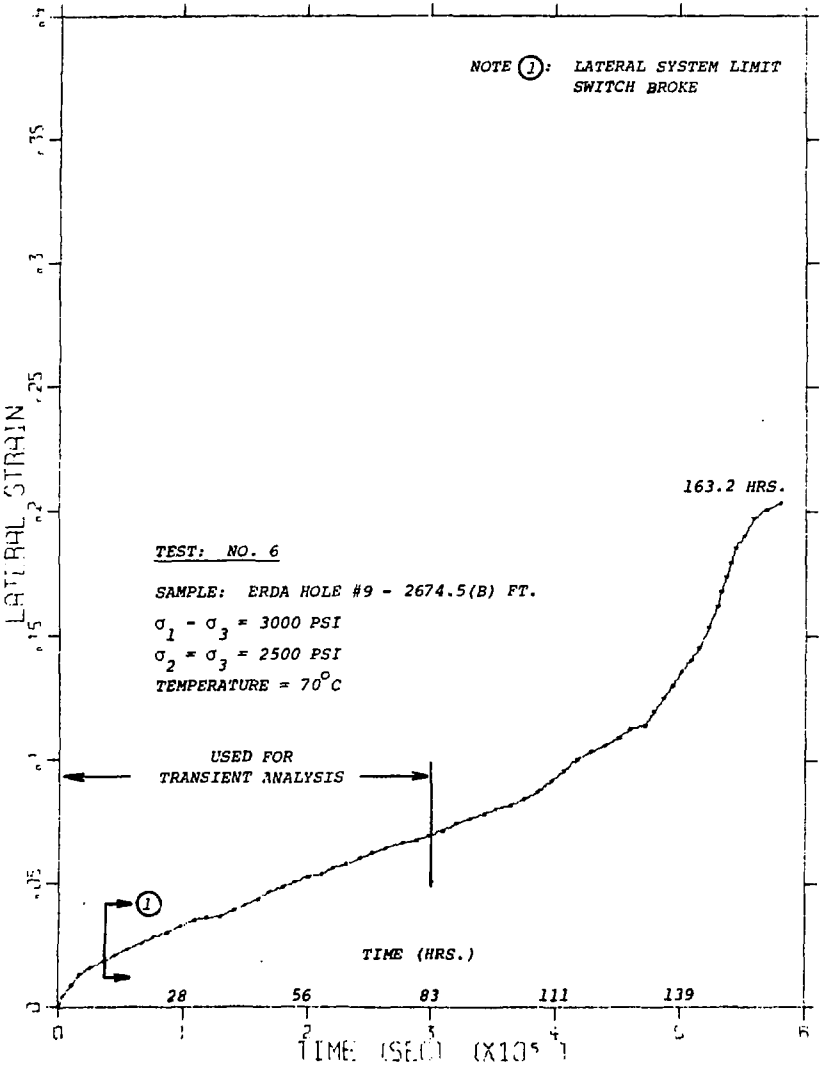

Figure C-2. Lateral Strain as a Function of Time, Test 6.

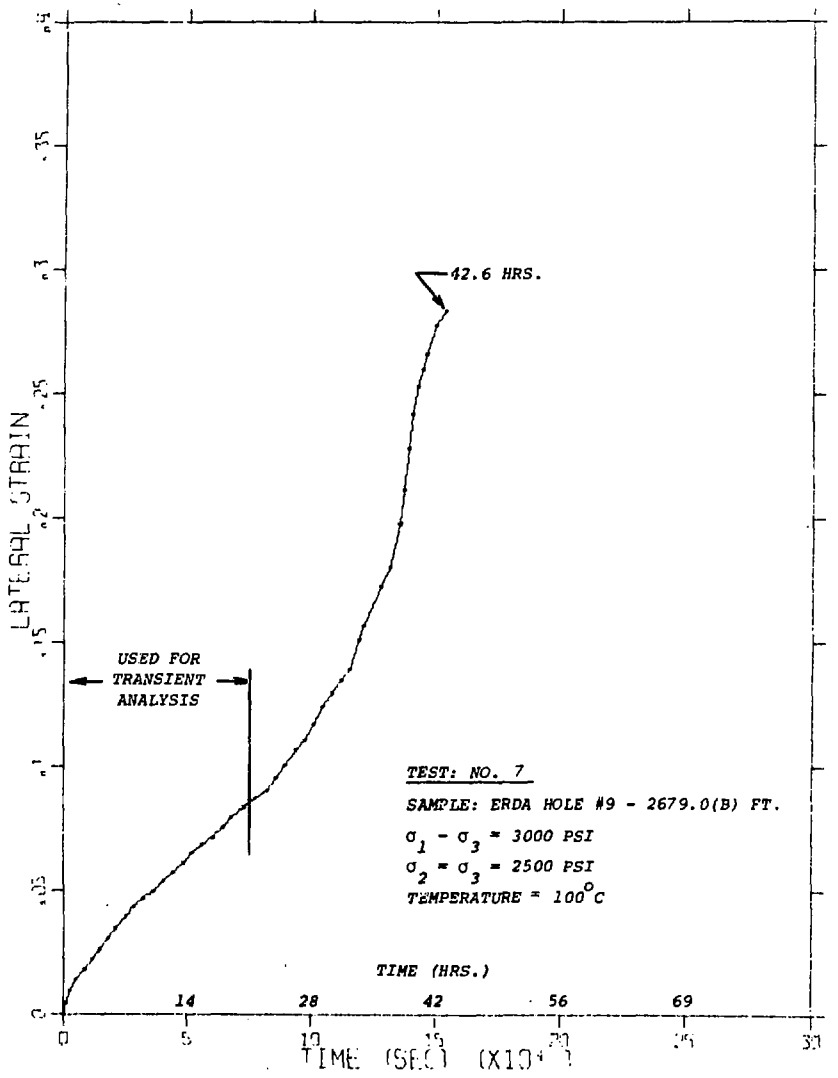

Figure C-3. Lateral Strain as a Function of Time, Test 7.

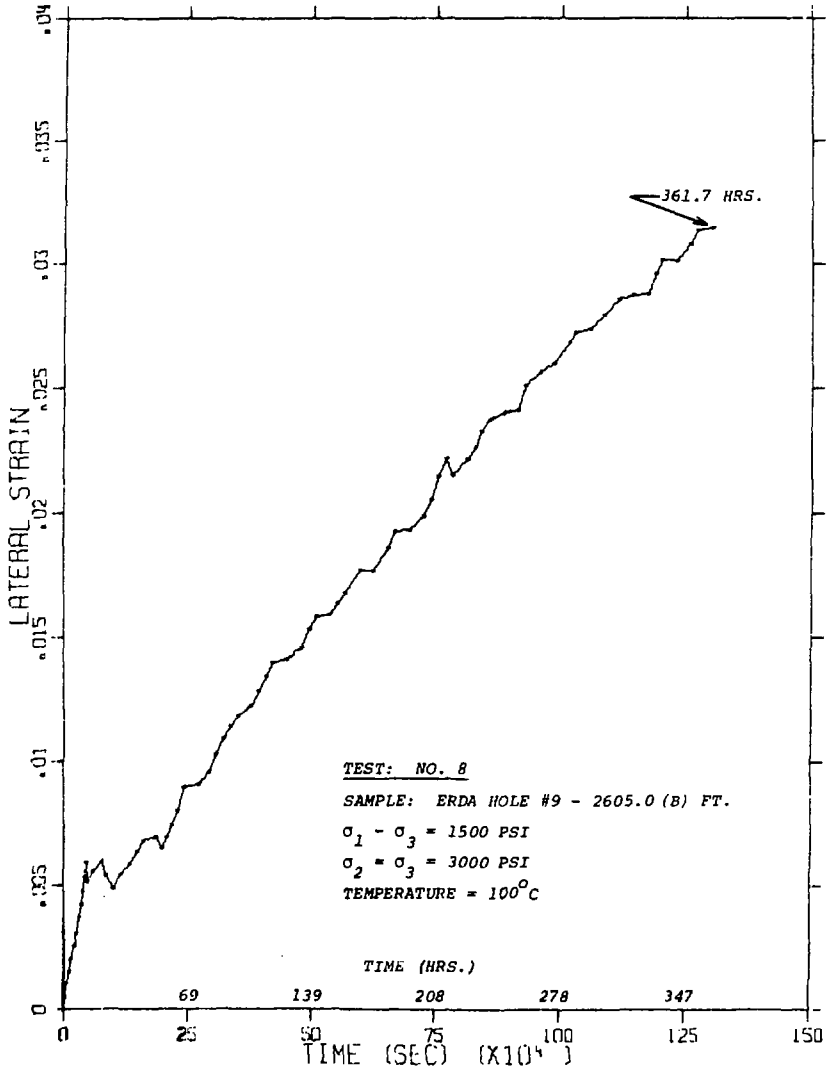

Figure C-4. Lateral Strain as a Function of Time, Test 8.

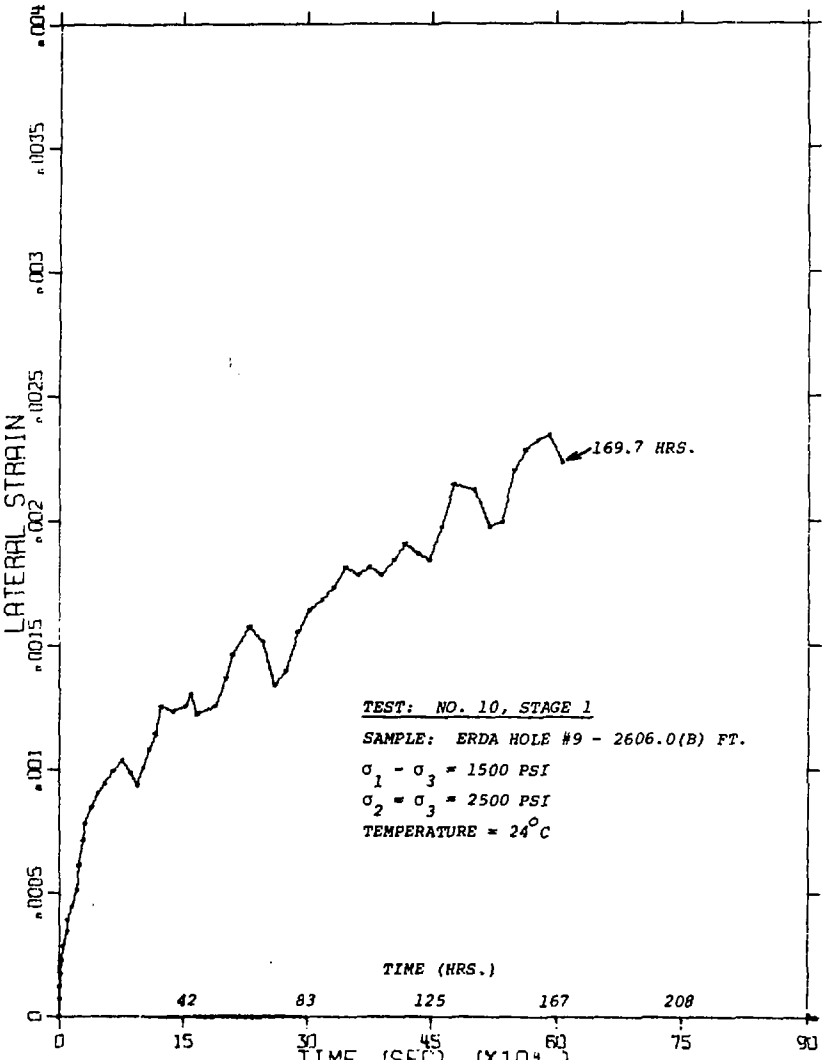

Figure C-5. Lateral Strain as a Function of Time, Test 10, Stage 1.

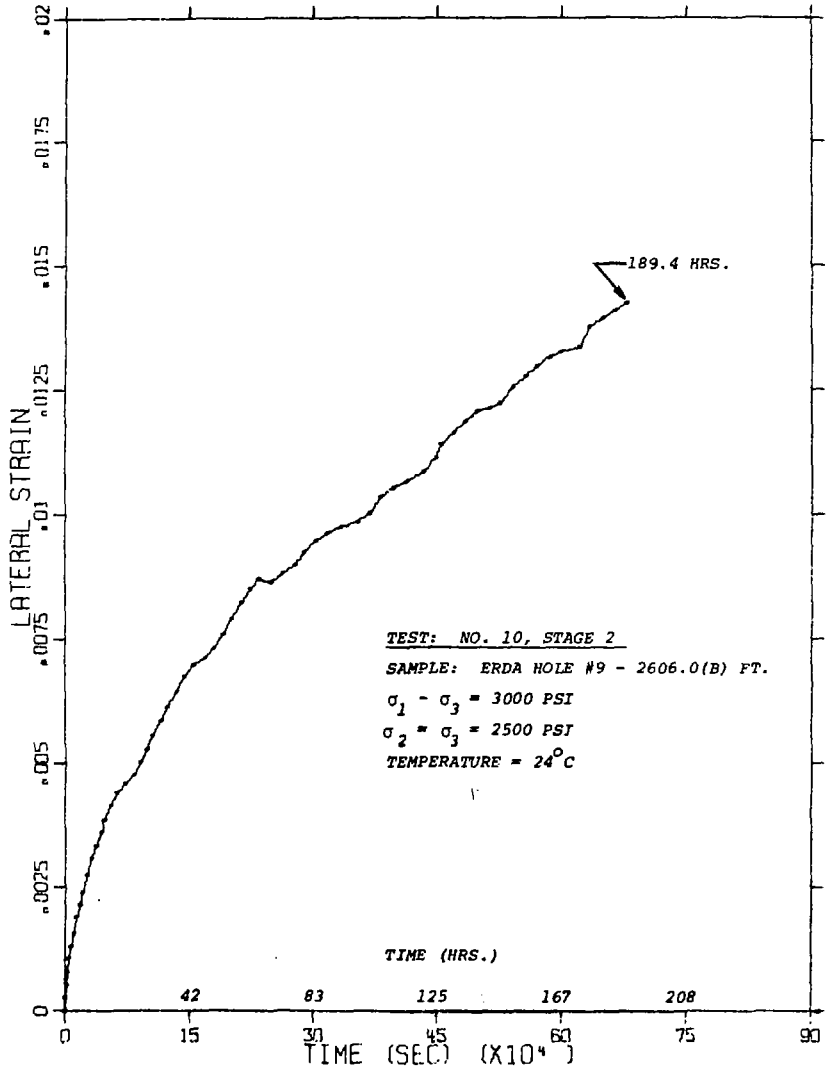

Figure C-6. Lateral Strain as a Function of Time, Test 10, Stage 2.

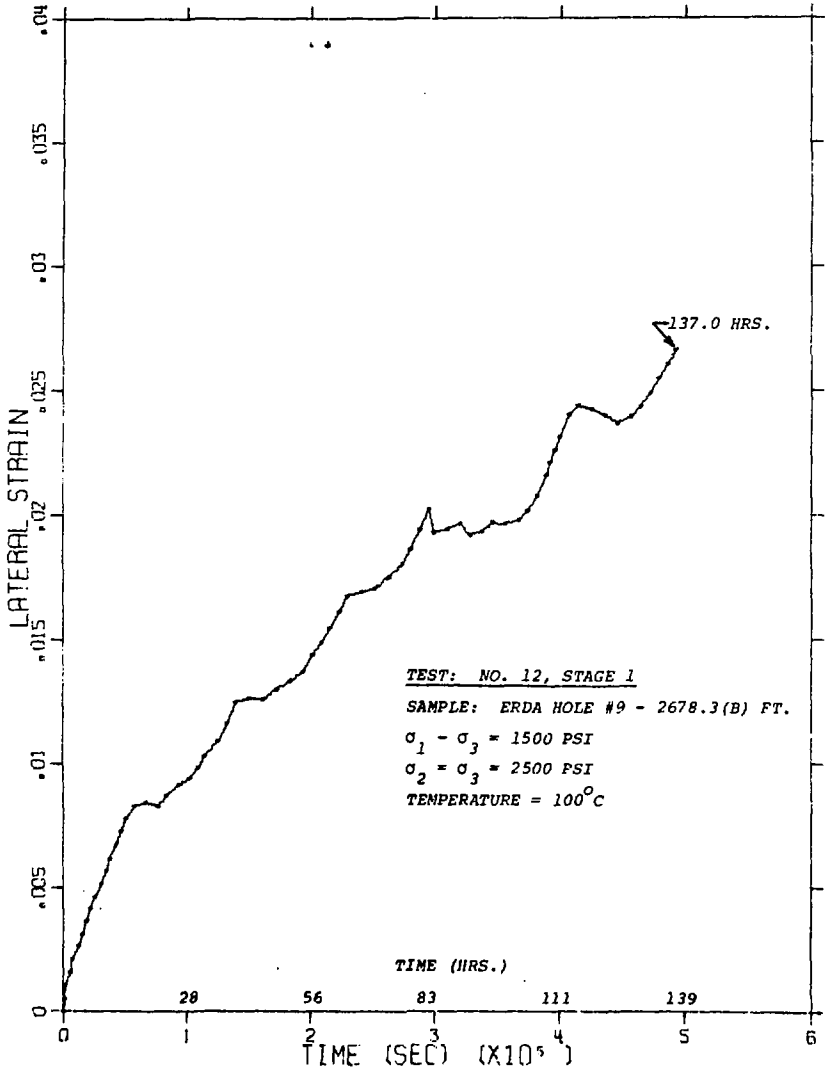

Figure C-7. Lateral Strain as a Function of Time, Test 12, Stage 1

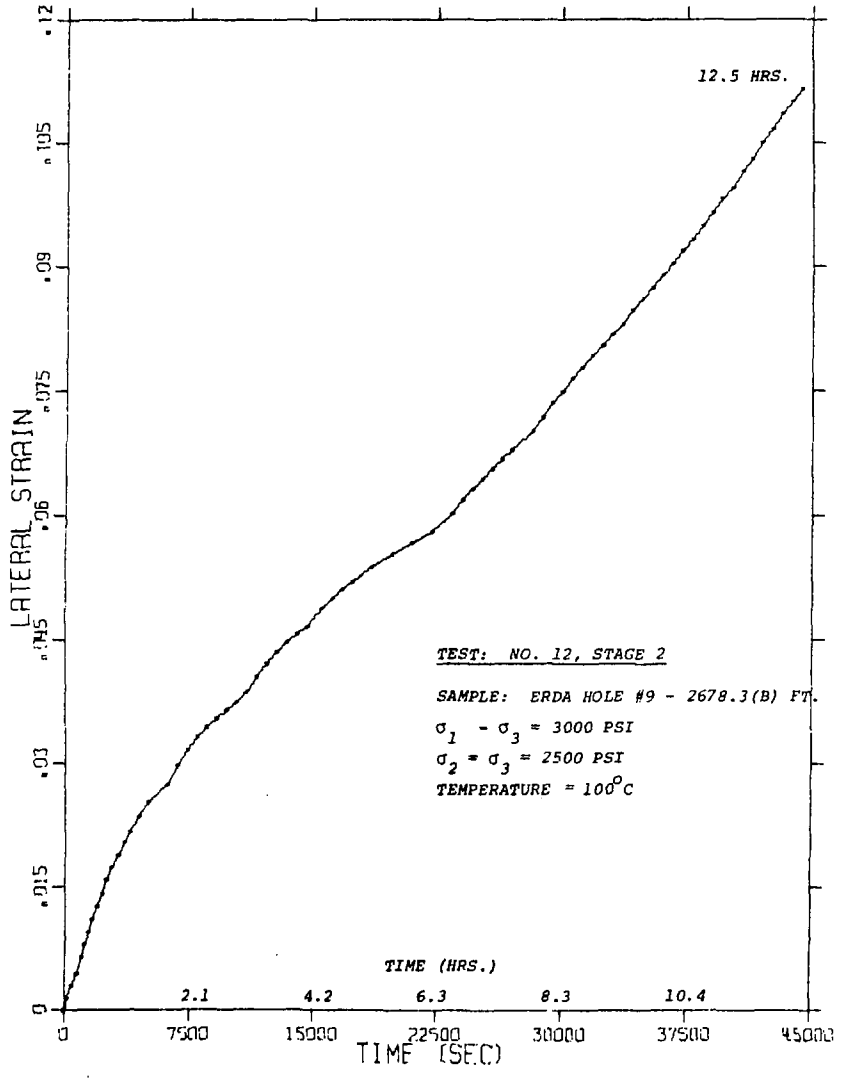

Figure C-8. Lateral Strain as a Function of Time, Test 12, Stage 2.

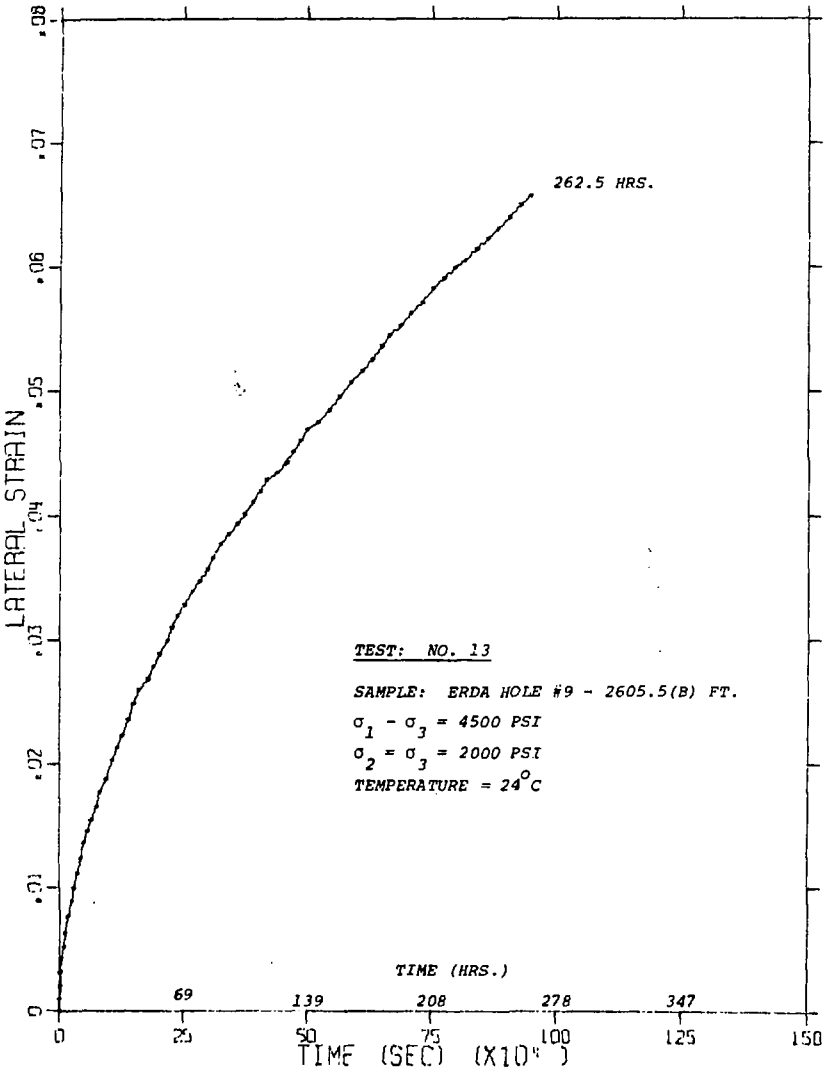

Figure C-9. Lateral Strain as a Function of Time, Test 13.

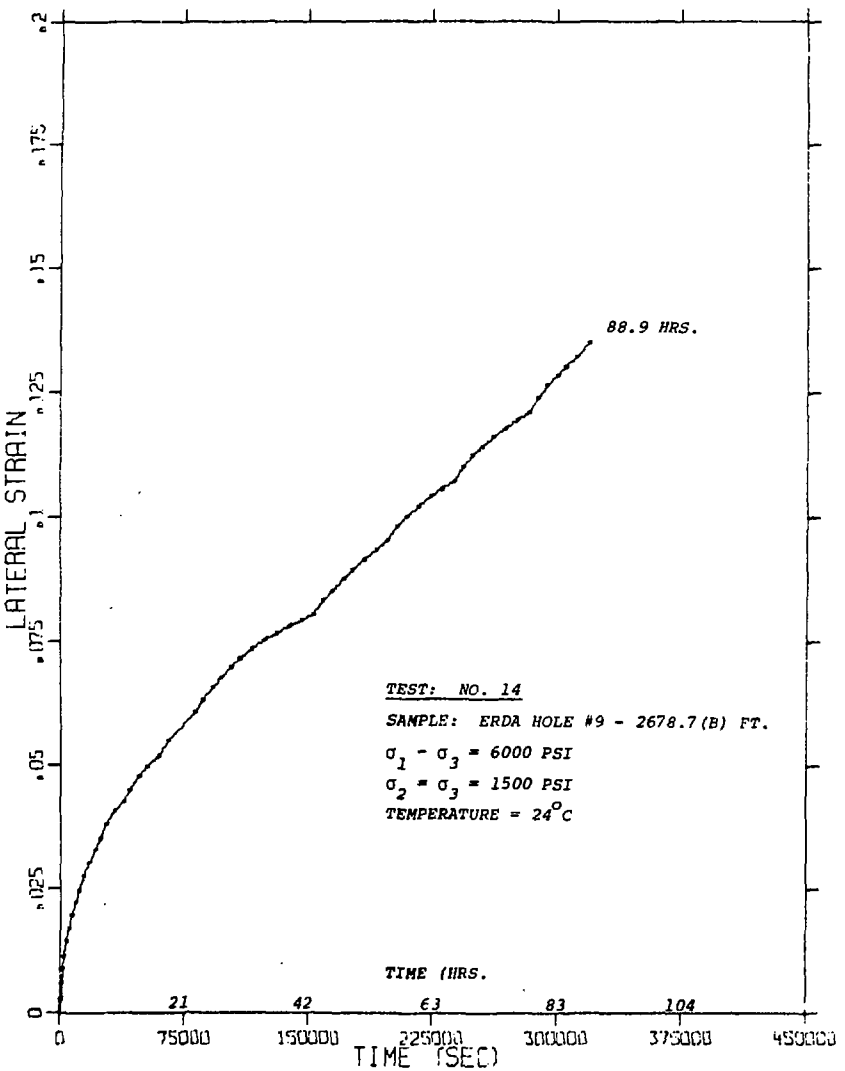

Figure C-10. Lateral Strain as a Function of Time, Test 14.

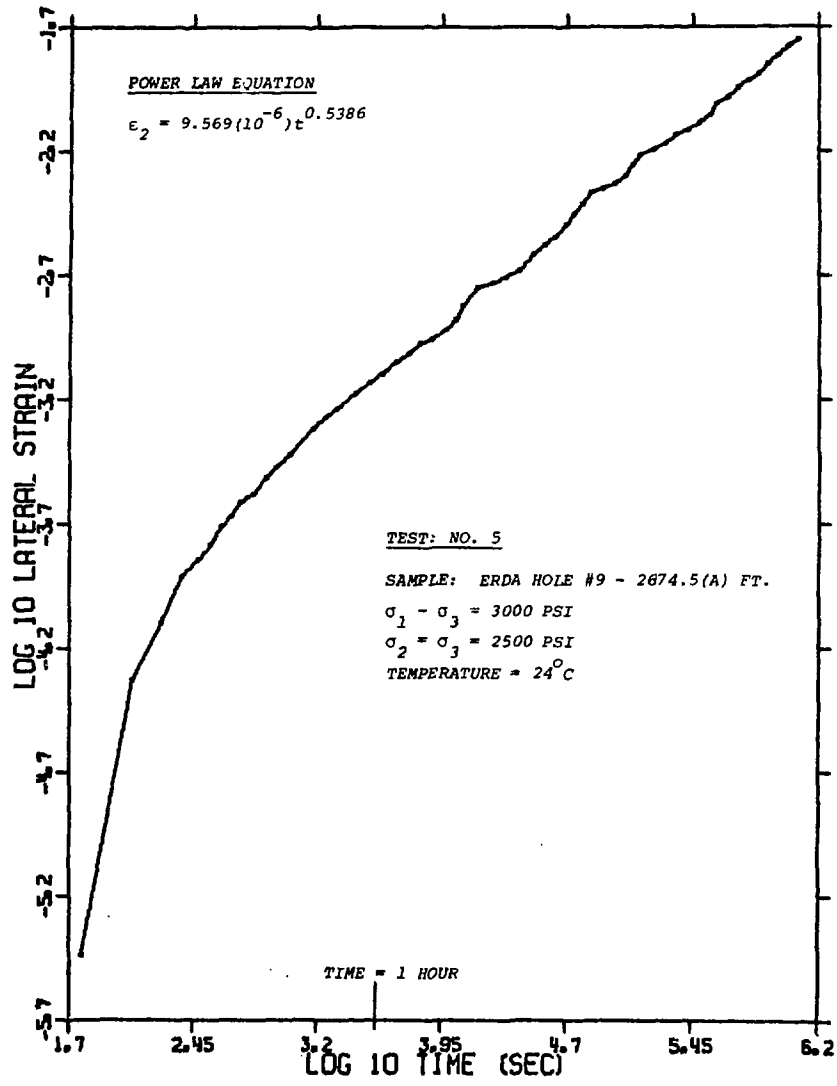

Figure C-11. Log_{10} Lateral Strain as a Function of Log_{10} Time (Sec.), Test 5.

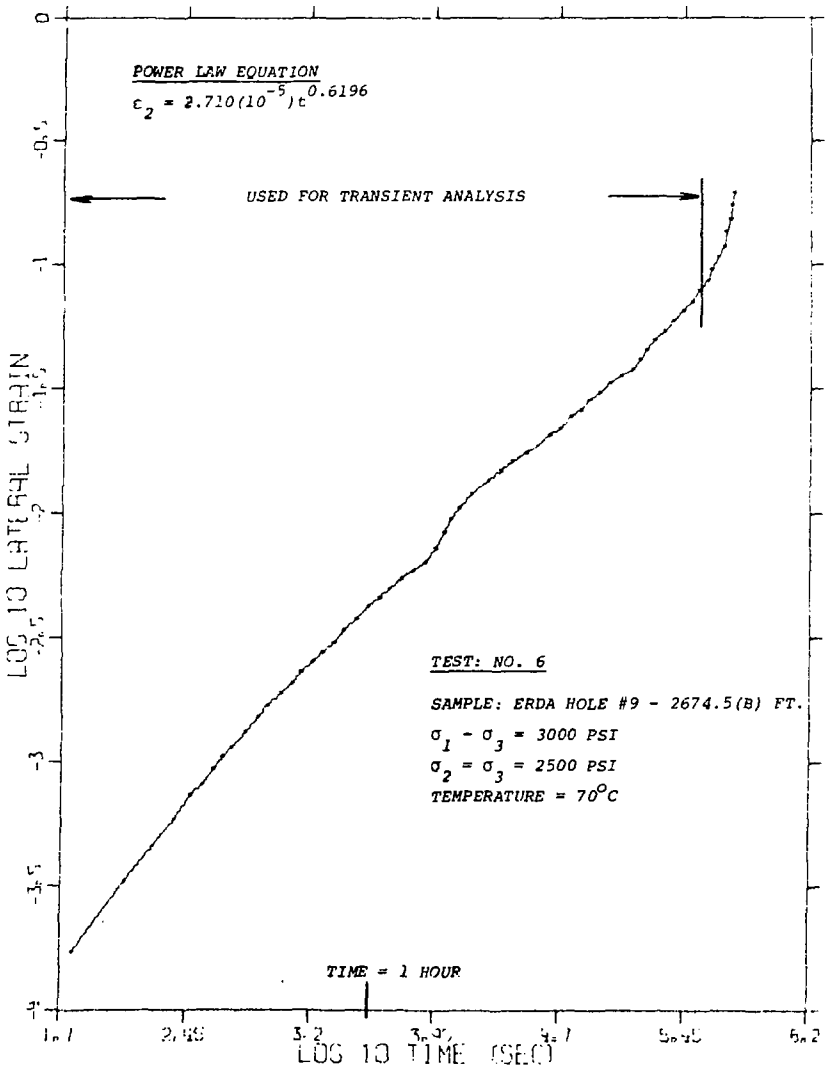

Figure C-12. Log_{10} Lateral Strain as a Function of Log_{10} Time (Sec.), Test 6.

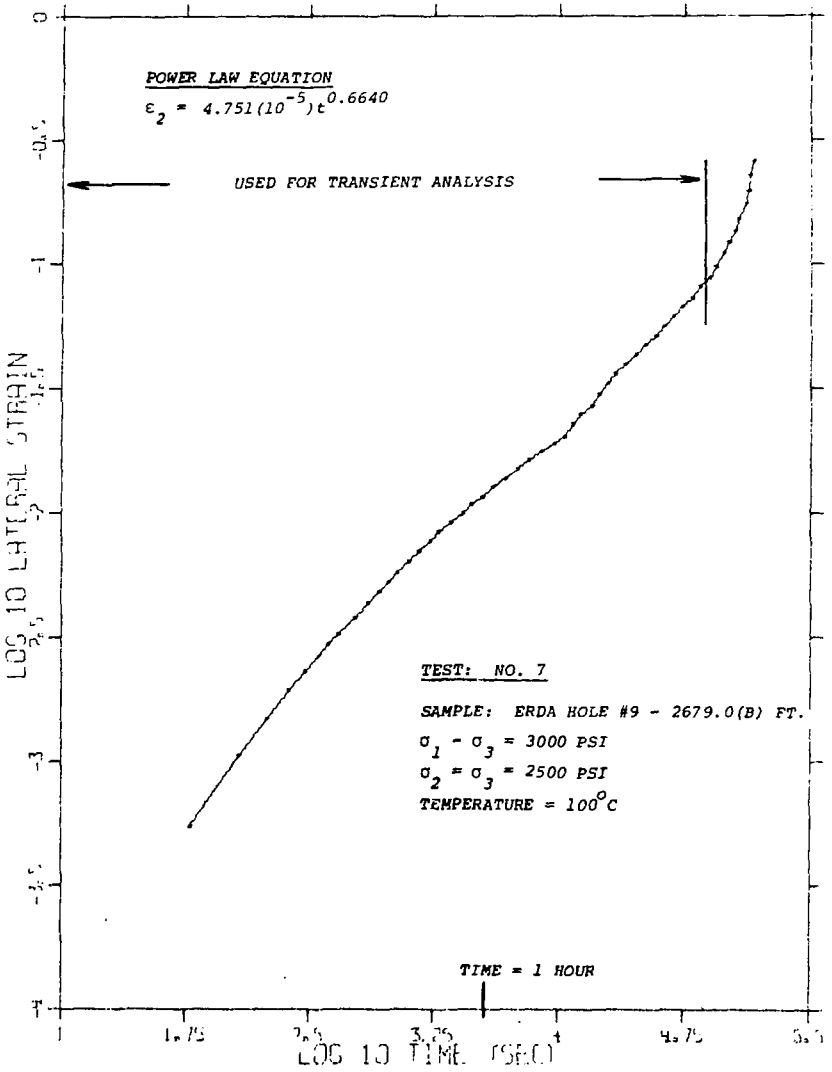

Figure C-13. Log_{10} Lateral Strain as a Function of Log_{10} Time (Sec.), Test 7.

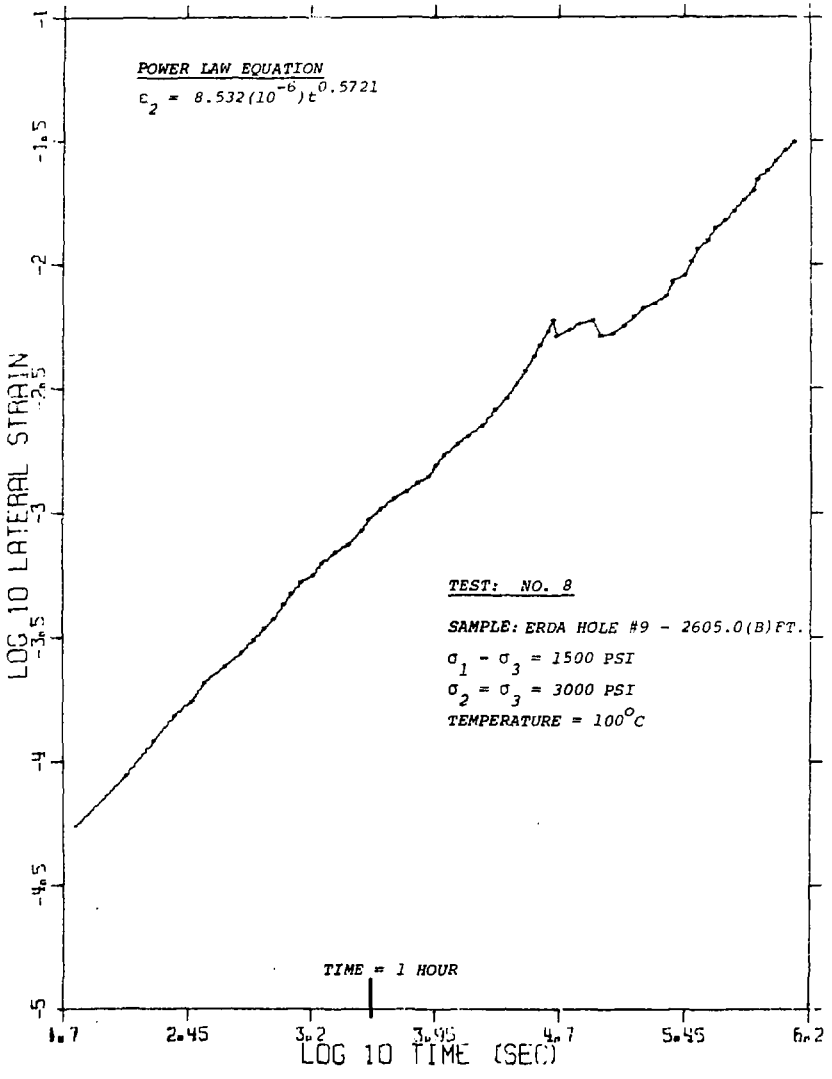

Figure C-14. Log_{10} Lateral Strain as a Function of Log_{10} Time (Sec.), Test 8.

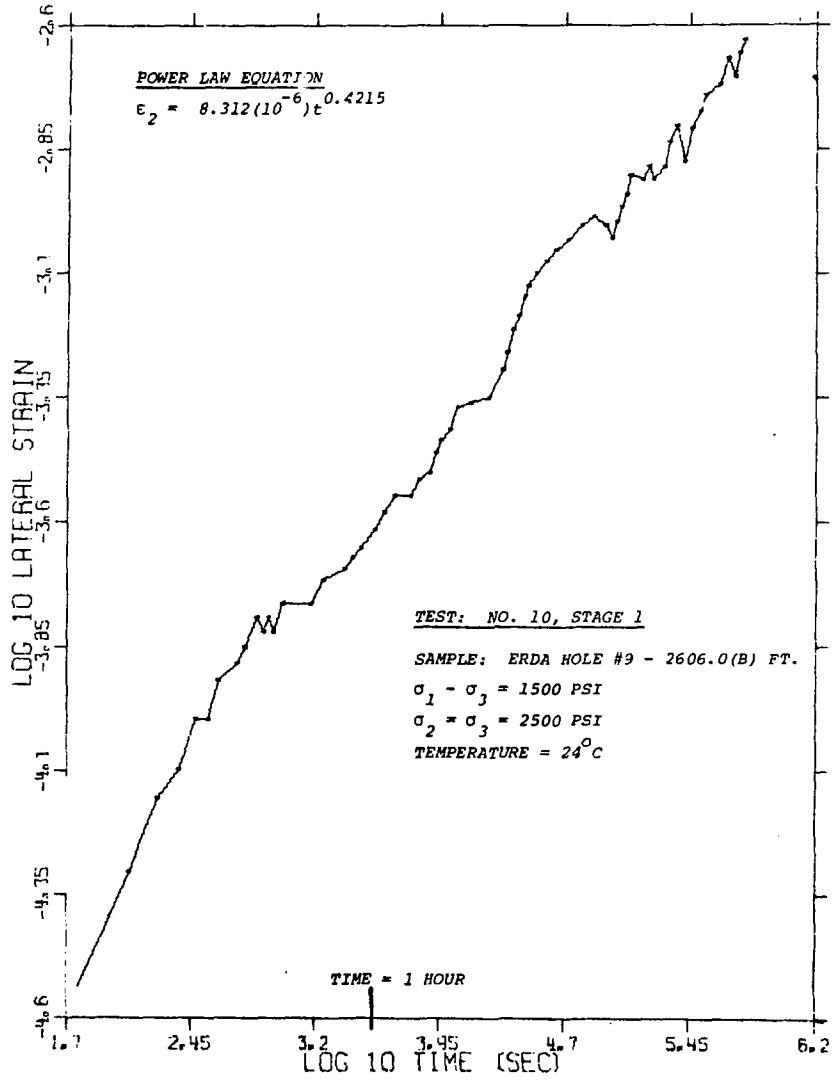

Figure C-15. Log_{10} Lateral Strain as a Function of Log_{10} Time (Sec.), Test 10, Stage 1.

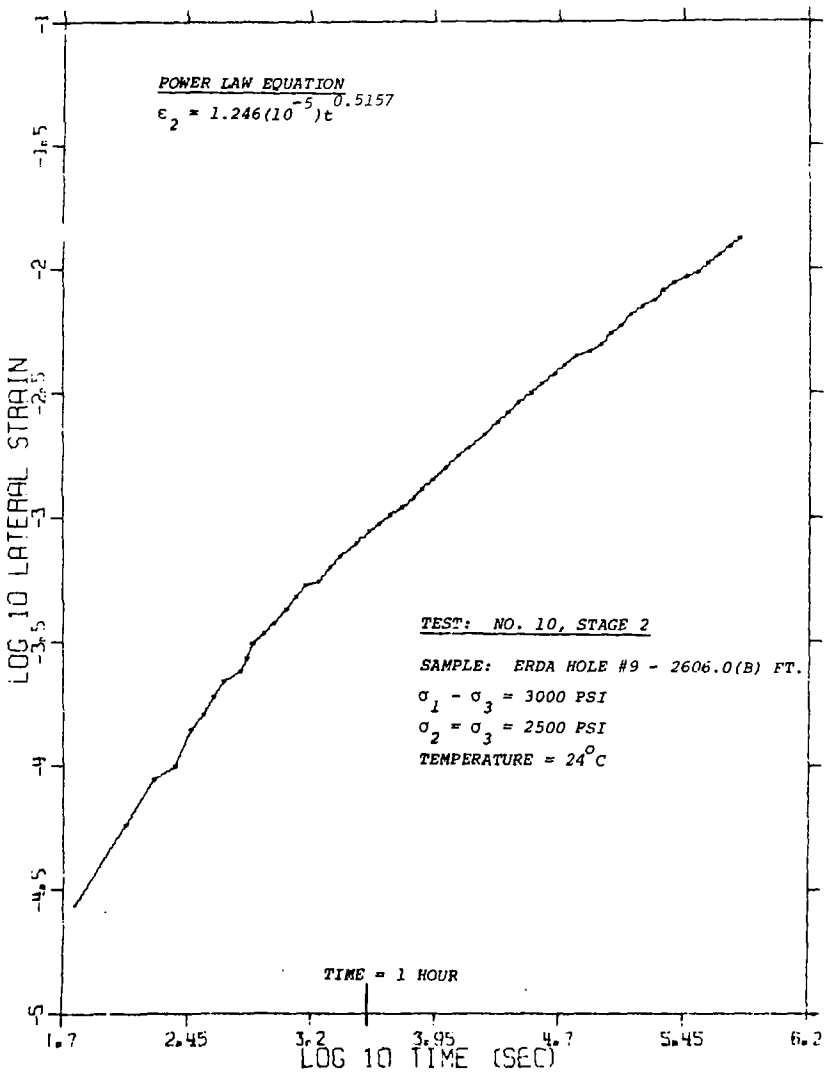

Figure C-16. Log_{10} Lateral Strain as a Function of Log_{10} Time (Sec.), Test 10, Stage 2.

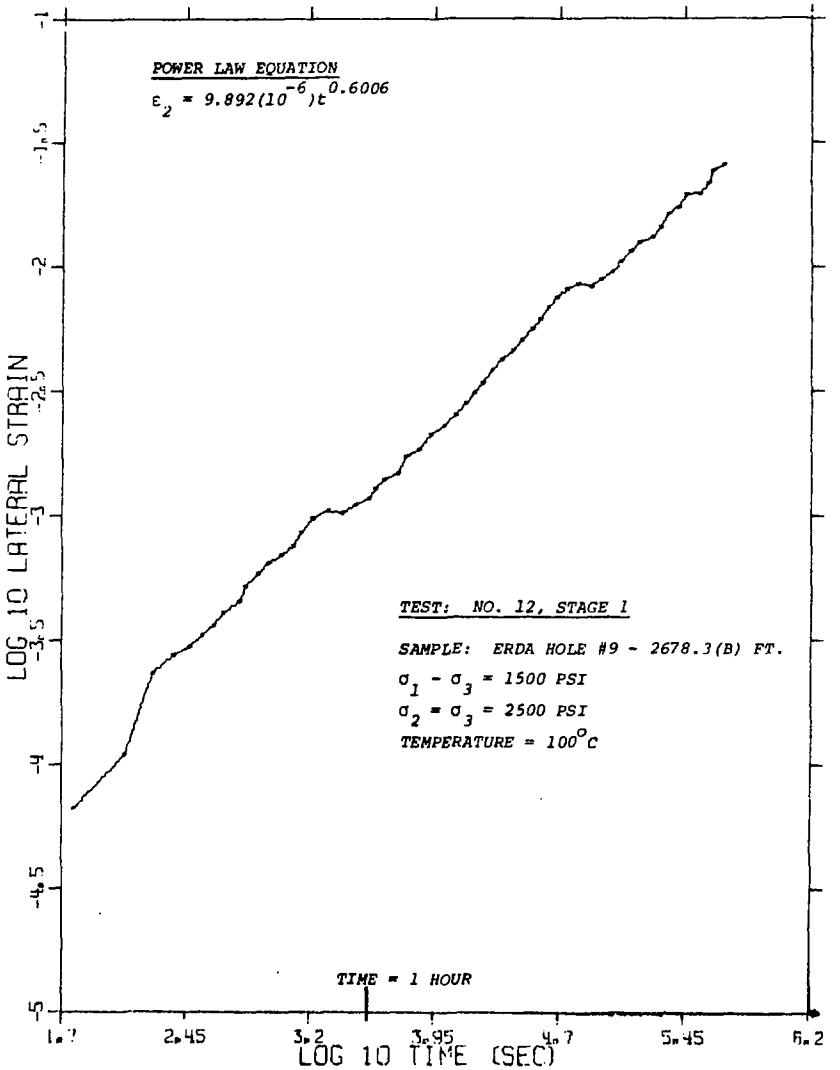

Figure C-17. Log_{10} Lateral Strain as a Function of Log_{10} Time (Sec.), Test 12, Stage 1.

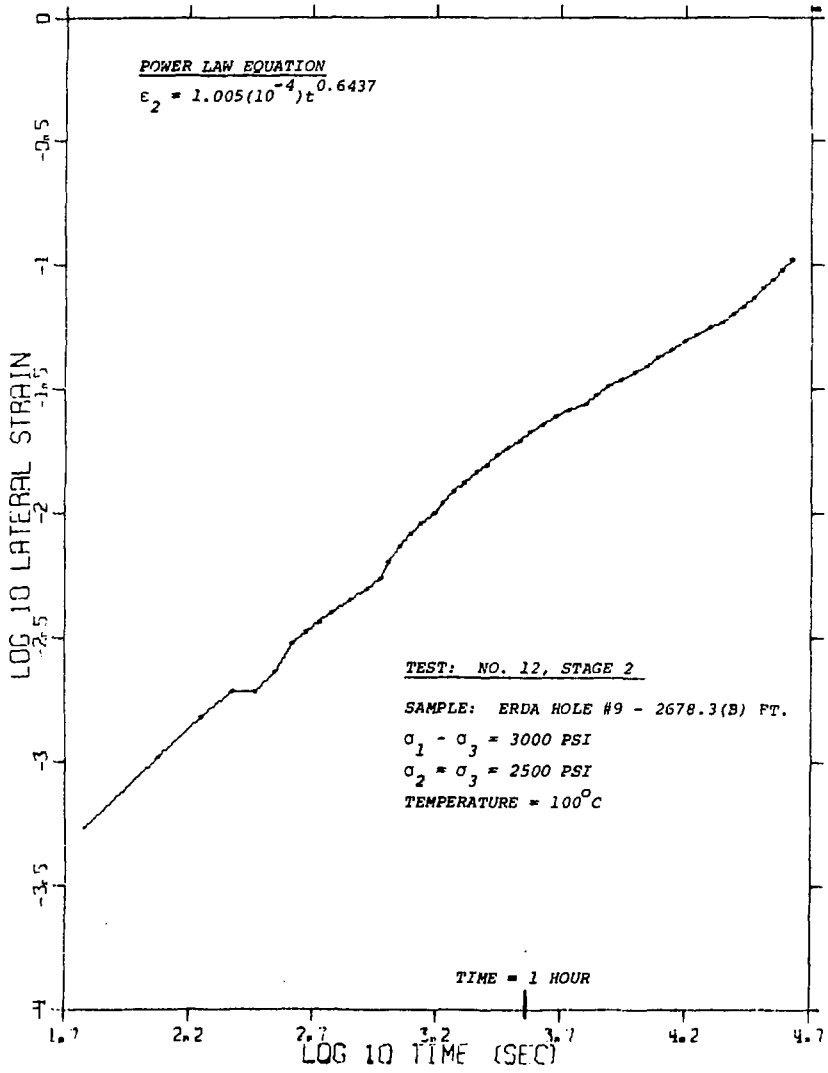

Figure C-18. Log_{10} Lateral Strain as a Function of Log_{10} Time (Sec.), Test 12, Stage 2.

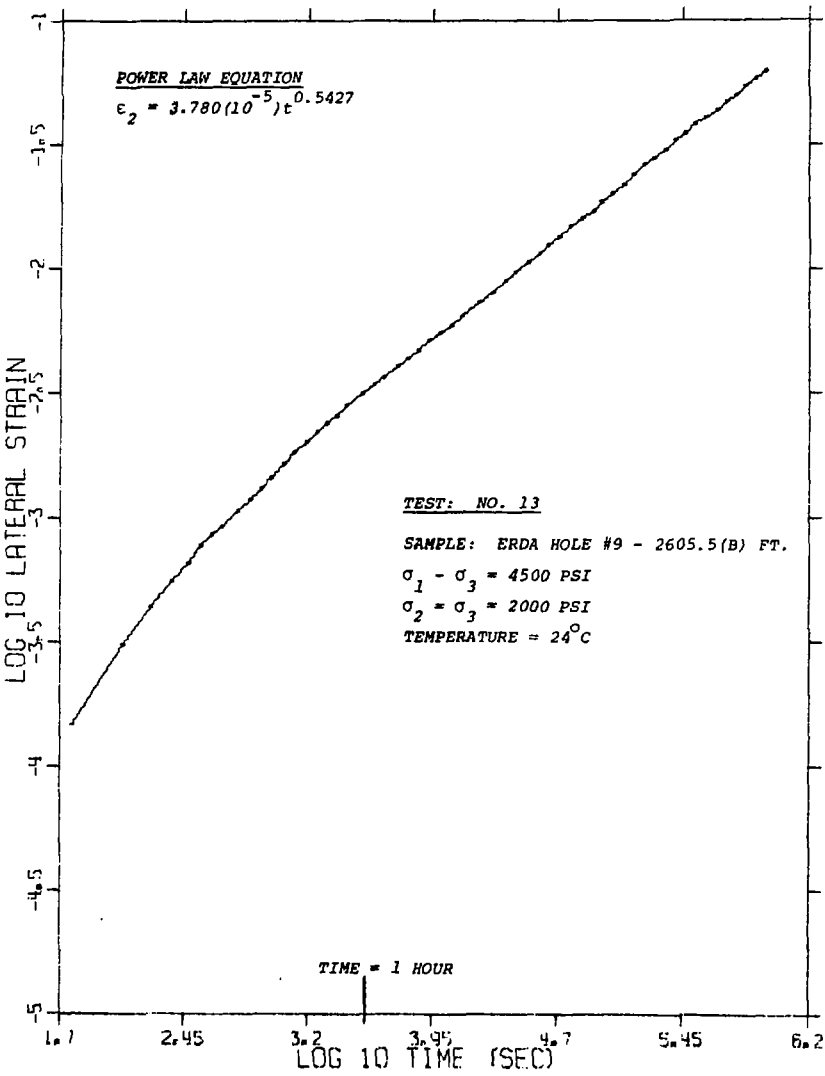

Figure C-19. Log_{10} Lateral Strain as a Function of Log_{10} Time (Sec.), Test 13.

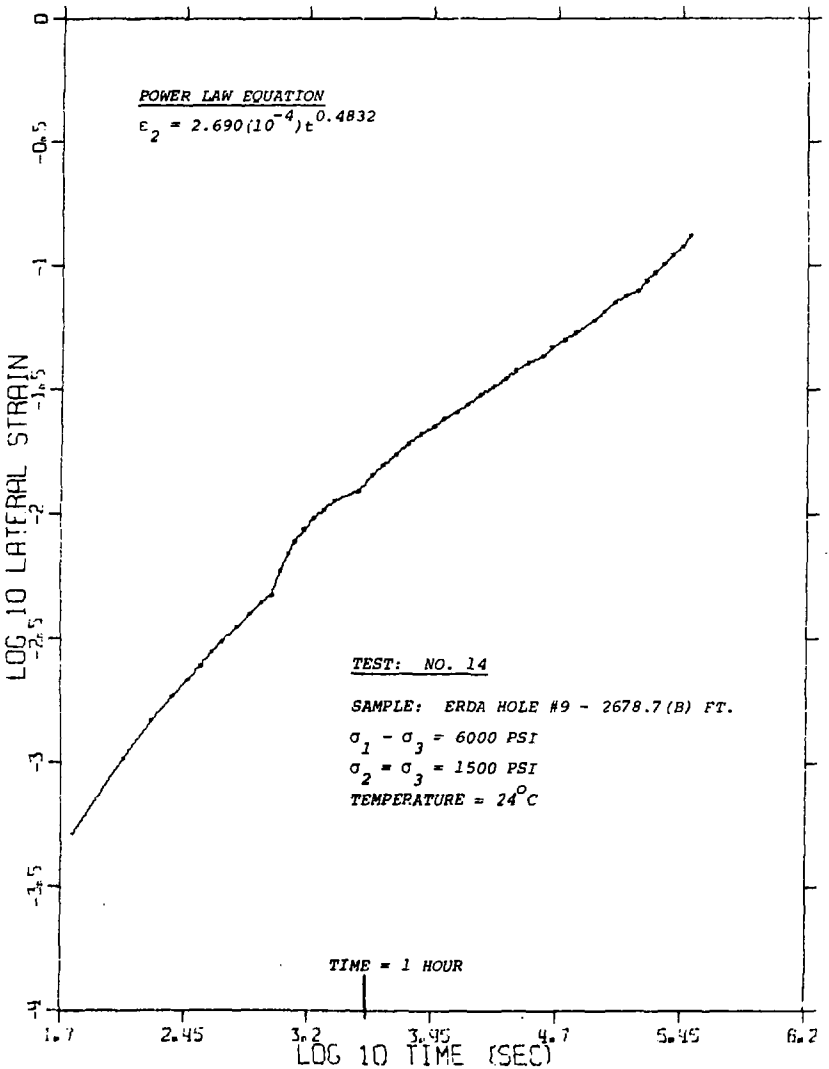

Figure C-20. Log_{10} Lateral Strain as a Function of Log_{10} Time (Sec.), Test 14.

APPENDIX D

SPECIMEN CHARACTERIZATION AND GEOMETRY BEFORE AND AFTER TESTING

This special appendix is for the purpose of presenting a physical description of the test specimens as they were set up for testing. In addition, geometrical measurements of length and diameter are given of the specimen before test initiation (L_o, D_o) and after test completion (L_f, D_f). In some tests the specimens underwent large strains ($\varepsilon_1 > 25\%$) and the area of the specimen increased such that the piston penetrated the salt, leaving a small circumferential ridge about the ends. In these instances, two measurements of final length are given; L_{f_1} is a measurement from piston surface to piston surface while L_{f_2} is a measurement from ridge to ridge (approximate). Several measurements of diameter are given for each specimen as barrelling was evident to various degrees in each. Further, cumulative axial strains were calculated ($\Delta L/L$) using average values and compared to the total axial strain from experimental data. Radial (lateral) strain was similarily calculated ($\Delta D/D$).

TABLE D-1

SPECIMEN CHARACTERIZATION AND GEOMETRIES

TEST NO.	SPECIMEN ORIGIN L_o(IN.):D_o(IN.)	SPECIMEN CHARACTERIZATION	L_{f_1} (IN)	L_{f_2} (IN)	DIAMETERS(IN.)
1	9-2668.5(A) 4.096:1.967	Very lg. XTL, gray impurities, anhydrite idioblasts epoxy caps on bottom end, few small chips on end	4.070	--	1/4 = 1.97 MID = 1.98 1/4 = 1.97
CUMULATIVE EXPERIMENTAL STRAINS ($\varepsilon_1/\varepsilon_2$) = 1.05%/-- STRAINS ON BASIS OF DEFORMED SPECIMEN ($\varepsilon_1/\varepsilon_2$) = 0.63%/0.32%					
2	9-2668.5(B) 4.055:1.967	Excellent edges, epoxy cap on bottom, small XTL.	3.920	--	1/4 = 2.02 MID = 2.04 1/4 = 2.01
CUMULATIVE EXPERIMENT STRAINS ($\varepsilon_1/\varepsilon_2$) = 3.69%/-- STRAINS ON BASIS OF DEFORMED SPECIMEN ($\varepsilon_1/\varepsilon_2$) = 3.33%/2.86%					
3	9-2622.0 4.102:1.970	Excellent edges; very minor cap, small XTL (0.1 in.)	3.625	--	1/8 = 2.06 1/4 = 2.20 MID = 2.24 1/4 = 2.21 1/8 = 2.08
CUMULATIVE EXPERIMENTAL STRAIN ($\varepsilon_1/\varepsilon_2$) = 11.71%/-- STRAINS ON BASIS OF DEFORMED SPECIMEN ($\varepsilon_1/\varepsilon_2$) = 11.63%/9.54%					
4	9-2678.0(A) 4.089:1.973	Small chips on one end w/mostly sm. XTL, other end 1/2 sm, 1/2 lg XTL, gray coloration, minor epoxy cap	?	?	?
SPECIMEN FAILED					
5	9-2674.5(A) 4.003:1.977	Very lg. XTL on one end, med. other end, small XTL along one edge, minor chips	3.816	--	1/4 = 1.998 MID = 2.039 1/4 = 2.022
CUMULATIVE EXPERIMENTAL STRAINS ($\varepsilon_1/\varepsilon_2$) = 4.90%/2.09% STRAINS ON BASIS OF DEFORMED SPECIMEN ($\varepsilon_1/\varepsilon_2$) = 4.67%/2.14%					

TABLE D-1 (CONT'D)

TEST NO.	SPECIMEN ORIGIN L_o(IN.):D_o(IN.)	SPECIMEN CHARACTERIZATION	L_{f_1} (IN)	L_{f_2} (IN)	DIAMETERS (IN.)
6	9-2674.5(B) 4.083:1.977	Most small XTL one end, all small other end, small throughout, gray coloration	2.25	2.41 2.55 2.37	1/8 = 2.60 1/4 = 2.67 MID = 2.69 1/4 = 2.64 1/8 = 2.36
CUMULATIVE EXPERIMENTAL STRAINS (ϵ_1/ϵ_2) = 44.54%/21.20% STRAINS ON BASIS OF DEFORMED SPECIMEN (ϵ_1/ϵ_2) = 44.89%/31.11%					
7	9-2679.0(B) 4.090:1.998	Minor gray impurities, not as much as other specimens most small XTL(75%), others large(25%)	2.31 2.39 2.31	2.55 2.51 2.50	1/8 = 2.59 1/4 = 2.70 MID = 2.69 1/4 = 2.63 1/8 = 2.55
CUMULATIVE EXPERIMENTAL STRAINS (ϵ_1/ϵ_2) = 40.99%/28.84% STRAINS ON BASIS OF DEFORMED SPECIMEN (ϵ_1/ϵ_2) = 42.87%/31.73%					
8	9-2605.0(B) 4.042:1.99	Most small XTL one end w/lg. XTL in center, otherwise small XTL, gray impurities throughout	3.771	--	1/8 = 2.06 1/4 = 2.09 MID = 2.08 1/4 = 2.06 1/8 = 2.04
CUMULATIVE EXPERIMENTAL STRAINS (ϵ_1/ϵ_2) = 6.75%/3.23% STRAINS ON BASIS OF DEFORMED SPECIMEN (ϵ_1/ϵ_2) = 6.70%/3.35%					
9	9-2678.0(B) 4.096:1.967	One small chip on top; large XTLs	?	--	?
SPECIMEN FAILED					
10	9-2606.0(B) 4.026:1.998	Small XTL, minor impurities	3.87	--	1/4 = 2.03 MID = 2.04 1/4 = 2.03
CUMULATIVE EXPERIMENTAL STRAINS (ϵ_1/ϵ_2) = 3.89%/1.92% STRAINS ON BASIS OF DEFORMED SPECIMEN (ϵ_1/ϵ_2) = 3.87%/1.77%					

TABLE D-1 (CONT'D)

TEST NO.	SPECIMEN ORIGIN L_o(IN.):D_o(IN.)	SPECIMEN CHARACTERIZATION	L_{f_1} (IN)	L_{f_2} (IN)	DIAMETERS (IN.)
11	9-2679.0(A) 4.032:1.998	Most large XTL, minor impurities upper end, arrow points to upper end	3.301 3.296 3.290	4.10 3.01 BROKEN EDGES	1/8 = 2.31 1/4 = 2.34 MID = 2.37 1/4 = 2.34 1/8 = 2.30
	CUMULATIVE EXPERIMENTAL STRAINS ($\varepsilon_1/\varepsilon_2$) = 15.40%/-- STRAINS ON BASIS OF DEFORMED SPECIMEN ($\varepsilon_1/\varepsilon_2$) = 18.26%/16.72%				
12	9-2678.3(D) 4.061:1.995	Small to medium XTL, gray coloration	2.991	3.11 3.06 3.13	1/8 = 2.25 1/4 = 2.33 MID = 2.42 1/4 = 2.30 1/8 = 2.26
	CUMULATIVE EXPERIMENTAL STRAINS($\varepsilon_1/\varepsilon_2$) = 27.70%/14.72% STRAINS ON BASIS OF DEFORMED SPECIMEN($\varepsilon_1/\varepsilon_2$) = 26.35%/15.89%				
13	9-2605.5(B) 4.077:1.998	Small XTL, minor impurities	3.49	3.53 3.52 3.50	1/8 = 2.13 1/4 = 2.19 MID = 2.18 1/4 = 2.18 1/8 = 2.11
	CUMULATIVE EXPERIMENTAL STRAINS ($\varepsilon_1/\varepsilon_2$) = 12.96%/6.81% STRAINS ON BASIS OF DEFORMED SPECIMEN ($\varepsilon_1/\varepsilon_2$) = 14.40%/8.01%				
14	9-2678.7(B) 4.018:1.997	Small to medium XTL, gray impurities diagonally oriented	2.90	3.08 3.01 3.10	1/8 = 2.29 1/4 = 2.38 MID = 2.41 1/4 = 2.50 1/8 = 2.31
	CUMULATIVE EXPERIMENTAL STRAINS ($\varepsilon_1/\varepsilon_2$) = 27.14%/15.62% STRAINS ON BASIS OF DEFORMED SPECIMEN ($\varepsilon_1/\varepsilon_2$) = 27.82%/19.08%				